UNIVERSITÀ
DEGLI STUDI
DI BRESCIA

DOTTORATO DI RICERCA IN GENETICA MOLECOLARE, BIOTECNOLOGIE E MEDICINA SPERIMENTALE

settore scientifico disciplinare
MED/26 NEUROLOGIA

XXXVI CICLO

TITOLO TESI

Advanced neuroimaging in genetic neurodegenerative diseases

Dottoranda:
Dott.ssa Marta Pengo
Matricola 734974

Relatore:
Chiar.mo Prof. Eugenio Monti

Correlatore:
Chiar.ma Prof.ssa Barbara Borroni

INDEX

ABSTRACT (*Italian*) 5

ABSTRACT (*English*) 7

CHAPTER 1 - INTRODUCTION 11

Advanced neuroimaging 11

Advanced neuroimaging in genetic Frontotemporal dementia 16

Advanced neuroimaging in Huntington's disease 23

CHAPTER 2 – REVIEW 44

Dissecting the many faces of Frontotemporal dementia: an imaging perspective 44

EXPERIMENTAL SECTION 75

CHAPTER 3 – STUDY 1 77

Differences and similarities between familial and sporadic Frontotemporal dementia: an Italian single-centre cohort study 77

CHAPTER 4 – STUDY 2 100

Early neurotransmitters changes in prodromal Frontotemporal Dementia: a GENFI study 100

CHAPTER 5 – STUDY 3 125

Impaired glymphatic system in genetic Frontotemporal Dementia: a GENFI study 125

CHAPTER 6 – STUDY 4 145

Visual networks dynamic functional connectivity is associated with neurofilament light and expected clinical onset in premanifest Huntington's disease 145

ABSTRACT (*Italian*)

Questo lavoro di tesi è il risultato del percorso di tre anni di Dottorato in Genetica molecolare, Biotecnologie e Medicina Sperimentale (ciclo XXXVI), durante i quali ho avuto l'opportunità di occuparmi di studi di neuroimaging avanzato in forme genetiche di malattie neurodegenerative.

Le malattie neurodegenerative genetiche rivestono un particolare interesse nella ricerca in quanto permettono di studiare la fase preclinica, in cui iniziano a svilupparsi alterazioni cerebrali che possono essere rilevate con approcci di neuroimaging avanzato, con profonde implicazioni per lo sviluppo di possibili approcci terapeutici.

Il neuroimaging avanzato è costituito da diverse metodiche non invasive, che permettono di studiare la struttura e la funzione cerebrali (*Capitolo 1*); le principali sono rappresentate dalla risonanza magnetica (RM) strutturale, la RM di diffusione e la RM funzionale. Le differenti tecniche sono in grado di indagare aspetti diversi delle patologie neurodegenerative, come viene illustrato nella Review sulla Demenza frontotemporale (FTD) (*Capitolo 2*).

La sezione sperimentale della tesi è una raccolta di studi sviluppati nel corso del Dottorato, in cui sono state applicate diverse metodiche di neuroimaging avanzato nelle forme genetiche di FTD (*Capitoli 3, 4 e 5*) e nella malattia di Huntington (*Capitolo 6*). Come sarà illustrato, la ricerca di biomarcatori fluidi, come i neurofilamenti, risulta cruciale e complementare al neuroimaging, per una caratterizzazione approfondita di queste patologie.

Il primo studio (*Capitolo 3*) è stato condotto su una coorte di pazienti con FTD seguiti presso la Clinica Neurologica dell'Università di Brescia, allo scopo di confrontare le forme genetiche e quelle sporadiche della malattia. I risultati hanno evidenziato che le forme familiari e quelle sporadiche rappresentano entità cliniche simili, ma con differenti meccanismi biologici, diversa gravità di atrofia cerebrale al neuroimaging strutturale, e differenti velocità di progressione.

Il secondo ed il terzo studio (*Capitoli 4 e 5*, rispettivamente) sono stati condotti su una vasta coorte internazionale di soggetti con FTD genetica in fase presintomatica e sintomatica, inclusi nel GENFI (*Genetic Frontotemporal Dementia Initiative*). I due studi avevano lo scopo di indagare, rispettivamente, le alterazioni neurotrasmettitoriali e del sistema glinfatico, attraverso metodiche specifiche di neuroimaging avanzato. In particolare, nel primo studio è stato utilizzato *JuSpace*, un toolbox che permette di confrontare i pattern di alterazioni cerebrali con la distribuzione di specifici sistemi neurotrasmettoriali. È stato, quindi, possibile evidenziare, indirettamente ed in vivo, come le diverse mutazioni responsabili di FTD genetica siano associate a differenti deficit neurotrasmettoriali nella fase prodromica. Il secondo studio, invece, ha dimostrato che le alterazioni del sistema glinfatico risultano evidenti nelle fasi cliniche e costituiscono un possibile biomarcatore di progressione di malattia. In questo lavoro è stata applicata una particolare metodica denominata DTI-ALPS (*Diffusion tensor image analysis along the perivascular space*) per indagare l'attività del sistema glinfatico.

Infine, l'ultimo studio (*Capitolo 6*) si occupa di risonanza magnetica funzionale nella fase preclinica della malattia di Huntington, ed è stato realizzato in collaborazione con il Centro Huntington dell'University College London (Londra, UK). In questo lavoro, abbiamo dimostrato alterazioni precoci dei network visivi, che predicono la concentrazione dei neurofilamenti e l'esordio atteso della malattia.

ABSTRACT (*English*)

This thesis work is the result of a three-year PhD program in Molecular Genetics, Biotechnology, and Experimental Medicine (cycle XXXVI), during which I had the opportunity to focus on advanced neuroimaging studies in genetic forms of neurodegenerative diseases.

Genetic neurodegenerative diseases are of particular interest in research as they allow for the study of the preclinical phase, where early brain alterations begin to develop and can be detected through advanced neuroimaging approaches, with profound implications for the development of potential therapeutic approaches.

Advanced neuroimaging encompasses various non-invasive techniques, that enable the study of brain structure and function (*Chapter 1*). They include structural magnetic resonance imaging (MRI), diffusion-weighted imaging and functional MRI. These different techniques can investigate various aspects of neurodegenerative pathologies, as illustrated in the Review on Frontotemporal Dementia (FTD) (*Chapter 2*).

The experimental section of the thesis is a collection of studies conducted during the PhD, where various advanced neuroimaging techniques were applied in genetic forms of FTD (*Chapters 3, 4, and 5*) and in Huntington's disease (HD) (*Chapter 6*). As will be explained, the search for fluid biomarkers, such as neurofilaments, is crucial and complementary to neuroimaging for a comprehensive characterization of these pathologies.

The first study (*Chapter 3*) was conducted on a cohort of FTD patients followed at the Neurological Clinic of the University of Brescia, with the aim of comparing genetic and sporadic forms of the disease. We found that familial and sporadic FTD are very similar clinical entities, but with different biological mechanisms, diverse atrophy severity at structural MRI, and different rates of progression.

The second and third studies (*Chapters 4 and 5*) were conducted on a large international cohort of subjects with genetic FTD from GENFI (Genetic Frontotemporal Dementia Initiative). The two

studies aimed to investigate, respectively, neurotransmitter alterations and changes of the glymphatic system, through specific advanced neuroimaging techniques. In particular, in the first study, we applied *JuSpace*, a toolbox able to explore if the spatial pattern of observed brain changes in the disease of interest are related to the distribution of specific neurotrasmitters pathways. Therefore, it allows to investigate, indirectly and in vivo, neurotransmitter deficits. We highlighted that different mutations responsible for genetic FTD are associated with diverse neurochemical deficits in the prodromal phase. In the second study, on the other hand, we found that glymphatic system alterations are evident in the clinical phase and constitute a possible disease progression biomarker. We applied a technique called DTI-ALPS (Diffusion tensor image analysis along the perivascular space) to investigate in vivo the glymphatic system.

Finally, the last study (*Chapter 6*) focused on functional MRI in the preclinical phase of HD. It is the result of the collaboration with the HD Center at University College London (London, UK). In this work, we demonstrated early alterations in visual networks, which predicted neurofilament concentration and the expected disease onset.

CHAPTER 1 - INTRODUCTION

Advanced neuroimaging

Structural MRI

Structural MRI is generally used for the quantitative measurements of morphological information including volume, cortical thickness and surface area. By means of volumetric T1-weighted MRI it is possible to detect changes in grey matter (GM) and white matter (WM) structure, determine volumes of specific regions of interest and the rate of atrophy. In addition, postprocessing techniques can be applied to structural images, such as investigations of whole-brain changes at voxel-level through voxel-based morphometry or measurement of cortical thickness.

Diffusion Weighted Imaging

Diffusion Weighted Imaging (DWI) investigates WM microstructure within brain tissue by using specific sequences sensitive to the motion of water molecules. Water movement in free space is isotropic, it can move in any number of directions. However, along the main axis of a WM fiber, diffusion occurs in one direction and diffusivity is anisotropic. When WM breaks down due to axonal damage or demyelination, for example, there is increased diffusion in directions other than long the axons. In theory, diffusion MRI might provide information about neuronal damage or dysfunction that precedes volumetric loss.

The most widely-studied diffusion technique in neurodegenerative diseases is Diffusion Tensor Imaging (DTI). It was introduced as a more efficient and accurate means of measuring anisotropy due to its independence of orientation within the scanner. The fractional anisotropy (FA) index captures the degree of anisotropy within a WM tract, and FA maps are derived from the estimated tensors where the brighter the voxel intensity, the greater the degree of FA. Mean diffusivity (MD), an average of diffusivity in all three directions, parallel (axial) diffusivity (AD) and perpendicular

(radial) diffusivity (RD) are also determined. Typically, reductions in DTI metrics of FA and increases in MD are seen across various neurodegenerative diseases[1–3].

DTI data can be analyzed using a whole brain or a regional/tract-based hypothesis-driven approach. Techniques such as tract-based spatial statistics (TBSS) are used to investigate changes in WM microstructure across the whole brain, while tractography examines diffusivity within specific tracts. More recently, studies have used whole-brain tractography approaches to investigate structural networks across the brain. Recent advances in diffusion acquisition and modelling techniques including the use of neurite orientation and density imaging (NODDI) methods provide the potential to improve the sensitivity of diffusion MRI measures.

Functional MRI

Functional MRI (fMRI) is used to investigate brain activity during a task (task-fMRI) or spontaneous activity occurring at rest (resting-state fMRI, rsfMRI). fMRI uses the neurovascular coupling of neuronal activity and blood flow (Blood Oxygen Level-Dependent, BOLD) to obtain an indirect measure of neuronal activity in response to performing a task or a function. Increases in brain activity cause increased metabolic activity, which leads to regional increases in blood flow (hemodynamic response). This causes a local shift in the ratio of oxygenated to deoxygenated blood, enabling the measurements of the BOLD MRI signal. Indeed, when hemoglobin becomes deoxygenated, it becomes paramagnetic relative to oxygenated hemoglobin, and as such changes in the proportion of oxyhemoglobin to deoxyhemoglobin, due to local neuronal activity, produce measurable changes in the BOLD signal. fMRI uses rapid gradient echo planar imaging (EPI) as this facilitates the acquisition of the large number of images necessary to detect the subtle changes in the BOLD signal. In the present work we focus on rsfMRI, whereas task-based fMRI is beyond the scope of our studies. rsfMRI data can be analyzed to investigate functional connectivity between brain regions at rest. Functional connectivity determines temporal correlations in activity across the brain or in specific

networks. Seed-based analyses and independent component analysis are both used to investigate whole-brain network activity. Seed-based analysis is partly hypothesis-driven looking at the correlation between activity within specific, pre-defined region and that across the rest of the brain. In choosing a specific seed region, the nature of the behavior of the associated network(s) can then be examined. Independent component analysis, alternatively, is a purely data-driven approach, whereby the signals within the fMRI data are separated into orthogonal components each of which represents a set of temporally correlated data comprising maps depicting either functional networks or noise. Finally, functional connectomics uses either a hypothesis-driven or purely data-driven approach to investigate whole-brain connectivity and is traditionally analyzed using graph theory metrics. The brain is parcellated into a number of regions using a pre-specified atlas and connections between every set of regions are calculated to produce a large connectivity matrix. Data decomposition is generally performed on these data to enable interpretation. Alternatively, empirical evidence can be used to limit the number of connections that form the basis for the analysis once the matrices have been produced.

Arterial Spin Labeling

Arterial Spin Labeling (ASL) is a technique which can produce quantitative images of perfusion. Since brain perfusion (defined as the amount of blood delivered to a unit of tissue per unit of time) is a well-known indicator of tissue metabolism and function, ASL is a promising technique to study brain function. The concept behind ASL is very similar, conceptually, to tracer injection perfusion measurements (e.g., bolus tracking MRI, PET etc.) except that, instead of injecting a tracer into the blood stream and tracking its accumulation into the tissue, the tracer consists of the blood water in the arteries itself. The tracer is created by inverting the magnetization of the blood in the arteries that feed the organ of interest with a train of radiofrequency pulses. As this “labeled” blood flows into the tissue, it reduces the available magnetization in the tissue. As a result, images collected downstream

of the labeling appear slightly darker. By subtracting the labeled images from a set of control images, it is possible to calculate the amount of blood that entered the organ since the beginning of the labeling period.

ALS is a promising technique in neurodegenerative research, since it reveals alterations in brain perfusion that correlate very well with metabolism measured with FDG-PET[4,5]. Moreover, cognitive decline is strongly associated with hypoperfusion, which can also be a predictor of conversion from mild cognitive impairment to dementia[6,7].

Advanced neuroimaging in genetic neurodegenerative diseases: an overview

Advanced neuroimaging techniques provide invaluable insights into in-vivo pathophysiology and are crucial to detect early structural and functional changes that develop many years before the clinical onset of genetic neurodegenerative diseases. Inherited conditions represent a unique opportunity to explore the presymptomatic stage in order to define the best timepoint for therapeutic interventions. Actually, mutation carriers represent the ideal target population for the development of disease-modifying therapies; thus, definying neuroimaging and biofluid biomarkers in the preclinical as well as clinical stages is a priority in order to stratify patients for clinical trials and to assess the efficacy of therapeutic interventions in this population.

The most widely-studied imaging acquisition is the structural volumetric MRI scan, with broad implications in clinical as well as research settings. As we will illustrate in this introduction, characteristic patterns of brain atrophy have been related to specific mutations, that support the differential diagnosis in clinical practice. Structural neuroimaging biomarkers appear key in the symptomatic phase, even though very early changes are detectable many decades before the disease onset. Conversely, advanced MRI methods such as DTI, fMRI and ASL are currently used in research and might be more sensitive in the earliest, presymptomatic, phase of genetic neurodegenerative diseases[8–13]. These MRI techniques have the advantage to be safe, non-invasive, repeatable, can be

combined in a single session, and do not involve radiation exposure. However, they have been investigated at a group level, and currently are not applicable in clinical practice at a single-patient level. Moreover, fMRI studies are limited by a wide variation in analytical methods used, such as independent component analysis, seed-based or region-of-interest based approaches[14]. Measures of structural connectivity derived from diffusion MRI suffer from similar pitfalls[15].

Advanced neuroimaging in genetic Frontotemporal dementia

Frontotemporal dementia (FTD) encompasses a heterogeneous group of neurodegenerative disorders with a wide range of clinical, genetic and neuropathological features[16]. The disease is characterized by progressive behavioral and personality changes, dysexecutive and language deficits. It is frequently associated with motor disturbances, such as parkinsonism or motor neuron disease. Different phenotypes have been classically defined on the basis of presenting clinical symptoms: the behavioral variant of FTD (bvFTD)[17], characterized by early behavioral and personality alterations; the agrammatic variant of primary progressive aphasia (avPPA)[18], with progressive deficits in speech, grammar and word output; the semantic variant of PPA (svPPA)[18], a progressive disorder of semantic knowledge and naming. The occurrence of associated motor symptoms, as in progressive supranuclear palsy (PSP), corticobasal syndrome (CBS) and motor neuron disease (FTD-MND) further enriches the spectrum of FTD-related disorders[19].

FTD is genetic in about a third of cases[20], with mutations in *microtubule-associated protein tau* (*MAPT*), *progranulin* (*GRN*) and *chromosome 9 open reading frame 72* (*C9orf72*) being the commonest causes[21]. The identification of FTD causative genes has represented a giant step forward to characterize the heterogeneity of the disorder, at clinical, molecular and imaging level and to explore the presymptomatic stage of the disease. Each of the most common genetic groups displays a differential and characteristic pattern of cortical atrophy [22] with early changes appearing during the prodromal disease stages, up to twenty years before phenoconversion [23,24]. These results have been made possible by well-established international networks such as the European and Canadian based Genetic Frontotemporal dementia Initiative (GENFI), the US based ARTFL/LEFFTDS, and the Australian DINAD, which have collected cross-sectional and longitudinal data of FTD patients with monogenic disease [23,25]. In addition, the recently established consortia in Latin America (ReDLat) and New Zealand (FTDGeNZ) will be able to further elucidate the natural history of the disease [26,27].

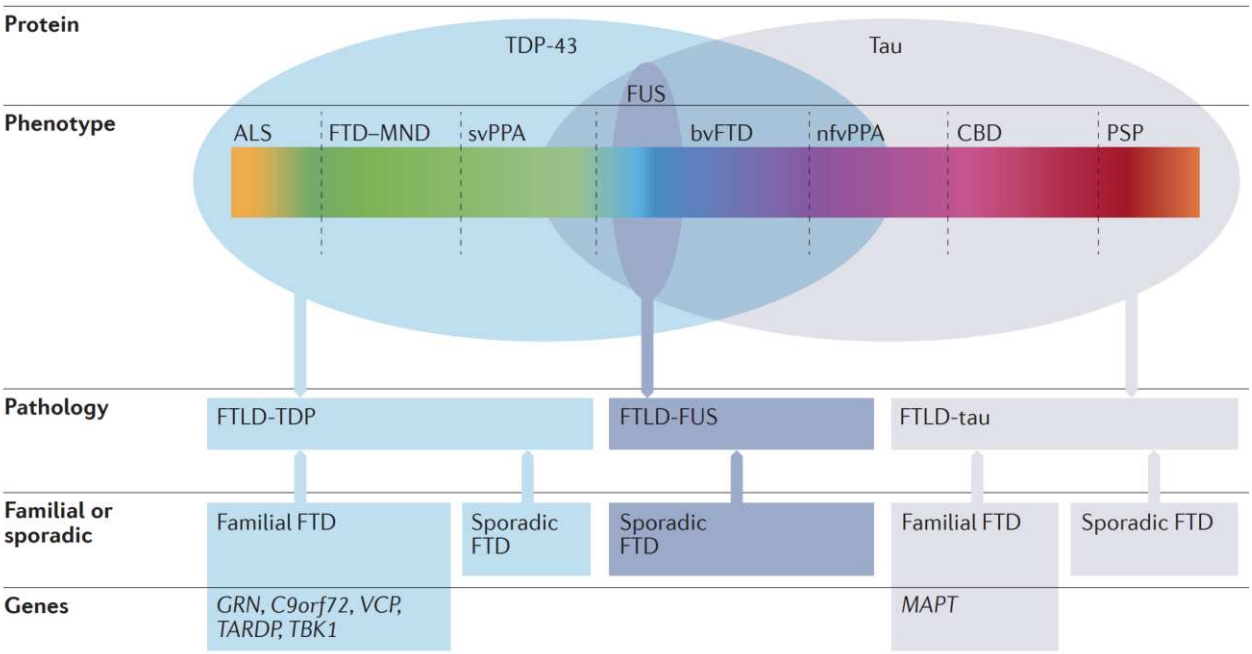

Figure 1. Clinical, pathological and genetic heterogeneity of FTD. Genetic forms of Frontotemporal dementia (FTD) have predictable pathology: GRN mutations and C9orf72 repeat expansions result in TDP-43 pathology, whereas MAPT mutations result in tau pathology. bvFTD = behavioral variant FTD; nfvPPA = non-fluent variant of Primary Progressive Aphasia; svPPA = semantic variant of Primary Progressive Aphasia; CBD = corticobasal degeneration; PSP = progressive supranuclear palsy; ALS = amyotrophic lateral sclerosis; FTD-MND = Frontotemporal dementia-Amyotrophic lateral sclerosis; TDP-43 = transactive response DNA-binding protein 43. FUS = RNA-binding protein FUS. *Adapted from Meeter et al, Nat Rev Neurol 2017.*

Presymptomatic genetic Frontotemporal dementia

Individuals with FTD-associated mutations develop GM atrophy and hypometabolism at least ten years before symptom onset, whereas WM abnormalities and functional connectivity alterations are seen even earlier, supporting the hypothesis of FTD as a network-based disease. Therefore, DTI and fMRI seem the most promising techniques to explore presymptomatic stages, with a greater sensitivity than structural MRI [9–11,28–30]. Traditionally, brain networks have been regarded as static over time. However, a recently introduced evolution of the brain connectome, the so-called chronnectome, allows to capture the dynamic functioning of the brain across time [31–33]. This approach has been demonstrated to be even more sensitive than traditional resting state fMRI approaches in

presymptomatic phases [34,35]. ASL MRI is also a promising non-invasive imaging biomarker in presymptomatic carriers. Indeed, cerebral blood flow differences appeared earlier than 10 years before the expected onset in key FTD regions in the GENFI cohort [13].

The different genetic groups, such as *GRN, C9orf72* and *MAPT* mutations, are characterized by variability in both timing and location of early GM and WM changes. In *C9orf72* mutation carriers GM and WM alterations appear very early, up to 30 years before symptoms onset. Atrophy begins at least 25 years before symptom onset in subcortical areas, including the thalamus, then involves the insula and the occipital cortex. After that, 10-20 years before expected onset, the pathology becomes evident in the frontal and temporal lobes and subsequently in the cerebellum[23]. WM deficits appear earlier than GM changes; they are detected by means of DTI at least 20 years before onset, particularly posteriorly initially[36–39]. During the presymptomatic stage, intrinsic connectivity network alterations are described in the Salience Network (SN), sensorimotor and Default Mode Network (DMN) and to the medial pulvinar, and these abnormalities are evident as early as the third decade of life[40].

GRN mutation carriers show no or only minimal atrophy in presymptomatic stage, thus representing the most challenging group to investigate in these disease stage. In studies including large cohorts, GM differences between carriers and non-carriers appeared in the insula at 15 years before expected onset, then in the temporal and parietal lobes at 10 years before expected onset, finally the striatum at 5 years before expected onset[23,24]. Prominent asymmetry was found in atrophy at 5 years before expected symptom onset[23]. DTI studies showed contrasting results in these patients. Some works demonstrated WM involvement of the same tracts affected during the disease stage, including the superior longitudinal and uncinate fasciculi, the corticospinal tract and the anterior corpus callosum[8,41]. Alterations might become evident 10 years before symptom onset. On the other hand, other studies failed to demonstrate DTI alterations[9,39]. In *GRN* mutation carriers, rsfMRI appears the most promising technique in detecting early changes. The first studies explored SN and DMN, which show prominent alterations in patients with sporadic FTD. For the SN, an increased functional connectivity was found in 9 presymptomatic *GRN* mutation carriers[10], while another study of 27

presymptomatic *GRN* mutation carriers revealed connectivity disruption of an anterior midcingulate seed region and parietal regions including precuneus, posterior cingulate and lateral parietal cortex[9]. These studies did not show DMN differences in presymptomatic carriers compared to HC. On the other hand, a study of 5 carriers showed no differences within functional networks[28]. Lee et al showed that presymptomatic carriers have hyperconnectivity within the four networks that correspond to the most common clinical syndromes reported during the symptomatic stage of *GRN*, namely the SN for bvFTD, a left frontal opercular network (avPPA), a perirolandic network (CBS), and the DMN for Alzheimer's Disease[42]. Thalamic hyperconnectivity was a common feature in all four cases. A recent GENFI study investigated spatial network configurations and their dynamic changes over time, the so-called spatial chronnectome, in a large population of *GRN* mutation carriers[43]. The authors considered the SN, the DMN and the language network, and found that carriers spent more time in networks' spatial configurations involving the insula and parietal lobe. These alterations correlated significantly with the expected age at onset and with cognitive tests.

Studies in presymptomatic *MAPT* mutation carriers showed contrasting results, probably because of the differences in cohort size and subject heterogeneity[30,39,44,45]. The largest study at present found volume loss in hippocampus and amygdala at 15 years before expected onset, temporal lobe at 10 years before expected onset and insula at 5 years before expected onset[23]. WM deficits might precede structural abnormalities, appearing 20-30 years before estimate onset. Frontotemporal tracts such as the uncinate fasciculus and parahippocampal cingulum bundle demonstrate the earliest involvement[9,38]. fMRI studies showed contrasting results, probably because of small cohorts[9,30].

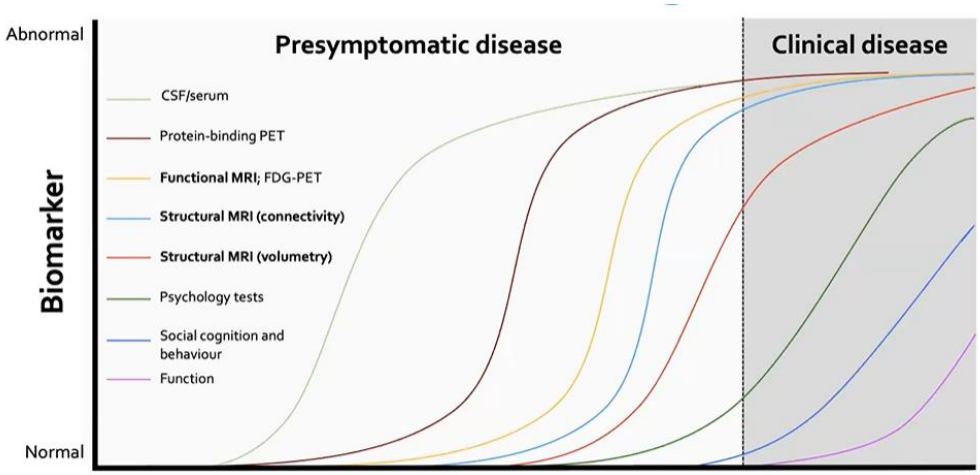

Figure 2. Disease progression model of genetic FTD. Alterations of fluid and neuroimaging biomarkers and clinical assessment in genetic Frontotemporal dementia (FTD) from the presymptomatic to the clinical stages. *Adapted from Prof Rohrer.*

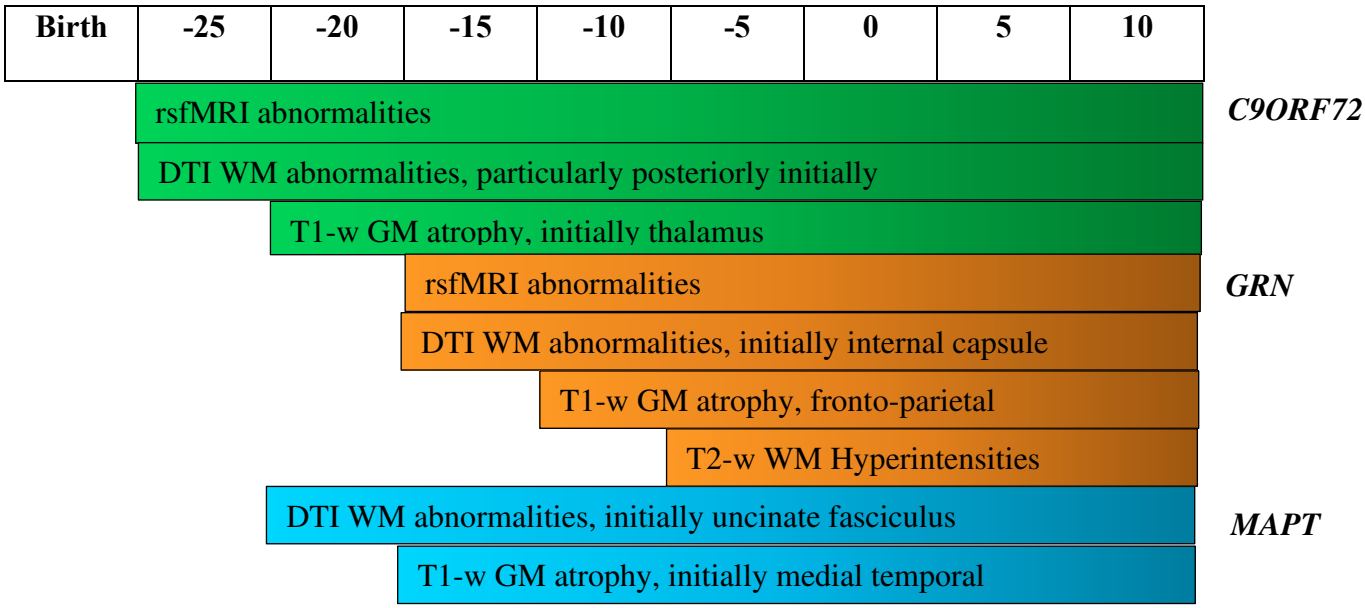

Figure 3. **Imaging biomarkers profiles across the lifespan of C9orf72, GRN and MAPT.** RsfMRI = resting state functional MRI; DTI = Diffusion Tensor Imaging; T1-w = T1-weighted; GM = grey matter. *Adapted from Graeves and Rohrer, J Neurol 2019.*

Symptomatic genetic Frontotemporal dementia

Symptomatic stages of the disease can be investigated accurately with structural MRI. Comparable atrophy for all three mutation groups was observed in a network involving the insula, orbitofrontal lobe and anterior cingulate. Beside these areas, each mutation group develops a characteristic pattern of cortical atrophy[24]. *C9orf72* mutation carriers present atrophy symmetrically involving dorsolateral, medial and orbitofrontal lobes. Anterior temporal lobes, thalamus, parietal and occipital lobes and cerebellum are also affected [23,24,46–52]. Cases of patients with mild, slowly progressive or even severe dementia with minimal or no atrophy have been reported [47,53,54]. Interestingly, a comparable pattern of functional network alterations despite various atrophy patterns have been described in *C9orf72* expansion carriers. In particular, they are characterized by reduced connectivity in the salience network and sensorimotor networks, whereas default mode network connectivity is similar to HC, unlike sporadic FTD [40].

GRN mutations carriers display a characteristic striking asymmetrical atrophy involving frontotemporal but also parietal cortices [23,24,46,51,55–57]. Both left- and right-sided predominant atrophy can be observed, even in the same family. *GRN* mutation carriers can present WM hyperintensities, even in the presymptomatic stages, that might be due to microglial activation and microglial dystrophy [58–62].

The distribution of atrophy in patients with *MAPT* mutation symmetrically involves the anterior and mesial temporal lobes, whereas orbitofrontal, lateral prefrontal and parietal regions are less altered [23,24,46,51,55]. A differential involvement of the temporal lobe has been described according to the diverse mutations in the *MAPT* gene [55].

Rate of atrophy varies in the different forms of genetic FTD. It is faster in those with *GRN* mutations and slower in *MAPT* mutation carriers. *C9orf72* mutation carriers show the greatest heterogeneity in the progression of brain atrophy [63,64]. In *GRN* mutation carriers, after clinical onset, the rate of atrophy

is greater in the temporal cortex and becomes more asymmetrical in the following stages of the disease [23].

Besides the most frequent mutations, more rare pathogenic mutations are associated with genetic FTD. At present, neuroimaging findings in these patients are described in case reports or in limited number of cases and future international studies with larger cohorts are warranted in this field.

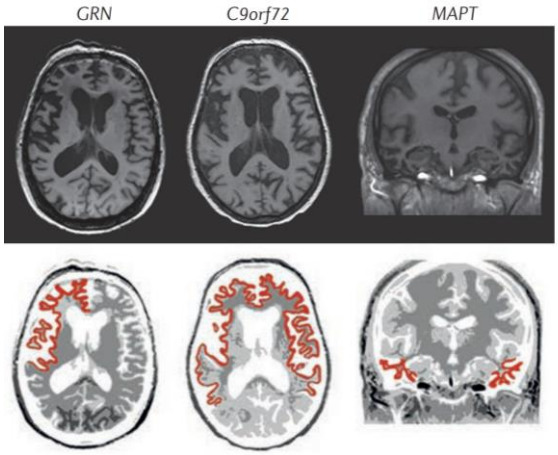

Figure 4. Grey matter atrophy in genetic FTD. Characteristic patterns of grey matter atrophy (in red) in different genetic subtypes of FTD. Patients with *GRN* mutations often exhibit asymmetrical frontotemporoparietal atrophy. Patients with a *C9orf72* repeat expansion present mostly with a generalized symmetrical atrophy. Patients with *MAPT* mutations exhibit marked symmetrical temporal atrophy. *Adapted from Meeter et al, Nat Rev Neurol 2017.*

Advanced neuroimaging in Huntington's disease

Huntington's disease (HD) is an inherited, autosomal dominant, neurodegenerative disorder, characterized by progressive cognitive impairment, psychiatric features and movement disorders[65]. It is caused by a CAG trinucleotide repeat expansion in exon 1 of huntingtin gene (*HTT*) on chromosome 4. This is translated into full length mutant huntingtin protein (mHTT) with an expanded polyglutamine stretch, which is toxic to neurons.

The monogenic nature of HD means that we have the unique opportunity to study the disease well before it manifests in gene carriers, with broad implications for biomarkers research and therapeutic development. Studies of premanifest populations have used models that utilize the positive association of CAG repeat length and age of disease onset to stratify groups in terms of proximity to disease onset[66,67]. For example, the disease burden score is a function of age and CAG repeat length that provides a proxy measure to lifetime toxic mHTT load[66]. To date, biomarker research has included small-scale studies as well as large international studies including TRACK-HD[68,69] and PREDICT-HD[70,71], which have provided the opportunity to study many potential neuroimaging biomarkers for HD in well-defined cohorts.

Premanifest Huntington's disease

The gradual loss of medium spiny GABAergic neurons of the caudate and putamen is the neuropathologic hallmark of HD[72]. Atrophy of the caudate and putamen can be detected from 15 to 20 years before the expected disease onset in neuroimaging studies, and this atrophy generally increases from one stage to the next[68,70,73,74]. Caudate and putamen are the imaging biomarkers to show atrophy the earliest, thus have been introduced as biomarker of neurodegeneration in the recently developed HD Integrated Staging System[75], which has profound implications in clinical research. Putamen volume reduction was documented even in a cohort of premanifest HD (preHD) subjects very far from expected onset (approximately 24 years), whereas caudate volume was not

significantly different compared to controls[76]. Longitudinal rates of atrophy in preHD are elevated; estimates of annual rates of change vary between studies but suggest atrophy of up to 4% and 3% per year in the caudate and putamen, respectively[77].

Two large longitudinal studies, TRACK-HD and PREDICT-HD, found that baseline striatal volume and atrophy rates predicted conversion to manifest HD, suggesting that these are promising biomarkers in clinical trials[73,78,79]. Striatal measures correlate with measures of disease burden and with clinical outcomes of disease progression. In particular, striatal atrophy shows significant correlations with UHDRS total motor score[79,80]; caudate volume reduction is related to deficits in verbal learning, working memory and emotion recognition, whereas putamen atrophy is associated with executive functions and emotion recognition[79,81,82].

Atrophy in preHD is described not only in the striatum, but is more widespread. For example, whole brain and grey matter volume has been shown to be reduced cross-sectionally[68,80] and longitudinally from the premanifest stages[69,83,84], even though the effect sizes are smaller compared to striatal and white matter measures. A previous work suggested that striatal and white matter loss occur early in the disease prior to symptom manifestation and that there is an acceleration of grey matter loss around the time of clinical conversion[84]. It would appear that, although there is some localized cortical involvement in preHD, e.g. in the occipital lobe, it is at the time of disease onset that pathology becomes more widespread throughout the cortex.

In agreement with early histopathology studies, neuroimaging shows that while the striatum is the first brain area to be affected by the HD mutation, neuronal loss soon spreads to the WM during premanifest stages. Both TRACK-HD and PREDICT-HD found progressive WM atrophy in preHD[69,74,85], that correlates with motor function[74,80,86,87], cognitive function[80,87,88] and total functional capacity[89,90]. Many studies pointed to increasing disorganization of WM microstructure in HD, with a reduction in FA, an increase in RD from the premanifest stage and an increase in AD as the disease progresses[91–95]. During the premanifest HD stages, microstructural WM alterations follow a centrifugal pattern, beginning in the basal ganglia[90,96,97] and deep white matter[98], then extending to

more superficial areas[92,99]. In cross-sectional studies, diffusion metric alterations have been demonstrated in premanifest HD, in particular in the corpus callosum, internal capsule and thalamic radiations[92,100–102].

Emerging findings suggest that functional imaging might detect alterations in preHD before structural brain damage[103–107]. Moreover, functional imaging findings could shed light into the spatiotemporal spreading of brain alteration in HD, unraveling detrimental and compensatory mechanisms that could pave the way to new interventions. Many studies suggest a decrease in somatomotor network functional connectivity in preHD[108–110], associated with worse motor[109] and cognitive abilities[108]. Emerging evidence supports an early involvement of posterior connectivity. Dumas and colleagues demonstrated a decrease in visual network connectivity[111]. McColgan and Gregory found an anterior-posterior dissociation in preHD, with increased connectivity in anterior regions and a decrease in posterior regions[112]. Interestingly, in a cohort of preHD very far from disease onset, posterior connectivity was associated with the concentration of neurofilament light in cerebrospinal fluid[107]. On the other hand, results concerning the involvement of executive, DMN and subcortical networks during the premanifest stages are nonconclusive.[109,111,113,114]

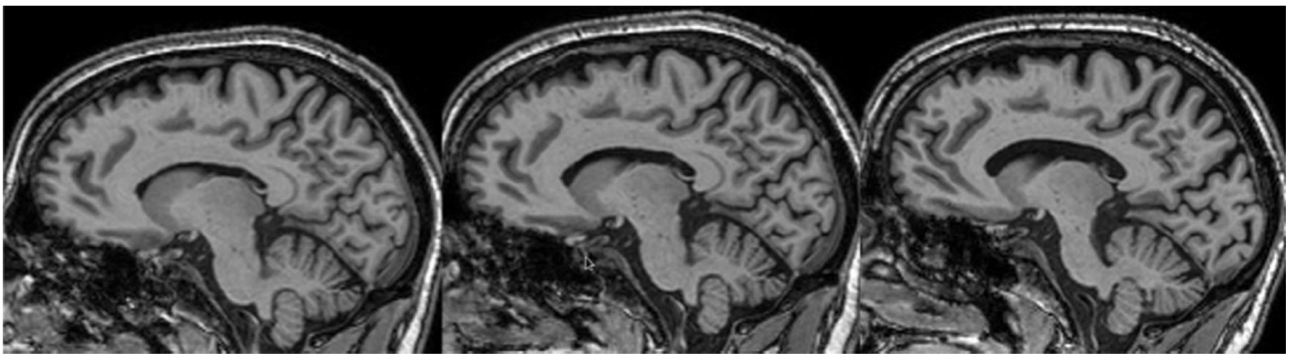

Figure 5. Longitudinal grey matter changes in HD. T1-weighted MRI scans of a gene carrier aged (left to right) 51, 54 (premanifest) and 57 (early HD) showing progressive caudate volume loss later accompanied by cortical atrophy. *Reproduced from Scahill et al, Hand Clin Neurol 2017.*

Symptomatic Huntington's disease

After the clinical onset, atrophy becomes more evident and is widespread throughout the brain. Atrophy of the basal ganglia is well-documented in manifest HD[68,115–117]. Other subcortical structures, such as the globus pallidus, nucleus accumbens, the cingulate, thalamus and hippocampus, show significant volume loss compared to controls. Significant correlations between total motor score and volumetric measures of the subcortical structures have been demonstrated[80,118–120]. In early manifest HD, total grey matter volume at baseline significantly predicted the decline in total functional capacity[73], thus suggesting it might be explored as prognostic neuroimaging biomarker.

Cortical involvement becomes much more widespread after phenoconversion[68]. Interestingly, the topography of cortical thinning is associated with clinical phenotype, thus explaining much clinical heterogeneity observed in HD[121]. Moreover, cortical thinning is associated with progressive functional decline, as measured by the total function capacity[121]; therefore, it is a potential biomarker of disease progression.

Diffusion metric changes become widespread as well, involving the frontal, parietal and occipital white matter[90,122]. DTI alterations are correlated with a number of clinical measures, including total motor score, finger tapping, executive functions[91], apathy[123] and depression[124].

Functional connectivity alterations become more global during the manifest stage. Several studies reported aberrant sensorimotor network increased connectivity[97,125,126], which correlated with worse motor functions[125,126] and impaired cognitive abilities[97]. On the other hand, visual network is characterized by reduced connectivity, which was related to worse visuomotor cognition and higher disease burden scores[111,127]. Executive network displays a divergent pattern, showing decreased connectivity in parietal and subcortical structures and increased connectivity in the frontal cortex. Finally, contrasting results have been reported on DMN and subcortical networks, with increased or decreased connectivity[109,125,126,128–130], and further studies are warranted in this field.

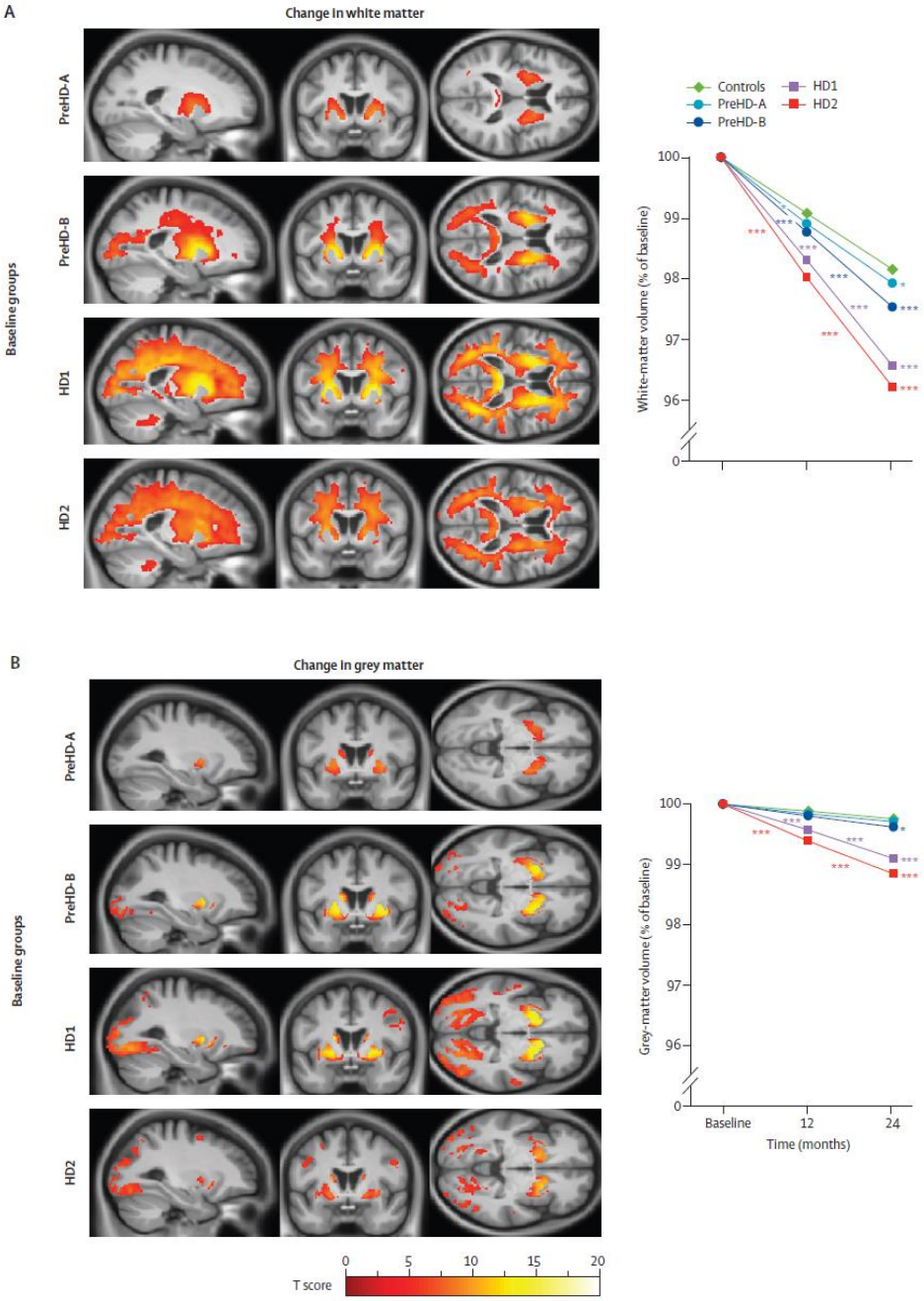

Figure 6. Longitudinal changes in grey and white matter in premanifest and early manifest HD. Parametric maps from the TRACK-HD study showing regions with statistically significant atrophy in (A) white matter and (B) grey matter over 24 months, relative to controls. Corresponding longitudinal plots show mean values at baseline, 12 months and 24 months. Significant change differences relative to controls over 0-12, 12-24, and 0-24 months are represented by *p < 0.05, **p < 0.01 and ***p 0.001. Individuals in the premanifest group were divided in preHD-A (> 10.8 years from predicted onset) and preHD-B (< 10.8 years from predicted onset). Patients with early HD were divided into two subgroups (HD1 and HD 2) on the basis of their score on the total functional capacity scale. *Reproduced from Tabrizi et al, Lancet Neurology 2012.*

References

1. Zhang Y, Schuff N, Du A-T, et al. White matter damage in frontotemporal dementia and Alzheimer's disease measured by diffusion MRI. *A J Neurol*. doi:10.1093/brain/awp071
2. Atkinson-Clement C, Pinto S, Eusebio A, Coulon O. Diffusion tensor imaging in Parkinson's disease: Review and meta-analysis. *Neuroimage (Amst)*. 2017;16:98. doi:10.1016/J.NICL.2017.07.011
3. Slattery CF, Zhang J, Paterson RW, et al. ApoE influences regional white-matter axonal density loss in Alzheimer's disease. *Neurobiol Aging*. 2017;57:8-17. doi:10.1016/J.NEUROBIOLAGING.2017.04.021
4. Verfaillie SCJ, Adriaanse SM, Binnewijzend MAA, et al. Cerebral perfusion and glucose metabolism in Alzheimer's disease and frontotemporal dementia: two sides of the same coin? *Eur Radiol*. 2015;25(10):3050-3059. doi:10.1007/S00330-015-3696-1
5. Tosun D, Schuff N, Rabinovici GD, et al. Diagnostic utility of ASL-MRI and FDG-PET in the behavioral variant of FTD and AD. *Ann Clin Transl Neurol*. 2016;3(10):740-751. doi:10.1002/ACN3.330
6. Chao LL, Buckley ST, Kornak J, et al. ASL perfusion MRI predicts cognitive decline and conversion from MCI to dementia. *Alzheimer Dis Assoc Disord*. 2010;24(1):19-27. doi:10.1097/WAD.0B013E3181B4F736
7. Wierenga CE, Hays CC, Zlatar ZZ. Cerebral Blood Flow Measured by Arterial Spin Labeling MRI as a Preclinical Marker of Alzheimer's Disease. *J Alzheimers Dis*. 2014;42(Suppl 4):S411. doi:10.3233/JAD-141467
8. Borroni B, Alberici A, Premi E, et al. Brain magnetic resonance imaging structural changes in a pedigree of asymptomatic progranulin mutation carriers. *Rejuvenation Res*. 2008;11(3):585-595. doi:10.1089/REJ.2007.0623
9. Dopper EGP, Rombouts SARB, Jiskoot LC, et al. Structural and functional brain

connectivity in presymptomatic familial frontotemporal dementia. *Neurology*. 2014;83(2). doi:10.1212/WNL.0000000000000583

10. Borroni B, Alberici A, Cercignani M, et al. Granulin mutation drives brain damage and reorganization from preclinical to symptomatic FTLD. *NBA*. 2012;33(10):2506-2520. doi:10.1016/j.neurobiolaging.2011.10.031
11. Lee SE, Sias AC, Kosik EL, et al. Thalamo-cortical network hyperconnectivity in preclinical progranulin mutation carriers. *NeuroImage Clin*. 2019;22. doi:10.1016/J.NICL.2019.101751
12. Alexander C, Zeithamova D, Hsiung GYR, Mackenzie IR, Jacova C. Decreased Prefrontal Activation during Matrix Reasoning in Predementia Progranulin Mutation Carriers. *J Alzheimers Dis*. 2018;62(2):583-589. doi:10.3233/JAD-170716
13. Mutsaerts HJMM, Mirza SS, Petr J, et al. Cerebral perfusion changes in presymptomatic genetic frontotemporal dementia: a GENFI study. *Brain*. 2019;142(4):1108-1120. doi:10.1093/BRAIN/AWZ039
14. Hohenfeld C, Werner CJ, Reetz K. Resting-state connectivity in neurodegenerative disorders: Is there potential for an imaging biomarker? *NeuroImage Clin*. 2018;18:849-870. doi:10.1016/J.NICL.2018.03.013
15. Farquharson S, Tournier JD, Calamante F, et al. White matter fiber tractography: why we need to move beyond DTI. *J Neurosurg*. 2013;118(6):1367-1377. doi:10.3171/2013.2.JNS121294
16. Bang J, Spina S, Miller BL. Frontotemporal dementia. *Lancet (London, England)*. 2015;386(10004):1672-1682. doi:10.1016/S0140-6736(15)00461-4
17. Rascovsky K, Hodges JR, Knopman D, et al. behavioural variant of frontotemporal dementia. Published online 2011:2456-2477. doi:10.1093/brain/awr179
18. Gorno-Tempini ML, Hillis AE, Weintraub S, et al. Classification of primary progressive aphasia and its variants. *Neurology*. 2011;76(11):1006-1014. doi:10.1212/WNL.0B013E31821103E6

19. Borroni B, Benussi A. Recent advances in understanding frontotemporal degeneration. *F1000Research*. 2019;8. doi:10.12688/F1000RESEARCH.20330.1

20. Rohrer JD, Guerreiro R, Vandrovcova J, et al. The heritability and genetics of frontotemporal lobar degeneration. *Neurology*. 2009;73(18):1451. doi:10.1212/WNL.0B013E3181BF997A

21. Borroni B, Padovani A. Dementia: a new algorithm for molecular diagnostics in FTLD. *Nat Rev Neurol*. 2013;9(5):241-242. doi:10.1038/NRNEUROL.2013.72

22. Chen Q, Kantarci K. Imaging Biomarkers for Neurodegeneration in Presymptomatic Familial Frontotemporal Lobar Degeneration. *Front Neurol*. 2020;11. doi:10.3389/FNEUR.2020.00080

23. Rohrer JD, Nicholas JM, Cash DM, et al. Presymptomatic cognitive and neuroanatomical changes in genetic frontotemporal dementia in the Genetic Frontotemporal dementia Initiative (GENFI) study: a cross-sectional analysis. *Lancet Neurol*. 2015;14(3):253-262. doi:10.1016/S1474-4422(14)70324-2

24. Cash DM, Bocchetta M, Thomas DL, et al. Patterns of gray matter atrophy in genetic frontotemporal dementia: results from the GENFI study. *Neurobiol Aging*. 2018;62:191-196. doi:10.1016/J.NEUROBIOLAGING.2017.10.008

25. Moore KM, Nicholas J, Grossman M, et al. Age at symptom onset and death and disease duration in genetic frontotemporal dementia: an international retrospective cohort study. *Lancet Neurol*. 2020;19(2):145-156. doi:10.1016/S1474-4422(19)30394-1

26. Ibanez A, Yokoyama JS, Possin KL, et al. The Multi-Partner Consortium to Expand Dementia Research in Latin America (ReDLat): Driving Multicentric Research and Implementation Science. *Front Neurol*. 2021;12. doi:10.3389/FNEUR.2021.631722

27. Ryan B, Baker A, Ilse C, et al. Diagnosing pre-clinical dementia: the NZ Genetic Frontotemporal Dementia Study (FTDGeNZ). *N Z Med J*. 2018;131(1476):88-91. Accessed September 1, 2022. https://pubmed.ncbi.nlm.nih.gov/29879731/

28. Pievani M, Paternicò D, Benussi L, et al. Pattern of structural and functional brain

abnormalities in asymptomatic granulin mutation carriers. *Alzheimers Dement*. 2014;10(5 Suppl):S354-S363.e1. doi:10.1016/J.JALZ.2013.09.009

29. Premi E, Cauda F, Costa T, et al. Looking for Neuroimaging Markers in Frontotemporal Lobar Degeneration Clinical Trials: A Multi-Voxel Pattern Analysis Study in Granulin Disease. *J Alzheimers Dis*. 2016;51(1):249-262. doi:10.3233/JAD-150340

30. Whitwell JL, Josephs KA, Avula R, et al. Altered functional connectivity in asymptomatic MAPT subjects: a comparison to bvFTD. *Neurology*. 2011;77(9):866-874. doi:10.1212/WNL.0B013E31822C61F2

31. Allen EA, Damaraju E, Plis SM, Erhardt EB, Eichele T, Calhoun VD. Tracking whole-brain connectivity dynamics in the resting state. *Cereb Cortex*. 2014;24(3):663-676. doi:10.1093/CERCOR/BHS352

32. Calhoun VD, Miller R, Pearlson G, Adali T. The chronnectome: time-varying connectivity networks as the next frontier in fMRI data discovery. *Neuron*. 2014;84(2):262-274. doi:10.1016/J.NEURON.2014.10.015

33. Chang C, Glover GH. Time-frequency dynamics of resting-state brain connectivity measured with fMRI. *Neuroimage*. 2010;50(1):81-98. doi:10.1016/J.NEUROIMAGE.2009.12.011

34. Premi E, Calhoun VD, Diano M, et al. The inner fluctuations of the brain in presymptomatic Frontotemporal Dementia: The chronnectome fingerprint. *Neuroimage*. 2019;189:645-654. doi:10.1016/J.NEUROIMAGE.2019.01.080

35. Premi E, Giunta M, Iraji A, et al. Dissemination in time and space in presymptomatic granulin mutation carriers: a GENFI spatial chronnectome study. *Neurobiol Aging*. 2021;108:155-167. doi:10.1016/J.NEUROBIOLAGING.2021.09.001

36. Bertrand A, Wen J, Rinaldi D, et al. Early Cognitive, Structural, and Microstructural Changes in Presymptomatic C9orf72 Carriers Younger Than 40 Years. *JAMA Neurol*. 2018;75(2):236-245. doi:10.1001/JAMANEUROL.2017.4266

37. Papma JM, Jiskoot LC, Panman JL, et al. Cognition and gray and white matter characteristics

of presymptomatic C9orf72 repeat expansion. *Neurology*. 2017;89(12):1256-1264. doi:10.1212/WNL.0000000000004393

38. Jiskoot LC, Bocchetta M, Nicholas JM, et al. Presymptomatic white matter integrity loss in familial frontotemporal dementia in the GENFI cohort: A cross-sectional diffusion tensor imaging study. *Ann Clin Transl Neurol*. 2018;5(9):1025-1036. doi:10.1002/ACN3.601

39. Panman JL, Jiskoot LC, Bouts MJRJ, et al. Gray and white matter changes in presymptomatic genetic frontotemporal dementia: a longitudinal MRI study. *Neurobiol Aging*. 2019;76:115-124. doi:10.1016/J.NEUROBIOLAGING.2018.12.017

40. Lee SE, Khazenzon AM, Trujillo AJ, et al. Altered network connectivity in frontotemporal dementia with C9orf72 hexanucleotide repeat expansion. *Brain*. 2014;137(Pt 11):3047-3060. doi:10.1093/BRAIN/AWU248

41. Olm CA, McMillan CT, Irwin DJ, et al. Longitudinal structural gray matter and white matter MRI changes in presymptomatic progranulin mutation carriers. *NeuroImage Clin*. 2018;19:497-506. doi:10.1016/J.NICL.2018.05.017

42. Lee SE, Sias AC, Kosik EL, et al. NeuroImage : Clinical Thalamo-cortical network hyperconnectivity in preclinical progranulin mutation carriers. *NeuroImage Clin*. 2019;22(March):101751. doi:10.1016/j.nicl.2019.101751

43. Premi E, Giunta M, Iraji A, et al. Dissemination in time and space in presymptomatic granulin mutation carriers: a GENFI spatial chronnectome study. *Neurobiol Aging*. 2021;108:155-167. doi:10.1016/j.neurobiolaging.2021.09.001

44. Domínguez-Vivero C, Wu L, Lee S, et al. Structural Brain Changes in Pre-Clinical FTD MAPT Mutation Carriers. *J Alzheimers Dis*. 2020;75(2):595-606. doi:10.3233/JAD-190820

45. Olney NT, Ong E, Goh SYM, et al. Clinical and volumetric changes with increasing functional impairment in familial frontotemporal lobar degeneration. *Alzheimers Dement*. 2020;16(1):49-59. doi:10.1016/J.JALZ.2019.08.196

46. Whitwell JL, Weigand SD, Boeve BF, et al. Neuroimaging signatures of frontotemporal

dementia genetics: C9ORF72, tau, progranulin and sporadics. *Brain*. 2012;135(Pt 3):794-806. doi:10.1093/BRAIN/AWS001

47. Boeve BF, Boylan KB, Graff-Radford NR, et al. Characterization of frontotemporal dementia and/or amyotrophic lateral sclerosis associated with the GGGGCC repeat expansion in C9ORF72. *Brain*. 2012;135(Pt 3):765-783. doi:10.1093/BRAIN/AWS004

48. Irwin DJ, McMillan CT, Brettschneider J, et al. Cognitive decline and reduced survival in C9orf72 expansion frontotemporal degeneration and amyotrophic lateral sclerosis. *J Neurol Neurosurg Psychiatry*. 2013;84(2):163-169. doi:10.1136/JNNP-2012-303507

49. Mahoney CJ, Beck J, Rohrer JD, et al. Frontotemporal dementia with the C9ORF72 hexanucleotide repeat expansion: clinical, neuroanatomical and neuropathological features. *Brain*. 2012;135(Pt 3):736-750. doi:10.1093/BRAIN/AWR361

50. Sha SJ, Takada LT, Rankin KP, et al. Frontotemporal dementia due to C9ORF72 mutations: clinical and imaging features. *Neurology*. 2012;79(10):1002-1011. doi:10.1212/WNL.0B013E318268452E

51. Rohrer JD, Lashley T, Schott JM, et al. Clinical and neuroanatomical signatures of tissue pathology in frontotemporal lobar degeneration. *Brain*. 2011;134(Pt 9):2565-2581. doi:10.1093/BRAIN/AWR198

52. Bocchetta M, Todd EG, Peakman G, et al. Differential early subcortical involvement in genetic FTD within the GENFI cohort. *NeuroImage Clin*. 2021;30. doi:10.1016/J.NICL.2021.102646

53. Devenney E, Hornberger M, Irish M, et al. Frontotemporal dementia associated with the C9ORF72 mutation: a unique clinical profile. *JAMA Neurol*. 2014;71(3):331-339. doi:10.1001/JAMANEUROL.2013.6002

54. Khan BK, Yokoyama JS, Takada LT, et al. Atypical, slowly progressive behavioural variant frontotemporal dementia associated with C9ORF72 hexanucleotide expansion. *J Neurol Neurosurg Psychiatry*. 2012;83(4):358-364. doi:10.1136/JNNP-2011-301883

55. Josephs KA, Whitwell JL, Jack CR, et al. Voxel-based morphometry patterns of atrophy in FTLD with mutations in MAPT or PGRN. *Neurology*. 2009;72(9):813-820. doi:10.1212/01.WNL.0000343851.46573.67

56. Le Ber I, Camuzat A, Hannequin D, et al. Phenotype variability in progranulin mutation carriers: a clinical, neuropsychological, imaging and genetic study. *Brain*. 2008;131(Pt 3):732-746. doi:10.1093/BRAIN/AWN012

57. Beck J, Rohrer JD, Campbell T, et al. A distinct clinical, neuropsychological and radiological phenotype is associated with progranulin gene mutations in a large UK series. *Brain*. 2008;131(Pt 3):706-720. doi:10.1093/BRAIN/AWM320

58. Ameur F, Colliot O, Caroppo P, et al. White matter lesions in FTLD: distinct phenotypes characterize GRN and C9ORF72 mutations. *Neurol Genet*. 2016;2(1). doi:10.1212/NXG.0000000000000047

59. Paternicò D, Premi E, Gazzina S, et al. Neurobiology of Aging White matter hyperintensities characterize monogenic frontotemporal dementia with granulin mutations. *Neurobiol Aging*. 2016;38:176-180. doi:10.1016/j.neurobiolaging.2015.11.011

60. Sudre CH, Bocchetta M, Cash D, et al. White matter hyperintensities are seen only in GRN mutation carriers in the GENFI cohort. *NeuroImage Clin*. 2017;15:171-180. doi:10.1016/J.NICL.2017.04.015

61. Sudre CH, Bocchetta M, Heller C, et al. White matter hyperintensities in progranulin-associated frontotemporal dementia: A longitudinal GENFI study. *NeuroImage Clin*. 2019;24. doi:10.1016/J.NICL.2019.102077

62. Woollacott IOCC, Bocchetta M, Sudre CH, et al. Pathological correlates of white matter hyperintensities in a case of progranulin mutation associated frontotemporal dementia. *Neurocase*. 2018;24(3):166-174. doi:10.1080/13554794.2018.1506039

63. Whitwell JL, Weigand SD, Gunter JL, et al. Trajectories of brain and hippocampal atrophy in FTD with mutations in MAPT or GRN. *Neurology*. 2011;77(4):393-398.

doi:10.1212/WNL.0B013E318227047F

64. Whitwell JL, Boeve BF, Weigand SD, et al. Brain atrophy over time in genetic and sporadic frontotemporal dementia: a study of 198 serial magnetic resonance images. *Eur J Neurol*. 2015;22(5):745-752. doi:10.1111/ENE.12675

65. Tabrizi SJ, Wild EJ. Huntington disease: new insights into molecular pathogenesis and therapeutic opportunities. *Nat Rev Neurol*. doi:10.1038/s41582-020-0389-4

66. Penney JB, Vonsattel JP, MacDonald ME, Gusella JF, Myers RH. CAG repeat number governs the development rate of pathology in Huntington's disease. *Ann Neurol*. 1997;41(5):689-692. doi:10.1002/ANA.410410521

67. Langbehn DR, Brinkman RR, Falush D, Paulsen JS, Hayden MR. A new model for prediction of the age of onset and penetrance for Huntington's disease based on CAG length. *Clin Genet*. 2004;65(4):267-277. doi:10.1111/J.1399-0004.2004.00241.X

68. Tabrizi SJ, Langbehn DR, Leavitt BR, et al. Biological and clinical manifestations of Huntington's disease in the longitudinal TRACK-HD study: cross-sectional analysis of baseline data. *Lancet Neurol*. 2009;8(9):791-801. doi:10.1016/S1474-4422(09)70170-X

69. Tabrizi SJ, Scahill RI, Durr A, et al. Biological and clinical changes in premanifest and early stage Huntington's disease in the TRACK-HD study: the 12-month longitudinal analysis. *Lancet Neurol*. 2011;10(1):31-42. doi:10.1016/S1474-4422(10)70276-3

70. Paulsen JS, Langbehn DR, Stout JC, et al. Detection of Huntington's disease decades before diagnosis: the Predict-HD study. *J Neurol Neurosurg Psychiatry*. 2008;79(8):874-880. doi:10.1136/JNNP.2007.128728

71. Paulsen JS, Ph D, Long JD, et al. imaging measures : A 12-year prospective observational study. 2015;13(12):1193-1201. doi:10.1016/S1474-4422(14)70238-8.Prediction

72. Vonsattel JPG, Keller C, Cortes Ramirez EP. Huntington's disease - neuropathology. *Handb Clin Neurol*. 2011;100:83-100. doi:10.1016/B978-0-444-52014-2.00004-5

73. Tabrizi SJ, Scahill RI, Owen G, et al. Predictors of phenotypic progression and disease onset

in premanifest and early-stage Huntington's disease in the TRACK-HD study: analysis of 36-month observational data. *Lancet Neurol*. 2013;12(7):637-649. doi:10.1016/S1474-4422(13)70088-7

74. Aylward EH, Nopoulos PC, Ross CA, et al. Longitudinal change in regional brain volumes in prodromal Huntington disease. *J Neurol Neurosurg Psychiatry*. 2011;82(4):405-410. doi:10.1136/JNNP.2010.208264

75. Tabrizi SJ, Schobel S, Gantman EC, et al. A biological classification of Huntington's disease: the Integrated Staging System. *Lancet Neurol*. 2022;21(7):632-644. doi:10.1016/S1474-4422(22)00120-X

76. Scahill RI, Zeun P, Osborne-Crowley K, et al. Biological and clinical characteristics of gene carriers far from predicted onset in the Huntington's disease Young Adult Study (HD-YAS): a cross-sectional analysis. *Lancet Neurol*. 2020;19(6):502-512. doi:10.1016/S1474-4422(20)30143-5

77. Georgiou-Karistianis N, Scahill R, Tabrizi SJ, Squitieri F, Aylward E. Structural MRI in Huntington's disease and recommendations for its potential use in clinical trials. *Neurosci Biobehav Rev*. 2013;37(3):480-490. doi:10.1016/J.NEUBIOREV.2013.01.022

78. Paulsen JS, Long JD, Ross CA, et al. Prediction of manifest Huntington's disease with clinical and imaging measures: a prospective observational study. *Lancet Neurol*. 2014;13(12):1193-1201. doi:10.1016/S1474-4422(14)70238-8

79. Aylward EH, Liu D, Nopoulos PC, et al. Striatal volume contributes to the prediction of onset of Huntington disease in incident cases. *Biol Psychiatry*. 2012;71(9):822-828. doi:10.1016/J.BIOPSYCH.2011.07.030

80. Paulsen JS, Nopoulos PC, Aylward E, et al. Striatal and white matter predictors of estimated diagnosis for Huntington disease. *Brain Res Bull*. 2010;82(3-4):201-207. doi:10.1016/J.BRAINRESBULL.2010.04.003

81. Harrington DL, Liu D, Smith MM, et al. Neuroanatomical correlates of cognitive functioning

in prodromal Huntington disease. *Brain Behav*. 2014;4(1):29-40. doi:10.1002/BRB3.185

82. Jurgens CK, Van De Wiel L, Van Es ACGM, et al. Basal ganglia volume and clinical correlates in "preclinical" Huntington's disease. *J Neurol*. 2008;255(11):1785-1791. doi:10.1007/S00415-008-0050-4

83. Kipps CM, Duggins AJ, Mahant N, Gomes L, Ashburner J, McCusker EA. Progression of structural neuropathology in preclinical Huntington's disease: a tensor based morphometry study. *J Neurol Neurosurg Psychiatry*. 2005;76(5):650-655. doi:10.1136/JNNP.2004.047993

84. Tabrizi SJ, Scahill RI, Owen G, et al. Predictors of phenotypic progression and disease onset in premanifest and early-stage Huntington's disease in the TRACK-HD study: Analysis of 36-month observational data. *Lancet Neurol*. 2013;12(7):637-649. doi:10.1016/S1474-4422(13)70088-7

85. Tabrizi SJ, Reilmann R, Roos RAC, et al. Potential endpoints for clinical trials in premanifest and early Huntington's disease in the TRACK-HD study: analysis of 24 month observational data. *Lancet Neurol*. 2012;11(1):42-53. doi:10.1016/S1474-4422(11)70263-0

86. Jech R, Klempíř J, Vymazal J, et al. Variation of selective gray and white matter atrophy in Huntington's disease. *Mov Disord*. 2007;22(12):1783-1789. doi:10.1002/MDS.21620

87. Scahill RI, Hobbs NZ, Say MJ, et al. Clinical impairment in premanifest and early Huntington's disease is associated with regionally specific atrophy. *Hum Brain Mapp*. 2013;34(3):519-529. doi:10.1002/HBM.21449

88. Beglinger LJ, Nopoulos PC, Jorge RE, et al. White matter volume and cognitive dysfunction in early Huntington's disease. *Cogn Behav Neurol*. 2005;18(2):102-107. doi:10.1097/01.WNN.0000152205.79033.73

89. Della Nave R, Ginestroni A, Tessa C, et al. Regional distribution and clinical correlates of white matter structural damage in Huntington disease: a tract-based spatial statistics study. *AJNR Am J Neuroradiol*. 2010;31(9):1675-1681. doi:10.3174/AJNR.A2128

90. Rosas HD, Tuch DS, Hevelone ND, et al. Diffusion tensor imaging in presymptomatic and

early Huntington's disease: Selective white matter pathology and its relationship to clinical measures. *Mov Disord*. 2006;21(9):1317-1325. doi:10.1002/MDS.20979

91. Poudel GR, Stout JC, Domínguez D JF, et al. White matter connectivity reflects clinical and cognitive status in Huntington's disease. *Neurobiol Dis*. 2014;65:180-187. doi:10.1016/J.NBD.2014.01.013

92. Poudel GR, Stout JC, Domínguez D. JF, et al. Longitudinal change in white matter microstructure in Huntington's disease: The IMAGE-HD study. *Neurobiol Dis*. 2015;74(1):406-412. doi:10.1016/J.NBD.2014.12.009

93. Gregory S, Scahill RI, Seunarine KK, et al. Neuropsychiatry and White Matter Microstructure in Huntington's Disease. *J Huntingtons Dis*. 2015;4(3):239-249. doi:10.3233/JHD-150160

94. Klöppel S, Draganski B, Golding C V., et al. White matter connections reflect changes in voluntary-guided saccades in pre-symptomatic Huntington's disease. *Brain*. 2008;131(Pt 1):196-204. doi:10.1093/BRAIN/AWM275

95. McColgan P, Seunarine KK, Razi A, et al. Selective vulnerability of Rich Club brain regions is an organizational principle of structural connectivity loss in Huntington's disease. *Brain*. 2015;138(Pt 11):3327-3344. doi:10.1093/BRAIN/AWV259

96. Mandelli ML, Savoiardo M, Minati L, et al. Decreased Diffusivity in the Caudate Nucleus of Presymptomatic Huntington Disease Gene Carriers: Which Explanation? *Am J Neuroradiol*. 2010;31(4):706-710. doi:10.3174/AJNR.A1891

97. Sánchez-Castañeda C, Cherubini A, Elifani F, et al. Seeking huntington disease biomarkers by multimodal, cross-sectional basal ganglia imaging. *Hum Brain Mapp*. 2013;34(7):1625-1635. doi:10.1002/HBM.22019

98. Phillips O, Squitieri F, Sanchez-Castaneda C, et al. Deep White Matter in Huntington's Disease. Published online 2014. doi:10.1371/journal.pone.0109676

99. Rosas HD, Wilkens P, Salat DH, et al. Complex spatial and temporally defined myelin and

axonal degeneration in Huntington disease. *NeuroImage Clin*. 2018;20:236-242. doi:10.1016/J.NICL.2018.01.029

100. Harrington DL, Long JD, Durgerian S, et al. Cross-Sectional and Longitudinal Multimodal Structural Imaging in Prodromal Huntington's Disease. *Mov Disord*. 2016;31(11):1664. doi:10.1002/MDS.26803

101. Stoffers D, Sheldon S, Kuperman JM, Goldstein J, Corey-Bloom J, Aron AR. Contrasting gray and white matter changes in preclinical Huntington disease: An MRI study. *Neurology*. 2010;74(15):1208. doi:10.1212/WNL.0B013E3181D8C20A

102. Rosas HD, Lee SY, Bender AC, et al. Altered white matter microstructure in the corpus callosum in Huntington's disease: implications for cortical "disconnection." *Neuroimage*. 2010;49(4):2995-3004. doi:10.1016/J.NEUROIMAGE.2009.10.015

103. Zimbelman JL, Paulsen JS, Mikos A, Reynolds NC, Hoffmann RG, Rao SM. fMRI detection of early neural dysfunction in preclinical Huntington's disease. *J Int Neuropsychol Soc*. 2007;13(5):758-769. doi:10.1017/S1355617707071214

104. Novak MJU, Warren JD, Henley SMD, Draganski B, Frackowiak RS, Tabrizi SJ. Altered brain mechanisms of emotion processing in pre-manifest Huntington's disease. *Brain*. 2012;135(Pt 4):1165-1179. doi:10.1093/BRAIN/AWS024

105. Paulsen JS. Functional imaging in Huntington's disease. *Exp Neurol*. 2009;216(2):272-277. doi:10.1016/J.EXPNEUROL.2008.12.015

106. Reading SAJ, Dziorny AC, Peroutka LA, et al. Functional brain changes in presymptomatic Huntington's disease. *Ann Neurol*. 2004;55(6):879-883. doi:10.1002/ANA.20121

107. McColgan P, Gregory S, Zeun P, et al. Neurofilament light-associated connectivity in young-adult Huntington's disease is related to neuronal genes. *Brain*. 2022;145(11):3953-3967. doi:10.1093/BRAIN/AWAC227

108. Koenig KA, Lowe MJ, Harrington DL, et al. Functional connectivity of primary motor cortex is dependent on genetic burden in prodromal Huntington disease. *Brain Connect*.

2014;4(7):535-546. doi:10.1089/BRAIN.2014.0271

109. Poudel GR, Egan GF, Churchyard A, Chua P, Stout JC, Georgiou-Karistianis N. Abnormal synchrony of resting state networks in premanifest and symptomatic Huntington disease: the IMAGE-HD study. *J Psychiatry Neurosci*. 2014;39(2):87-96. doi:10.1503/JPN.120226

110. Unschuld PG, Joel SE, Liu X, et al. Impaired cortico-striatal functional connectivity in prodromal Huntington's Disease. *Neurosci Lett*. 2012;514(2):204-209. doi:10.1016/J.NEULET.2012.02.095

111. Dumas EM, Van Den Bogaard SJA, Hart EP, et al. Reduced functional brain connectivity prior to and after disease onset in Huntington's disease. *NeuroImage Clin*. 2013;2(1):377-384. doi:10.1016/J.NICL.2013.03.001

112. McColgan P, Gregory S, Razi A, et al. White matter predicts functional connectivity in premanifest Huntington's disease. *Ann Clin Transl Neurol*. 2017;4(2):106-118. doi:10.1002/ACN3.384

113. Odish OFF, van den Berg-Huysmans AA, van den Bogaard SJA, et al. Longitudinal resting state fMRI analysis in healthy controls and premanifest Huntington's disease gene carriers: a three-year follow-up study. *Hum Brain Mapp*. 2015;36(1):110-119. doi:10.1002/HBM.22616

114. Gorges M, Müller HP, Mayer IMS, et al. Intact sensory-motor network structure and function in far from onset premanifest Huntington's disease. *Sci Rep*. 2017;7. doi:10.1038/SREP43841

115. Aylward EH, Li Q, Stine OC, et al. Longitudinal change in basal ganglia volume in patients with Huntington's disease. *Neurology*. 1997;48(2):394-399. doi:10.1212/WNL.48.2.394

116. Rosas HD, Goodman J, Chen YI, et al. Striatal volume loss in HD as measured by MRI and the influence of CAG repeat. *Neurology*. 2001;57(6):1025-1028. doi:10.1212/WNL.57.6.1025

117. Henley SMD, Wild EJ, Hobbs NZ, et al. Relationship between CAG repeat length and brain volume in premanifest and early Huntington's disease. *J Neurol*. 2009;256(2):203-212.

doi:10.1007/S00415-009-0052-X

118. Van Den Bogaard SJA, Dumas EM, Acharya TP, et al. Early atrophy of pallidum and accumbens nucleus in Huntington's disease. *J Neurol*. 2011;258(3):412-420. doi:10.1007/S00415-010-5768-0

119. Ginestroni A, Battaglini M, Diciotti S, et al. Magnetization transfer MR imaging demonstrates degeneration of the subcortical and cortical gray matter in Huntington disease. *AJNR Am J Neuroradiol*. 2010;31(10):1807-1812. doi:10.3174/AJNR.A2225

120. Aylward EH, Harrington DL, Mills JA, et al. Regional atrophy associated with cognitive and motor function in prodromal Huntington disease. *J Huntingtons Dis*. 2013;2(4):477-489. doi:10.3233/JHD-130076

121. Rosas HD, Salat DH, Lee SY, et al. Cerebral cortex and the clinical expression of Huntington's disease: complexity and heterogeneity. *Brain*. 2008;131(Pt 4):1057-1068. doi:10.1093/BRAIN/AWN025

122. Hobbs NZ, Cole JH, Farmer RE, et al. Evaluation of multi-modal, multi-site neuroimaging measures in Huntington's disease: Baseline results from the PADDINGTON study. *NeuroImage Clin*. 2012;2(1):204-211. doi:10.1016/J.NICL.2012.12.001

123. Delmaire C, Dumas EM, Sharman MA, et al. The structural correlates of functional deficits in early huntington's disease. *Hum Brain Mapp*. 2013;34(9):2141-2153. doi:10.1002/HBM.22055

124. Sprengelmeyer R, Orth M, Müller HP, et al. The neuroanatomy of subthreshold depressive symptoms in Huntington's disease: a combined diffusion tensor imaging (DTI) and voxel-based morphometry (VBM) study. *Psychol Med*. 2014;44(9):1867-1878. doi:10.1017/S003329171300247X

125. Wolf RC, Sambataro F, Vasic N, et al. Abnormal resting-state connectivity of motor and cognitive networks in early manifest Huntington's disease. *Psychol Med*. 2014;44(15):3341-3356. doi:10.1017/S0033291714000579

126. Werner CJ, Dogan I, Saß C, et al. Altered resting-state connectivity in Huntington's disease. *Hum Brain Mapp*. 2014;35(6):2582-2593. doi:10.1002/HBM.22351

127. Coppen EM, van der Grond J, Hart EP, Lakke EAJF, Roos RAC. The visual cortex and visual cognition in Huntington's disease: An overview of current literature. *Behav Brain Res*. 2018;351:63-74. doi:10.1016/J.BBR.2018.05.019

128. Quarantelli M, Salvatore E, Delle Acque Giorgio SM, et al. Default-mode network changes in Huntington's disease: an integrated MRI study of functional connectivity and morphometry. *PLoS One*. 2013;8(8). doi:10.1371/JOURNAL.PONE.0072159

129. Dumas EM, Van Den Bogaard SJA, Hart EP, et al. Reduced functional brain connectivity prior to and after disease onset in Huntington's disease. *NeuroImage Clin*. 2013;2(1):377-384. doi:10.1016/j.nicl.2013.03.001

130. Sánchez-Castañeda C, de Pasquale F, Caravasso CF, et al. Resting-state connectivity and modulated somatomotor and default-mode networks in Huntington disease. *CNS Neurosci Ther*. 2017;23(6):488-497. doi:10.1111/CNS.12701

CHAPTER 2 – REVIEW

Dissecting the many faces of Frontotemporal dementia: an imaging perspective

Marta Pengo, Enrico Premi, Barbara Borroni

Published in *International Journal of Molecular Sciences*, 2022; doi: 10.3390/ijms232112867

Abstract

Frontotemporal dementia (FTD) is a heterogeneous clinical and neuropathological disorder characterized by behavioral abnormalities, executive dysfunctions and language deficits.

FTD encompasses a wide range of different pathological entities, associated with the accumulation of proteins such as tau and TPD-43. A family history of dementia is found in one third of cases, and several genes causing autosomal dominant inherited disease have been identified. The clinical symptoms are preceded by a prodromal phase, which has been mainly studied in cases carrying pathogenetic mutations. New experimental strategies are emerging, in both prodromal and clinical settings, and outcomes markers are needed to test their efficacy.

In this complex context, in the last few years advanced neuroimaging techniques have allowed a better characterization of FTD, supporting clinical diagnosis, improving the comprehension of genetic heterogeneity and the earliest stages of the disease, helping a more detailed classification of underlying proteinopathies and developing new outcome markers on clinical grounds.

In this review, we briefly discuss the contribution of brain imaging and the most recent techniques in deciphering the different aspects of FTD.

Introduction

Frontotemporal dementia (FTD) is a common cause of early-onset dementia [1,2], with devasting psychological and social implications for both patients and families.

FTD encompasses a heterogeneous group of neurodegenerative disorders with a wide range of clinical, genetic and neuropathological features [2–5]. The careful characterization of clinical features of the behavioral variant frontotemporal dementia (bvFTD) [3], the agrammatic or the semantic variant of primary progressive aphasia (avPPA and svPPA) [4], and the spectrum of frontotemporal lobar degeneration (FTLD) with extrapyramidal symptoms, such as corticobasal syndrome (CBS) and progressive supranuclear palsy (PSP), has enabled a better understanding of the heterogeneity of FTLD phenotypes [6].

Along with the heterogeneity of clinical presentations, a complex neuropathology is associated with the disease, characterized by FLTD-Tau, FTLD-TDP and FTLD-FET with respect to the deposition of tau protein, TAR DNA Binding Protein 43 (TDP-43) and FET family proteins, respectively [7,8].

In one third of cases, FTD is associated with an autosomal dominant inherited mutation in one of three main genes: microtubule-associated protein tau (*MAPT*), progranulin (*GRN*), and chromosome 9 open reading frame 72 (*C9orf72*) [9].

This heterogeneity, as well the lack of a clear-cut relationship between clinical phenotypes, genetic traits and neuropathological features, represents the main obstacle hampering the development of a unifying disease model and, as consequence, of disease modifying strategies of intervention.

In the last few years, advanced neuroimaging techniques have gone beyond the mere neuroanatomical description of frontotemporal atrophy or hypometabolism in FTD patients, and have helped in increasing the diagnostic accuracy, in disentangling the features associated with monogenic disease, in describing the earliest changes occurring in the prodromal phases, and in forecasting disease progression [10]. Moreover, new positron emission tomography tracers provided key information to define the underlying neuropathology [11–15]. These neuroimaging developments have contributed to

explore FTD pathogenesis and to identify novel potential biomarkers. Since at present there is a lack of disease modifying therapies in FTD and treatment relies on symptomatic interventions [16], brain imaging biomarkers might be crucial in facilitating the recruitment of patients in clinical trials.

In the present review, we discuss the most important brain imaging candidates that help decipherer the different aspects of FTD, and suggest an approach to further improve our knowledge in FTD-related imaging (Figure 1).

Neuroimaging & FTD phenotypes

The different FTD syndromes are characterized by an early involvement of the insula and the anterior cingulate, which are part of the salience network [17–20]. Besides this common feature, structural brain magnetic resonance imaging (MRI) and brain positron emission tomography with [F18] fluorodeoxyglucose (FDG-PET) show characteristic and distinctive neuroimaging patterns which can help accurately discriminate between different FTD phenotypes and are routinely used in clinical practice [3,4,21–27]. By means of volumetric T1-weighted MRI it is possible to detect changes in grey matter (GM) structure, determine volumes of specific regions of interest and the rate of atrophy. In addition, postprocessing techniques can be applied to structural images, such as investigations of changes at voxel-level through voxel-based morphometry or measurement of cortical thickness. On the other hand, FDG-PET allows the identification of alterations in brain metabolism that might precede GM atrophy [28,29].

Conversely, advanced MRI methods such as diffusion tensor imaging (DTI), functional MRI (fMRI) and arterial spin labeling (ASL) are currently used in research and might be more sensitive in the earliest phases of the disease [30–35]. DTI explores microstructural white matter (WM) alterations that anticipate GM loss in FTD [36,37], whereas fMRI is a technique sensitive to changes in functional brain connectivity. ASL reveals alterations in brain perfusion that correlate very well with metabolism measured with FDG-PET [38,39]. These MRI techniques have the advantage to be safe, non-invasive, repeatable, can be combined in a single session, and do not involve radiation exposure. However, they have been investigated at a group level, and currently are not applicable in clinical practice at a single-patient level. Moreover, fMRI studies are limited by a wide variation in analytical methods used, such as independent component analysis, seed-based or region-of-interest based approaches.

Atrophy in bvFTD involves the frontal and temporal lobes, the insula and the anterior cingulate cortex, reflecting the distribution of Von Economo neurons [22,23,40,41] (Figure 2). The pattern of atrophy in bvFTD is usually asymmetric, predominantly involving the right hemisphere, and is associated

with the core neuropsychiatric features, including disinhibition, apathy, loss of empathy and binge eating [42–47]. Degeneration of many subcortical structures is also observed in bvFTD, in the amygdala, hippocampus, basal ganglia and thalamus [48].

Brain FDG-PET shows areas of hypometabolism that reflect atrophic regions, but might be more sensitive than structural images in the initial stages of the disease [28,29]. Low glucose metabolism is observed in comparable brain structures, mainly in orbitofrontal, dorsolateral and medial prefrontal cortices, anterior temporal poles and basal ganglia [39,49,50].

The distribution of atrophy and hypometabolism helps differentiating FTD from Alzheimer's disease (AD) [25,29,51–58].

The avPPA is mainly identified by left-sided frontal and insula involvement, both at structural MRI and brain FDG-PET [24,26,27,59,60], while the svPPA presents with asymmetrical, typically left-sided, anteroinferior temporal lobe atrophy and hypometabolism [24,27] (Figure 2). A minority of patients can exhibit right-predominant patterns of atrophy/hypometabolism affecting the temporal lobe and may present clinically with prosopagnosia, memory impairment and behavioral changes [61–64].

Distinct patterns of metabolic abnormalities in primary progressive aphasia (PPA) are important not only for the differential diagnosis of the different syndromes, but also to predict progression to specific dementia subtypes [27]. In avPPA, hypometabolism involving parietal, subcortical and brainstem structures was associated with progression to CBS or to PSP. svPPA showing extended bilateral hypometabolism progressed to bvFTD overtime.

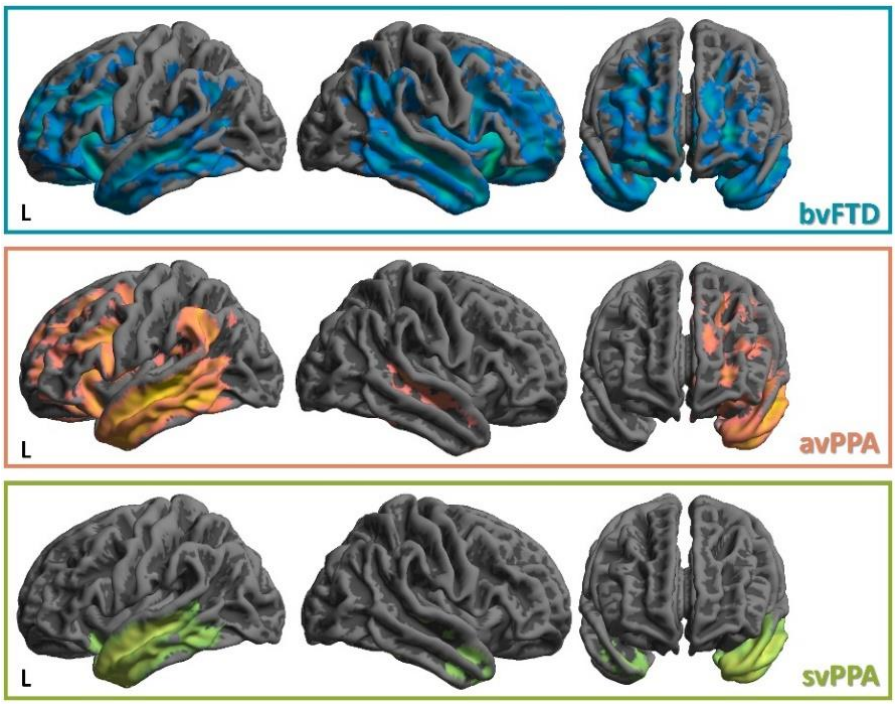

Figure 1. Representative VBM analysis in FTLD.

From our historical cohort of FTLD patients we performed a structural MRI analysis (Voxel Based Morphometry) to demonstrate the different patterns of gray matter atrophy. To this aim we considered the following cohort of subjects (80 healthy controls (63.1±7.9 years, 75% females); 122 bvFTD (64.8±7.9 years, 38% females): 68 avPPA (65.6±8.4 years, 66.2% females); 30 svPPA (63.6±8.4 years, 56.7% females). Age and gender were considered as nuisance variables in the statistical model. The findings (patient<healthy controls for each group) are superimposed on a 3D MRI template, clusters surviving a statistical threshold of $p<0.05$ FWE whole-brain correction for multiple comparisons are reported. VBM: voxel-based morphometry; MRI: magnetic resonance imaging; FWE: family-wise error.

Neuroimaging & neuropathology

One of the main goals of the current literature in FTD is to develop reliable imaging markers able to predict *in vivo* neuropathological hallmarks, namely tau or TDP-43 inclusions. Identifying biomarkers of misfolded proteins is extremely relevant for a precision medicine approach in future clinical trials. This would be key especially in non-monogenic cases, for which neuropathology is still unpredictable.

Up to now, at single-subject level, no brain MRI approaches hold the premises to identify neuropathology in FTD patients. Moreover, whereas the pattern of GM atrophy does not differ between FTLD-tau and FTLD-TDP [65], it has been described that FTLD-tau had significantly more WM degeneration in *post mortem* studies compared to FTLD-TDP [66].

Conversely, the field of PET imaging with tracers targeting different proteins has exploded in recent years. This technique holds the tremendous potential to define not only the underlying neuropathology of neurodegenerative diseases but also the pattern of distribution of unfolded proteins. Thus, this will be important also to investigate disease pathogenesis, for early and differential diagnosis and to monitor disease progression.

Tau PET first generation tracers have led to inconclusive results, because of the lack of specificity, subcortical WM uptake, and variable affinity for different tau isoforms [11–15]. These limitations have prompted the development of second generation of tau PET tracers. It has been demonstrated that these new radiotracer have a high affinity for tau neurofibrillary tangles, the hallmark of AD pathology [67,68]. In the same view, tau PET shows a good sensitivity in carriers of *MAPT* mutations that are more likely to cause an AD-like tau pathology [11,14,69,70]. However, these tracers bind only weakly if at all to 3-repeat tau in the Pick bodies of FTD and the 4-repeat linear tangles in dementias associated with PSP and CBS [68,71–75]. Moreover, although different studies demonstrated *in vivo* increased tau accumulation in the midbrain in PSP, discrepancies with autopsy studies and

considerable overlap with healthy controls (HC) underline the ongoing need for further investigations in this field [15,74,76].

No specific TDP-43 tracers are available yet. However, in different series of patients with svPPA, a disease typically characterized by TDP-43 pathology, tau PET signal was unexpectedly elevated with a spatial distribution mirroring areas of atrophy. These results raised concerns about the lack of specificity of tau tracers, suggesting a possible off-target biding to non-tau molecules [77–80]. PET ligands developed to bind tau neurofibrillary tangles in AD showed increase uptake also in bvFTD due to hexanucleotide repeat expansion in *C9orf72*, associated with TDP-43 deposition [12].

To conclude, it is clear that the field of PET imaging is extremely promising and progressing very rapidly. Nevertheless, further research is warranted in the spectrum of FTLD to clarify the aforementioned ambiguities. Furthermore, confirmation of *in vivo* findings with autopsy studies will be necessary for the validation of tau tracers in this field.

Neuroimaging & genetics

In recent years, the identification of new causative genes associated with FTD has represented a giant step forward to characterize the heterogeneity of the disorder, at clinical, molecular and imaging level. Moreover, exploring genetic FTD is crucial since it represents the ideal target population for the development of disease-modifying therapies and allows to unravel the prodromal disease stages in at-risk subjects [81–86]. Thus, definying biomarkers in the preclinical as well as clinical stages represents a priority in order to stratify patients for clinical trials and to assess the efficacy of therapeutic interventions in this population.

Each of the most common genetic groups, namely *GRN*, *MAPT* and *C9orf72* mutations, display a differential and characteristic pattern of cortical atrophy [87] with early changes appearing during the prodromal disease stages, up to twenty years before phenoconversion [82,88]. These results have been made possible by well-established international networks such as the European and Canadian based Genetic Frontotemporal dementia Initiative (GENFI, www.genfi.org), the US based ARTFL/LEFFTDS, and the Australian DINAD, which have collected cross-sectional and longitudinal data of FTD patients with monogenic disease [9,82]. In addition, the recently established consortia in Latin America (ReDLat) and New Zealand (FTDGeNZ) will be able to further elucidate the natural history of the disease [89,90].

Symptomatic stages of the disease can be investigated accurately with structural MRI. Comparable atrophy for all three mutation groups was observed in a network involving the insula, orbitofrontal lobe and anterior cingulate. Beside these areas, each mutation group develop a characteristic pattern of cortical atrophy [88]. *C9orf72* mutation carriers present atrophy symmetrically involving dorsolateral, medial and orbitofrontal lobes. Anterior temporal lobes, thalamus, parietal and occipital lobes and cerebellum are also affected [23,82,88,91–96]. Cases of patients with mild, slowly progressive or even severe dementia with minimal or no atrophy have been reported [91,97,98]. Interestingly, a comparable pattern of functional network alterations despite various atrophy patterns have been

described in *C9orf72* expansion carriers. In particular, they are characterized by reduced connectivity in the salience network and sensorimotor networks, whereas default mode network connectivity is similar to HC, unlike sporadic FTD [99].

GRN mutations carriers display a characteristic striking asymmetrical atrophy involving frontotemporal but also parietal cortices [23,82,88,95,100–102]. Both left- and right-sided predominant atrophy can be observed, even in the same family. *GRN* mutation carriers can present WM hyperintensities, even in the presymptomatic stages, that might be due to microglial activation and microglial dystrophy [103–107].

The distribution of atrophy in patients with *MAPT* mutation symmetrically involves the anterior and mesial temporal lobes, whereas orbitofrontal, lateral prefrontal and parietal regions are less altered [23,82,88,95,100]. A differential involvement of the temporal lobe has been described according to the diverse mutations in the *MAPT* gene [100].

Rate of atrophy varies in the different forms of genetic FTD. It is faster in those with *GRN* mutations and slower in *MAPT* mutation carriers. *C9orf72* mutation carriers show the greatest heterogeneity in the progression of brain atrophy [108,109]. In *GRN* mutation carriers, after clinical onset, the rate of atrophy is greater in the temporal cortex and becomes more asymmetrical in the following stages of the disease [82].

Besides the most frequent mutations, more rare pathogenic mutations are associated with genetic FTD. At present, neuroimaging findings in these patients are described in case reports or in limited number of cases and future international studies with larger cohorts are warranted in this field.

Neuroimaging & prodromal stages

Prodromal FTD may be defined as the presence of mild cognitive and/or behavioral changes without a significant impact on functional independence. The label of mild cognitive and/or behavioral and/or motor impairment (MCBMI) has been recently proposed in a consensus paper with the aim to capture the complexity of the clinical presentation in this disease stage [110].

In this context, the genetic forms have provided a privileged point of view for investigating the prodromal phases, assessing brain changes in at-risk mutation carriers.

Individuals with FTD-associated mutations develop GM atrophy and hypometabolism at least ten years before symptom onset, whereas WM abnormalities and functional connectivity alterations are seen even earlier, supporting the hypothesis of FTD as a network-based disease. Therefore, DTI and fMRI seem the most promising techniques to explore presymptomatic stages, with a greater sensitivity than structural MRI [31–33,111–113].

Traditionally, brain networks have been regarded as static over time. However, a recently introduced evolution of the brain connectome, the so-called chronnectome, allows to capture the dynamic functioning of the brain across time [114–116]. This approach has been demonstrated to be even more sensitive than traditional resting state fMRI approaches in presymptomatic phases [117,118]. ASL MRI is also a promising non-invasive imaging biomarker in presymptomatic carriers. Indeed, cerebral blood flow differences appeared earlier than 10 years before the expected onset in key FTD regions in the GENFI cohort [35].

The different genetic groups, such as *GRN, C9orf72* and *MAPT* mutations, are characterized by variability in both timing and location of early GM and WM changes.

In *C9orf72* mutation carriers GM and WM alterations appear very early, up to 30 years before symptoms onset; *GRN* mutation carriers show no or only minimal atrophy in presymptomatic stages, thus representing the most challenging group to investigate in these disease stages [30,32,121,122,33,34,82,88,99,112,119,120]. Conversely, studies in presymptomatic *MAPT* mutation carriers

showed contrasting results, probably because of the differences in cohort size and subject heterogeneity [113,121–123]; the largest study at present found early volume loss in hippocampus and amygdala at 15 years before expected onset [82].

Neuroimaging & disease progression

Conventional neuroimaging is routinely used for clinical diagnosis [124] and might also provide prognostic information [125,126]. Since FTD is characterized by great heterogeneity in clinical course, identifying imaging biomarkers of disease progression would be crucial also for inclusion in clinical trials.

The pattern of brain atrophy in FTD carries also prognostic information, as the degree of atrophy in the anterior cingulate and motor cortex predicted a faster disease progression [127], while diffuse brain atrophy was related to a worse prognosis than focal atrophy [128]. Functional brain imaging might also aid in defining prognosis. Hypoperfusion in the orbitomesial frontal cortex associated with the "pseudomanic behavior", characterized by disinhibition and abnormal social conduct, predicted a worse prognosis [129]. Moreover, hypoperfusion in the right orbitomesial frontal cortex and in the brainstem was associated with decreased survival [130,131]. Accordingly, different patterns of metabolic abnormalities in PPA are important to predict progression to specific dementia subtypes [27].

Along the disease course, the most suitable neuroimaging biomarker and the regions to evaluate could change. In this context, multivariate statistical approaches, like the multi-voxel pattern analysis (MVPA), might be useful for establishing the most accurate biomarker for clinical trials. By means of MVPA, it was demonstrated that in patients carrying *GRN* mutation, the most predictive measures were structural alterations, whereas in presymptomatic carriers, the best predictors markers were functional abnormalities, in particular the local connectivity measure (fALFF) [112].

Biological modulators and environmental factors, like education, have been proposed to contribute to heterogeneity in disease progression both in sporadic and genetic forms [132–136]. Neuroimaging might be of crucial relevance in evaluating the influence of these factors. Actually, disease modifiers can modulate brain atrophy [137] and brain connectivity [138] even in presymptomatic phases [139,140]. As a consequence, taking into account their effect of early brain damage is mandatory to stratify patients at risk of dementia, develop new therapies and eventually to monitor the efficacy of treatments.

Despite the relevance of neuroimaging as biomarker in FTD, at present its potential has been investigated mainly at group-level, to discriminate patients' groups from each other or from HC. However, this poses difficulties in clinical practice, since diagnostic and prognostic information at a single-subject level are essential. Recently developed tools might help to overcome this limitation. The preGRN-MRI tool was able to predict the expected MRI atrophy at follow-up using baseline MRI measures in presymptomatic *GRN* mutation carriers with good accuracy [141]. Therefore, this tool can be helpful in clinical trials since deviation of cortical thickness from the expected model might be a marker of treatment efficacy.

Moreover, machine-learning techniques are able to stratify *in vivo* disease subtypes and stages, and recent studies demonstrated their reliability to deal with the extreme heterogeneity of different neurodegenerative diseases. They therefore appear promising approaches in precision medicine, in order to stratify patients at very early disease stages. Subtype and stage inference (SuStaIn) is a computational approach that unravels phenotypic heterogeneity to distinguish patients' subgroups with similar pattern of disease progression [142]. In genetic FTD, using structural T1-weighted imaging, it was able to identify genotypes from imaging alone. Moreover, it could even reveal within-genotype heterogeneity, namely different subgroups in *C9orf72* and *MAPT* mutation carriers, characterized by diverse disease trajectories [142,143]. The contrastive trajectory inference (cTI) is another recently developed machine learning algorithm for staging and subtyping disease. It has been already applied for different neurodegenerative diseases, such as AD and Huntington disease [144]. A recent work explored its reliability also in genetic FTD [145]. Indeed, cTI could stage the disease in a heterogeneous cohort of genetic FTD, both presymptomatic and symptomatic, using only a combination of different neuroimaging modalities without clinical information. Machine learning appears therefore a promising approach to follow disease progression and monitor treatment efficacy in future clinical trials. A further development might be the combination with non-imaging biomarkers, e.g. neurofilament light chain, for optimal disease staging.

Conclusions and future perspectives

Neuroimaging appears a key biomarker in FTD. Whereas some techniques like structural MRI and FDG-PET are routinely used in clinical practice mainly for diagnostic purposes, novel emerging techniques are under development with different aims. PET with specific tracers and advanced neuroimaging approaches like fMRI and DTI will be essential to define the underlying neuropathology and investigate presymptomatic disease stages, respectively. Machine learning approaches will be crucial for early diagnosis, to evaluate disease progression and stratify patients for future clinical trials, and eventually also to combine neuroimaging with non-imaging biomarkers. All these advancements in neuroimaging research will be essential to develop and monitor new therapies in a pathology which is still orphan of disease-modifying treatments.

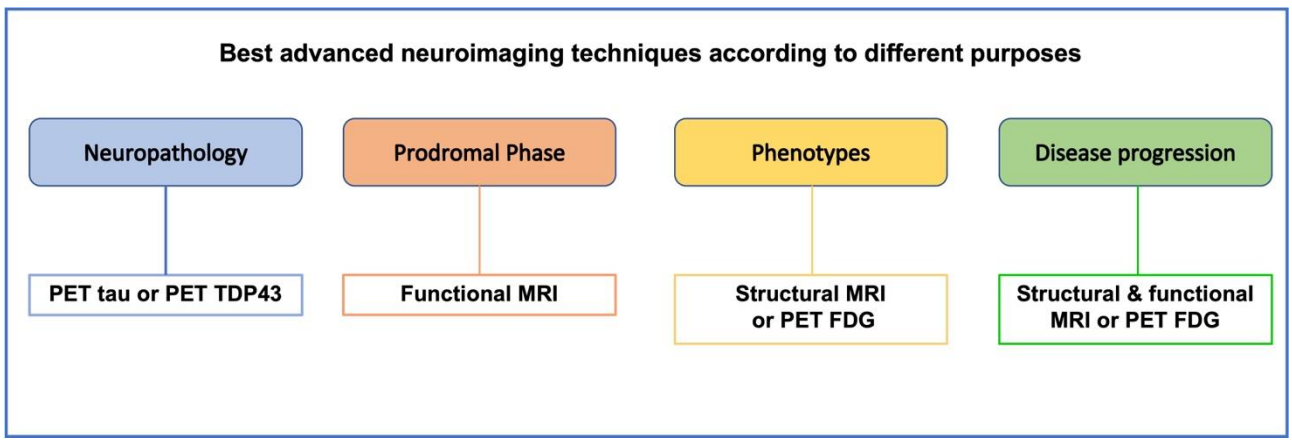

Figure 2. Proposed advanced neuroimaging techniques according to different aims.
Advanced neuroimaging allows to investigate different aspects of FTD, from defining neuropathology to early and differential diagnosis and disease progression. Different techniques are suitable for each of these aims.

References

1. RT V, L C, S M, et al. Epidemiology of early-onset dementia: a review of the literature. *Clin Pract Epidemiol Ment Health*. 2013;9(1):88-95. doi:10.2174/1745017901309010088
2. Bang J, Spina S, Miller BL. Frontotemporal dementia. *Lancet (London, England)*. 2015;386(10004):1672-1682. doi:10.1016/S0140-6736(15)00461-4
3. Rascovsky K, Hodges JR, Knopman D, et al. Sensitivity of revised diagnostic criteria for the behavioural variant of frontotemporal dementia. *Brain*. 2011;134(Pt 9):2456-2477. doi:10.1093/BRAIN/AWR179
4. Gorno-Tempini ML, Hillis AE, Weintraub S, et al. Classification of primary progressive aphasia and its variants. *Neurology*. 2011;76(11):1006-1014. doi:10.1212/WNL.0B013E31821103E6
5. Borroni B, Padovani A. Dementia: a new algorithm for molecular diagnostics in FTLD. *Nat Rev Neurol*. 2013;9(5):241-242. doi:10.1038/NRNEUROL.2013.72
6. Giunta M, Solje E, Gardoni F, Borroni B, Benussi A. Experimental Disease-Modifying Agents for Frontotemporal Lobar Degeneration. *J Exp Pharmacol*. 2021;13:359-376. doi:10.2147/JEP.S262352
7. MacKenzie IRA, Neumann M, Bigio EH, et al. Nomenclature and nosology for neuropathologic subtypes of frontotemporal lobar degeneration: an update. *Acta Neuropathol*. 2010;119(1):1-4. doi:10.1007/S00401-009-0612-2
8. Neumann M, Mackenzie IRA. Review: Neuropathology of non-tau frontotemporal lobar degeneration. *Neuropathol Appl Neurobiol*. 2019;45(1):19-40. doi:10.1111/NAN.12526
9. Moore KM, Nicholas J, Grossman M, et al. Age at symptom onset and death and disease duration in genetic frontotemporal dementia: an international retrospective cohort study. *Lancet Neurol*. 2020;19(2):145-156. doi:10.1016/S1474-4422(19)30394-1
10. Borroni B, Benussi A, Premi E, et al. Biological, Neuroimaging, and Neurophysiological Markers in Frontotemporal Dementia: Three Faces of the Same Coin. *J Alzheimers Dis*. 2018;62(3):1113-1123. doi:10.3233/JAD-170584
11. Jones DT, Knopman DS, Graff-Radford J, et al. In vivo 18 F-AV-1451 tau PET signal in MAPT mutation carriers varies by expected tau isoforms. *Neurology*. 2018;90(11):e947-e954. doi:10.1212/WNL.0000000000005117

12. Bevan-Jones RW, Cope TE, Jones SP, et al. [18 F]AV-1451 binding is increased in frontotemporal dementia due to C9orf72 expansion. 2018;5(10):1292-1296. Accessed September 1, 2022. https://pubmed.ncbi.nlm.nih.gov/30349864/

13. Ricci M, Cimini A, Camedda R, Chiaravalloti A, Schillaci O. Tau Biomarkers in Dementia: Positron Emission Tomography Radiopharmaceuticals in Tauopathy Assessment and Future Perspective. *Int J Mol Sci*. 2021;22(23). doi:10.3390/IJMS222313002

14. Tsai RM, Bejanin A, Lesman-Segev O, et al. 18 F-flortaucipir (AV-1451) tau PET in frontotemporal dementia syndromes. *Alzheimers Res Ther*. 2019;11(1). doi:10.1186/S13195-019-0470-7

15. Marquié M, Normandin MD, Vanderburg CR, et al. Validating novel tau positron emission tomography tracer [F-18]-AV-1451 (T807) on postmortem brain tissue. *Ann Neurol*. 2015;78(5):787-800. doi:10.1002/ANA.24517

16. Panza F, Lozupone M, Seripa D, et al. Development of disease-modifying drugs for frontotemporal dementia spectrum disorders. *Nat Rev Neurol*. 2020;16(4):213-228. doi:10.1038/S41582-020-0330-X

17. Ng ASL, Wang J, Ng KK, et al. Distinct network topology in Alzheimer's disease and behavioral variant frontotemporal dementia. *Alzheimers Res Ther*. 2021;13(1). doi:10.1186/S13195-020-00752-W

18. Day GS, Farb NAS, Tang-Wai DF, et al. Salience network resting-state activity: prediction of frontotemporal dementia progression. *JAMA Neurol*. 2013;70(10):1249-1253. doi:10.1001/JAMANEUROL.2013.3258

19. Filippi M, Agosta F, Scola E, et al. Functional network connectivity in the behavioral variant of frontotemporal dementia. *Cortex*. 2013;49(9):2389-2401. doi:10.1016/J.CORTEX.2012.09.017

20. Zhou J, Greicius MD, Gennatas ED, et al. Divergent network connectivity changes in behavioural variant frontotemporal dementia and Alzheimer's disease. *Brain*. 2010;133(Pt 5):1352-1367. doi:10.1093/BRAIN/AWQ075

21. Dukart J, Mueller K, Horstmann A, et al. Combined evaluation of FDG-PET and MRI improves detection and differentiation of dementia. *PLoS One*. 2011;6(3). doi:10.1371/JOURNAL.PONE.0018111

22. Pan PL, Song W, Yang J, et al. Gray matter atrophy in behavioral variant frontotemporal dementia: a

meta-analysis of voxel-based morphometry studies. *Dement Geriatr Cogn Disord*. 2012;33(2-3):141-148. doi:10.1159/000338176

23. Whitwell JL, Weigand SD, Boeve BF, et al. Neuroimaging signatures of frontotemporal dementia genetics: C9ORF72, tau, progranulin and sporadics. *Brain*. 2012;135(Pt 3):794-806. doi:10.1093/BRAIN/AWS001

24. Gorno-Tempini ML, Dronkers NF, Rankin KP, et al. Cognition and anatomy in three variants of primary progressive aphasia. *Ann Neurol*. 2004;55(3):335-346. doi:10.1002/ANA.10825

25. Poljansky S, Ibach B, Hirschberger B, et al. A visual [18F]FDG-PET rating scale for the differential diagnosis of frontotemporal lobar degeneration. *Eur Arch Psychiatry Clin Neurosci*. 2011;261(6):433-446. doi:10.1007/S00406-010-0184-0

26. Nestor PJ, Graham NL, Fryer TD, Williams GB, Patterson K, Hodges JR. Progressive non-fluent aphasia is associated with hypometabolism centred on the left anterior insula. *Brain*. 2003;126(Pt 11):2406-2418. doi:10.1093/BRAIN/AWG240

27. Cerami C, Dodich A, Greco L, et al. The Role of Single-Subject Brain Metabolic Patterns in the Early Differential Diagnosis of Primary Progressive Aphasias and in Prediction of Progression to Dementia. *J Alzheimers Dis*. 2017;55(1):183-197. doi:10.3233/JAD-160682

28. Mendez MF, Shapira JS, McMurtray A, Licht E, Miller BL. Accuracy of the clinical evaluation for frontotemporal dementia. *Arch Neurol*. 2007;64(6):830-835. doi:10.1001/ARCHNEUR.64.6.830

29. Womack KB, Diaz-Arrastia R, Aizenstein HJ, et al. Temporoparietal hypometabolism in frontotemporal lobar degeneration and associated imaging diagnostic errors. *Arch Neurol*. 2011;68(3):329-337. doi:10.1001/ARCHNEUROL.2010.295

30. Borroni B, Alberici A, Premi E, et al. Brain magnetic resonance imaging structural changes in a pedigree of asymptomatic progranulin mutation carriers. *Rejuvenation Res*. 2008;11(3):585-595. doi:10.1089/REJ.2007.0623

31. Dopper EGP, Rombouts SARB, Jiskoot LC, et al. Structural and functional brain connectivity in presymptomatic familial frontotemporal dementia. *Neurology*. 2014;83(2). doi:10.1212/WNL.0000000000000583

32. Borroni B, Alberici A, Cercignani M, et al. Granulin mutation drives brain damage and

reorganization from preclinical to symptomatic FTLD. *NBA*. 2012;33(10):2506-2520. doi:10.1016/j.neurobiolaging.2011.10.031

33. Lee SE, Sias AC, Kosik EL, et al. Thalamo-cortical network hyperconnectivity in preclinical progranulin mutation carriers. *NeuroImage Clin*. 2019;22. doi:10.1016/J.NICL.2019.101751

34. Alexander C, Zeithamova D, Hsiung GYR, Mackenzie IR, Jacova C. Decreased Prefrontal Activation during Matrix Reasoning in Predementia Progranulin Mutation Carriers. *J Alzheimers Dis*. 2018;62(2):583-589. doi:10.3233/JAD-170716

35. Mutsaerts HJMM, Mirza SS, Petr J, et al. Cerebral perfusion changes in presymptomatic genetic frontotemporal dementia: a GENFI study. *Brain*. 2019;142(4):1108-1120. doi:10.1093/BRAIN/AWZ039

36. Mahoney CJ, Ridgway GR, Malone IB, et al. Profiles of white matter tract pathology in frontotemporal dementia. *Hum Brain Mapp*. 2014;35(8):4163-4179. doi:10.1002/HBM.22468

37. Lam BYK, Halliday GM, Irish M, Hodges JR, Piguet O. Longitudinal white matter changes in frontotemporal dementia subtypes. *Hum Brain Mapp*. 2014;35(7):3547-3557. doi:10.1002/HBM.22420

38. Verfaillie SCJ, Adriaanse SM, Binnewijzend MAA, et al. Cerebral perfusion and glucose metabolism in Alzheimer's disease and frontotemporal dementia: two sides of the same coin? *Eur Radiol*. 2015;25(10):3050-3059. doi:10.1007/S00330-015-3696-1

39. Tosun D, Schuff N, Rabinovici GD, et al. Diagnostic utility of ASL-MRI and FDG-PET in the behavioral variant of FTD and AD. *Ann Clin Transl Neurol*. 2016;3(10):740-751. doi:10.1002/ACN3.330

40. Seeley WW, Crawford R, Rascovsky K, et al. Frontal paralimbic network atrophy in very mild behavioral variant frontotemporal dementia. *Arch Neurol*. 2008;65(2):249-255. doi:10.1001/ARCHNEUROL.2007.38

41. Schroeter ML, Laird AR, Chwiesko C, et al. Conceptualizing neuropsychiatric diseases with multimodal data-driven meta-analyses - the case of behavioral variant frontotemporal dementia. *Cortex*. 2014;57:22-37. doi:10.1016/J.CORTEX.2014.02.022

42. Rosen HJ, Allison SC, Schauer GF, Gorno-Tempini ML, Weiner MW, Miller BL. Neuroanatomical

correlates of behavioural disorders in dementia. *Brain*. 2005;128(Pt 11):2612-2625. doi:10.1093/BRAIN/AWH628

43. Peters F, Perani D, Herholz K, et al. Orbitofrontal dysfunction related to both apathy and disinhibition in frontotemporal dementia. *Dement Geriatr Cogn Disord*. 2006;21(5-6):373-379. doi:10.1159/000091898

44. Hornberger M, Geng J, Hodges JR. Convergent grey and white matter evidence of orbitofrontal cortex changes related to disinhibition in behavioural variant frontotemporal dementia. *Brain*. 2011;134(Pt 9):2502-2512. doi:10.1093/BRAIN/AWR173

45. Massimo L, Powers C, Moore P, et al. Neuroanatomy of apathy and disinhibition in frontotemporal lobar degeneration. *Dement Geriatr Cogn Disord*. 2009;27(1):96-104. doi:10.1159/000194658

46. Zamboni G, Huey ED, Krueger F, Nichelli PF, Grafman J. Apathy and disinhibition in frontotemporal dementia: Insights into their neural correlates. *Neurology*. 2008;71(10):736-742. doi:10.1212/01.WNL.0000324920.96835.95

47. Woolley JD, Gorno-Tempini ML, Seeley WW, et al. Binge eating is associated with right orbitofrontal-insular-striatal atrophy in frontotemporal dementia. *Neurology*. 2007;69(14):1424-1433. doi:10.1212/01.WNL.0000277461.06713.23

48. Halabi C, Halabi A, Dean DL, et al. Patterns of striatal degeneration in frontotemporal dementia. *Alzheimer Dis Assoc Disord*. 2013;27(1):74-83. doi:10.1097/WAD.0B013E31824A7DF4

49. Vijverberg EGB, Wattjes MP, Dols A, et al. Diagnostic Accuracy of MRI and Additional [18F]FDG-PET for Behavioral Variant Frontotemporal Dementia in Patients with Late Onset Behavioral Changes. *J Alzheimers Dis*. 2016;53(4):1287-1297. doi:10.3233/JAD-160285

50. Buhour MS, Doidy F, Laisney M, et al. Pathophysiology of the behavioral variant of frontotemporal lobar degeneration: A study combining MRI and FDG-PET. *Brain Imaging Behav*. 2017;11(1):240-252. doi:10.1007/S11682-016-9521-X

51. Ossenkoppele R, Pijnenburg YAL, Perry DC, et al. The behavioural/dysexecutive variant of Alzheimer's disease: clinical, neuroimaging and pathological features. *Brain*. 2015;138(Pt 9):2732-2749. doi:10.1093/BRAIN/AWV191

52. Ossenkoppele R, Singleton EH, Groot C, et al. Research Criteria for the Behavioral Variant of

Alzheimer Disease: A Systematic Review and Meta-analysis. *JAMA Neurol*. 2022;79(1):48-60. doi:10.1001/JAMANEUROL.2021.4417

53. Whitwell JL, Jack CR, Przybelski SA, et al. Temporoparietal atrophy: a marker of AD pathology independent of clinical diagnosis. *Neurobiol Aging*. 2011;32(9):1531-1541. doi:10.1016/J.NEUROBIOLAGING.2009.10.012

54. Lehmann M, Koedam ELGE, Barnes J, et al. Posterior cerebral atrophy in the absence of medial temporal lobe atrophy in pathologically-confirmed Alzheimer's disease. *Neurobiol Aging*. 2012;33(3):627.e1-627.e12. doi:10.1016/J.NEUROBIOLAGING.2011.04.003

55. Hartikainen P, Räsänen J, Julkunen V, et al. Cortical thickness in frontotemporal dementia, mild cognitive impairment, and Alzheimer's disease. *J Alzheimers Dis*. 2012;30(4):857-874. doi:10.3233/JAD-2012-112060

56. Du AT, Schuff N, Kramer JH, et al. Different regional patterns of cortical thinning in Alzheimer's disease and frontotemporal dementia. *Brain*. 2007;130(Pt 4):1159-1166. doi:10.1093/BRAIN/AWM016

57. Isella V, Crivellaro C, Formenti A, et al. Validity of cingulate-precuneus-temporo-parietal hypometabolism for single-subject diagnosis of biomarker-proven atypical variants of Alzheimer's Disease. *J Neurol*. 2022;269(8). doi:10.1007/S00415-022-11086-Y

58. Grimmer T, Diehl J, Drzezga A, Förstl H, Kurz A. Region-specific decline of cerebral glucose metabolism in patients with frontotemporal dementia: a prospective 18F-FDG-PET study. *Dement Geriatr Cogn Disord*. 2004;18(1):32-36. doi:10.1159/000077732

59. Grossman M, Mickanin J, Onishi K, et al. Progressive Nonfluent Aphasia: Language, Cognitive, and PET Measures Contrasted with Probable Alzheimer's Disease. *J Cogn Neurosci*. 1996;8(2):135-154. doi:10.1162/JOCN.1996.8.2.135

60. Grossman M. The non-fluent/agrammatic variant of primary progressive aphasia. *Lancet Neurol*. 2012;11(6):545-555. doi:10.1016/S1474-4422(12)70099-6

61. Chan D, Anderson V, Pijnenburg Y, et al. The clinical profile of right temporal lobe atrophy. *Brain*. 2009;132(Pt 5):1287-1298. doi:10.1093/BRAIN/AWP037

62. Josephs KA, Duffy JR, Strand EA, et al. Clinicopathological and imaging correlates of progressive

aphasia and apraxia of speech. *Brain*. 2006;129(Pt 6):1385-1398. doi:10.1093/BRAIN/AWL078

63. Kumfor F, Landin-Romero R, Devenney E, et al. On the right side? A longitudinal study of left- versus right-lateralized semantic dementia. *Brain*. 2016;139(Pt 3):986-998. doi:10.1093/BRAIN/AWV387

64. Erkoyun HU, Groot C, Heilbron R, et al. A clinical-radiological framework of the right temporal variant of frontotemporal dementia. *Brain*. 2020;143(9):2831-2843. doi:10.1093/BRAIN/AWAA225

65. Whitwell JL, Jack CR, Senjem ML, et al. MRI correlates of protein deposition and disease severity in postmortem frontotemporal lobar degeneration. *Neurodegener Dis*. 2009;6(3):106-117. doi:10.1159/000209507

66. McMillan CT, Irwin DJ, Avants BB, et al. White matter imaging helps dissociate tau from TDP-43 in frontotemporal lobar degeneration. *J Neurol Neurosurg Psychiatry*. 2013;84(9):949-955. doi:10.1136/JNNP-2012-304418

67. Ossenkoppele R, Rabinovici GD, Smith R, et al. Discriminative Accuracy of [18F]flortaucipir Positron Emission Tomography for Alzheimer Disease vs Other Neurodegenerative Disorders. *JAMA*. 2018;320(11):1151-1162. doi:10.1001/JAMA.2018.12917

68. Yap SY, Frias B, Wren MC, et al. Discriminatory ability of next-generation tau PET tracers for Alzheimer's disease. *Brain*. 2021;144(8):2284-2290. doi:10.1093/BRAIN/AWAB120

69. Smith R, Puschmann A, Schöll M, et al. 18F-AV-1451 tau PET imaging correlates strongly with tau neuropathology in MAPT mutation carriers. *Brain*. 2016;139(Pt 9):2372-2379. doi:10.1093/BRAIN/AWW163

70. Bevan Jones WR, Cope TE, Passamonti L, et al. [18 F]AV-1451 PET in behavioral variant frontotemporal dementia due to MAPT mutation. *Ann Clin Transl Neurol*. 2016;3(12):940-947. doi:10.1002/ACN3.366

71. Cho H, Choi JY, Hwang MS, et al. Subcortical 18 F-AV-1451 binding patterns in progressive supranuclear palsy. *Mov Disord*. 2017;32(1):134-140. doi:10.1002/MDS.26844

72. Smith R, Schain M, Nilsson C, et al. Increased basal ganglia binding of 18 F-AV-1451 in patients with progressive supranuclear palsy. *Mov Disord*. 2017;32(1):108-114. doi:10.1002/MDS.26813

73. Whitwell JL, Lowe VJ, Tosakulwong N, et al. [18F]AV-1451 tau-PET in progressive supranuclear

palsy. *Mov Disord*. 2017;32(1):124. doi:10.1002/MDS.26834

74. Passamonti L, Rodríguez PV, Hong YT, et al. 18F-AV-1451 positron emission tomography in Alzheimer's disease and progressive supranuclear palsy. *Brain*. 2017;140(3):781-791. doi:10.1093/BRAIN/AWW340

75. Brendel M, Barthel H, Van Eimeren T, et al. Assessment of 18F-PI-2620 as a Biomarker in Progressive Supranuclear Palsy. *JAMA Neurol*. 2020;77(11):1408-1419. doi:10.1001/JAMANEUROL.2020.2526

76. Sander K, Lashley T, Gami P, et al. Characterization of tau positron emission tomography tracer [18 F]AV-1451 binding to postmortem tissue in Alzheimer's disease, primary tauopathies, and other dementias. *Alzheimers Dement*. 2016;12(11):1116-1124. doi:10.1016/J.JALZ.2016.01.003

77. Josephs KA, Whitwell JL, Tosakulwong N, et al. TDP-43 and pathological subtype of Alzheimer's disease impact clinical features. *Ann Neurol*. 2015;78(5):697. doi:10.1002/ANA.24493

78. Lee H, Seo S, Lee SY, et al. [18F]-THK5351 PET Imaging in Patients With Semantic Variant Primary Progressive Aphasia. *Alzheimer Dis Assoc Disord*. 2018;32(1):62-69. doi:10.1097/WAD.0000000000000216

79. Bevan-Jones WR, Cope TE, Simon Jones P, et al. [18 F]AV-1451 binding in vivo mirrors the expected distribution of TDP-43 pathology in the semantic variant of primary progressive aphasia. *J Neurol Neurosurg Psychiatry*. 2018;89(10):1032-1037. doi:10.1136/JNNP-2017-316402

80. Makaretz SJ, Quimby M, Collins J, et al. Flortaucipir tau PET imaging in semantic variant primary progressive aphasia. *J Neurol Neurosurg Psychiatry*. 2018;89(10):1024-1031. doi:10.1136/JNNP-2017-316409

81. Rohrer JD, Boxer AL. The Frontotemporal Dementia Prevention Initiative: Linking Together Genetic Frontotemporal Dementia Cohort Studies. *Adv Exp Med Biol*. 2021;1281:113-121. doi:10.1007/978-3-030-51140-1_8

82. Rohrer JD, Nicholas JM, Cash DM, et al. Presymptomatic cognitive and neuroanatomical changes in genetic frontotemporal dementia in the Genetic Frontotemporal dementia Initiative (GENFI) study: a cross-sectional analysis. *Lancet Neurol*. 2015;14(3):253-262. doi:10.1016/S1474-4422(14)70324-2

83. Jiang J, Zhu Q, Gendron TF, et al. Gain of Toxicity from ALS/FTD-Linked Repeat Expansions in

C9ORF72 Is Alleviated by Antisense Oligonucleotides Targeting GGGGCC-Containing RNAs. *Neuron*. 2016;90(3):535-550. doi:10.1016/J.NEURON.2016.04.006

84. Arrant AE, Onyilo VC, Unger DE, Roberson ED. Progranulin Gene Therapy Improves Lysosomal Dysfunction and Microglial Pathology Associated with Frontotemporal Dementia and Neuronal Ceroid Lipofuscinosis. *J Neurosci*. 2018;38(9):2341-2358. doi:10.1523/JNEUROSCI.3081-17.2018

85. DeVos SL, Miller RL, Schoch KM, et al. Tau reduction prevents neuronal loss and reverses pathological tau deposition and seeding in mice with tauopathy. *Sci Transl Med*. 2017;9(374). doi:10.1126/SCITRANSLMED.AAG0481

86. Jadhav S, Avila J, Schöll M, et al. A walk through tau therapeutic strategies. *Acta Neuropathol Commun*. 2019;7(1):22. doi:10.1186/S40478-019-0664-Z

87. Chen Q, Kantarci K. Imaging Biomarkers for Neurodegeneration in Presymptomatic Familial Frontotemporal Lobar Degeneration. *Front Neurol*. 2020;11. doi:10.3389/FNEUR.2020.00080

88. Cash DM, Bocchetta M, Thomas DL, et al. Patterns of gray matter atrophy in genetic frontotemporal dementia: results from the GENFI study. *Neurobiol Aging*. 2018;62:191-196. doi:10.1016/J.NEUROBIOLAGING.2017.10.008

89. Ibanez A, Yokoyama JS, Possin KL, et al. The Multi-Partner Consortium to Expand Dementia Research in Latin America (ReDLat): Driving Multicentric Research and Implementation Science. *Front Neurol*. 2021;12. doi:10.3389/FNEUR.2021.631722

90. Ryan B, Baker A, Ilse C, et al. Diagnosing pre-clinical dementia: the NZ Genetic Frontotemporal Dementia Study (FTDGeNZ). *N Z Med J*. 2018;131(1476):88-91. Accessed September 1, 2022. https://pubmed.ncbi.nlm.nih.gov/29879731/

91. Boeve BF, Boylan KB, Graff-Radford NR, et al. Characterization of frontotemporal dementia and/or amyotrophic lateral sclerosis associated with the GGGGCC repeat expansion in C9ORF72. *Brain*. 2012;135(Pt 3):765-783. doi:10.1093/BRAIN/AWS004

92. Irwin DJ, McMillan CT, Brettschneider J, et al. Cognitive decline and reduced survival in C9orf72 expansion frontotemporal degeneration and amyotrophic lateral sclerosis. *J Neurol Neurosurg Psychiatry*. 2013;84(2):163-169. doi:10.1136/JNNP-2012-303507

93. Mahoney CJ, Beck J, Rohrer JD, et al. Frontotemporal dementia with the C9ORF72 hexanucleotide

repeat expansion: clinical, neuroanatomical and neuropathological features. *Brain*. 2012;135(Pt 3):736-750. doi:10.1093/BRAIN/AWR361

94. Sha SJ, Takada LT, Rankin KP, et al. Frontotemporal dementia due to C9ORF72 mutations: clinical and imaging features. *Neurology*. 2012;79(10):1002-1011. doi:10.1212/WNL.0B013E318268452E

95. Rohrer JD, Lashley T, Schott JM, et al. Clinical and neuroanatomical signatures of tissue pathology in frontotemporal lobar degeneration. *Brain*. 2011;134(Pt 9):2565-2581. doi:10.1093/BRAIN/AWR198

96. Bocchetta M, Todd EG, Peakman G, et al. Differential early subcortical involvement in genetic FTD within the GENFI cohort. *NeuroImage Clin*. 2021;30. doi:10.1016/J.NICL.2021.102646

97. Devenney E, Hornberger M, Irish M, et al. Frontotemporal dementia associated with the C9ORF72 mutation: a unique clinical profile. *JAMA Neurol*. 2014;71(3):331-339. doi:10.1001/JAMANEUROL.2013.6002

98. Khan BK, Yokoyama JS, Takada LT, et al. Atypical, slowly progressive behavioural variant frontotemporal dementia associated with C9ORF72 hexanucleotide expansion. *J Neurol Neurosurg Psychiatry*. 2012;83(4):358-364. doi:10.1136/JNNP-2011-301883

99. Lee SE, Khazenzon AM, Trujillo AJ, et al. Altered network connectivity in frontotemporal dementia with C9orf72 hexanucleotide repeat expansion. *Brain*. 2014;137(Pt 11):3047-3060. doi:10.1093/BRAIN/AWU248

100. Josephs KA, Whitwell JL, Jack CR, et al. Voxel-based morphometry patterns of atrophy in FTLD with mutations in MAPT or PGRN. *Neurology*. 2009;72(9):813-820. doi:10.1212/01.WNL.0000343851.46573.67

101. Le Ber I, Camuzat A, Hannequin D, et al. Phenotype variability in progranulin mutation carriers: a clinical, neuropsychological, imaging and genetic study. *Brain*. 2008;131(Pt 3):732-746. doi:10.1093/BRAIN/AWN012

102. Beck J, Rohrer JD, Campbell T, et al. A distinct clinical, neuropsychological and radiological phenotype is associated with progranulin gene mutations in a large UK series. *Brain*. 2008;131(Pt 3):706-720. doi:10.1093/BRAIN/AWM320

103. Ameur F, Colliot O, Caroppo P, et al. White matter lesions in FTLD: distinct phenotypes characterize

GRN and C9ORF72 mutations. *Neurol Genet*. 2016;2(1). doi:10.1212/NXG.0000000000000047

104. Paternicò D, Premi E, Gazzina S, et al. Neurobiology of Aging White matter hyperintensities characterize monogenic frontotemporal dementia with granulin mutations. *Neurobiol Aging*. 2016;38:176-180. doi:10.1016/j.neurobiolaging.2015.11.011

105. Sudre CH, Bocchetta M, Cash D, et al. White matter hyperintensities are seen only in GRN mutation carriers in the GENFI cohort. *NeuroImage Clin*. 2017;15:171-180. doi:10.1016/J.NICL.2017.04.015

106. Sudre CH, Bocchetta M, Heller C, et al. White matter hyperintensities in progranulin-associated frontotemporal dementia: A longitudinal GENFI study. *NeuroImage Clin*. 2019;24. doi:10.1016/J.NICL.2019.102077

107. Woollacott IOCC, Bocchetta M, Sudre CH, et al. Pathological correlates of white matter hyperintensities in a case of progranulin mutation associated frontotemporal dementia. *Neurocase*. 2018;24(3):166-174. doi:10.1080/13554794.2018.1506039

108. Whitwell JL, Weigand SD, Gunter JL, et al. Trajectories of brain and hippocampal atrophy in FTD with mutations in MAPT or GRN. *Neurology*. 2011;77(4):393-398. doi:10.1212/WNL.0B013E318227047F

109. Whitwell JL, Boeve BF, Weigand SD, et al. Brain atrophy over time in genetic and sporadic frontotemporal dementia: a study of 198 serial magnetic resonance images. *Eur J Neurol*. 2015;22(5):745-752. doi:10.1111/ENE.12675

110. Benussi A, Alberici A, Samra K, et al. Conceptual framework for the definition of preclinical and prodromal frontotemporal dementia. *Alzheimers Dement*. 2022;18(7):1408-1423. doi:10.1002/ALZ.12485

111. Pievani M, Paternicò D, Benussi L, et al. Pattern of structural and functional brain abnormalities in asymptomatic granulin mutation carriers. *Alzheimers Dement*. 2014;10(5 Suppl):S354-S363.e1. doi:10.1016/J.JALZ.2013.09.009

112. Premi E, Cauda F, Costa T, et al. Looking for Neuroimaging Markers in Frontotemporal Lobar Degeneration Clinical Trials: A Multi-Voxel Pattern Analysis Study in Granulin Disease. *J Alzheimers Dis*. 2016;51(1):249-262. doi:10.3233/JAD-150340

113. Whitwell JL, Josephs KA, Avula R, et al. Altered functional connectivity in asymptomatic MAPT

subjects: a comparison to bvFTD. *Neurology*. 2011;77(9):866-874. doi:10.1212/WNL.0B013E31822C61F2

114. Allen EA, Damaraju E, Plis SM, Erhardt EB, Eichele T, Calhoun VD. Tracking whole-brain connectivity dynamics in the resting state. *Cereb Cortex*. 2014;24(3):663-676. doi:10.1093/CERCOR/BHS352

115. Calhoun VD, Miller R, Pearlson G, Adali T. The chronnectome: time-varying connectivity networks as the next frontier in fMRI data discovery. *Neuron*. 2014;84(2):262-274. doi:10.1016/J.NEURON.2014.10.015

116. Chang C, Glover GH. Time-frequency dynamics of resting-state brain connectivity measured with fMRI. *Neuroimage*. 2010;50(1):81-98. doi:10.1016/J.NEUROIMAGE.2009.12.011

117. Premi E, Calhoun VD, Diano M, et al. The inner fluctuations of the brain in presymptomatic Frontotemporal Dementia: The chronnectome fingerprint. *Neuroimage*. 2019;189:645-654. doi:10.1016/J.NEUROIMAGE.2019.01.080

118. Premi E, Giunta M, Iraji A, et al. Dissemination in time and space in presymptomatic granulin mutation carriers: a GENFI spatial chronnectome study. *Neurobiol Aging*. 2021;108:155-167. doi:10.1016/J.NEUROBIOLAGING.2021.09.001

119. Caroppo P, Habert MO, Durrleman S, et al. Lateral Temporal Lobe: An Early Imaging Marker of the Presymptomatic GRN Disease? *J Alzheimer's Dis*. 2015;47(3):751-759. doi:10.3233/JAD-150270

120. Bertrand A, Wen J, Rinaldi D, et al. Early Cognitive, Structural, and Microstructural Changes in Presymptomatic C9orf72 Carriers Younger Than 40 Years. *JAMA Neurol*. 2018;75(2):236-245. doi:10.1001/JAMANEUROL.2017.4266

121. Olney NT, Ong E, Goh SYM, et al. Clinical and volumetric changes with increasing functional impairment in familial frontotemporal lobar degeneration. *Alzheimers Dement*. 2020;16(1):49-59. doi:10.1016/J.JALZ.2019.08.196

122. Panman JL, Jiskoot LC, Bouts MJRJ, et al. Gray and white matter changes in presymptomatic genetic frontotemporal dementia: a longitudinal MRI study. *Neurobiol Aging*. 2019;76:115-124. doi:10.1016/J.NEUROBIOLAGING.2018.12.017

123. Domínguez-Vivero C, Wu L, Lee S, et al. Structural Brain Changes in Pre-Clinical FTD MAPT

Mutation Carriers. *J Alzheimers Dis*. 2020;75(2):595-606. doi:10.3233/JAD-190820

124. Fumagalli GG, Basilico P, Arighi A, et al. Distinct patterns of brain atrophy in Genetic Frontotemporal Dementia Initiative (GENFI) cohort revealed by visual rating scales. *Alzheimers Res Ther*. 2018;10(1). doi:10.1186/S13195-018-0376-9

125. Anderl-Straub S, Lausser L, Lombardi J, et al. Predicting disease progression in behavioral variant frontotemporal dementia. *Alzheimer's Dement (Amsterdam, Netherlands)*. 2021;13(1). doi:10.1002/DAD2.12262

126. Illán-Gala I, Falgàs N, Friedberg A, et al. Diagnostic Utility of Measuring Cerebral Atrophy in the Behavioral Variant of Frontotemporal Dementia and Association With Clinical Deterioration. *JAMA Netw open*. 2021;4(3). doi:10.1001/JAMANETWORKOPEN.2021.1290

127. Agarwal S, Ahmed RM, D'Mello M, et al. Predictors of survival and progression in behavioural variant frontotemporal dementia. *Eur J Neurol*. 2019;26(5):774-779. doi:10.1111/ENE.13887

128. Lee JS, Jung NY, Jang YK, et al. Prognosis of Patients with Behavioral Variant Frontotemporal Dementia Who have Focal Versus Diffuse Frontal Atrophy. *J Clin Neurol*. 2017;13(3):234-242. doi:10.3988/JCN.2017.13.3.234

129. Borroni B, Grassi M, Agosti C, et al. Survival in frontotemporal lobar degeneration and related disorders: latent class predictors and brain functional correlates. *Rejuvenation Res*. 2009;12(1):33-43. doi:10.1089/REJ.2008.0812

130. Borroni B, Grassi M, Premi E, et al. Is long-term prognosis of frontotemporal lobar degeneration predictable by neuroimaging? Evidence from a single-subject functional brain study. *J Alzheimers Dis*. 2012;29(4):883-890. doi:10.3233/JAD-2012-112078

131. Le Ber I, Guedj E, Gabelle A, et al. Demographic, neurological and behavioural characteristics and brain perfusion SPECT in frontal variant of frontotemporal dementia. *Brain*. 2006;129(Pt 11):3051-3065. doi:10.1093/BRAIN/AWL288

132. Maiovis P, Ioannidis P, Gerasimou G, Gotzamani-Psarrakou A, Karacostas D. Cognitive Reserve Hypothesis in Frontotemporal Dementia: Evidence from a Brain SPECT Study in a Series of Greek Frontotemporal Dementia Patients. *Neurodegener Dis*. 2018;18(2-3):69-73. doi:10.1159/000486621

133. Borroni B, Premi E, Agosti C, et al. Revisiting brain reserve hypothesis in frontotemporal dementia:

evidence from a brain perfusion study. *Dement Geriatr Cogn Disord*. 2009;28(2):130-135. doi:10.1159/000235575

134. Premi E, Garibotto V, Alberici A, et al. Nature versus nurture in frontotemporal lobar degeneration: the interaction of genetic background and education on brain damage. *Dement Geriatr Cogn Disord*. 2012;33(6):372-378. doi:10.1159/000339366

135. Zhang M, Ferrari R, Tartaglia MC, et al. A C6orf10/LOC101929163 locus is associated with age of onset in C9orf72 carriers. *Brain*. 2018;141(10):2895-2907. doi:10.1093/BRAIN/AWY238

136. Pottier C, Zhou X, Perkerson RB, et al. Potential genetic modifiers of disease risk and age at onset in patients with frontotemporal lobar degeneration and GRN mutations: a genome-wide association study. *Lancet Neurol*. 2018;17(6):548-558. doi:10.1016/S1474-4422(18)30126-1

137. Premi E, Grassi M, Van Swieten J, et al. Cognitive reserve and TMEM106B genotype modulate brain damage in presymptomatic frontotemporal dementia: a GENFI study. *Brain*. 2017;140(6):1784-1791. doi:10.1093/BRAIN/AWX103

138. Premi E, Cristillo V, Gazzina S, et al. Expanding the role of education in frontotemporal dementia: a functional dynamic connectivity (the chronnectome) study. *Neurobiol Aging*. 2020;93:35-43. doi:10.1016/J.NEUROBIOLAGING.2020.04.021

139. Premi E, Formenti A, Gazzina S, et al. Effect of TMEM106B polymorphism on functional network connectivity in asymptomatic GRN mutation carriers. *JAMA Neurol*. 2014;71(2):216-221. doi:10.1001/JAMANEUROL.2013.4835

140. Gazzina S, Grassi M, Premi E, et al. Education modulates brain maintenance in presymptomatic frontotemporal dementia. *J Neurol Neurosurg Psychiatry*. 2019;90(10):1124-1130. doi:10.1136/JNNP-2019-320439

141. Premi E, Costa T, Gazzina S, et al. An Automated Toolbox to Predict Single Subject Atrophy in Presymptomatic Granulin Mutation Carriers. *J Alzheimers Dis*. 2022;86(1):205-218. doi:10.3233/JAD-215447

142. Young AL, Marinescu R V., Oxtoby NP, et al. Uncovering the heterogeneity and temporal complexity of neurodegenerative diseases with Subtype and Stage Inference. *Nat Commun*. 2018;9(1). doi:10.1038/S41467-018-05892-0

143. Young AL, Bocchetta M, Russell LL, et al. Characterizing the Clinical Features and Atrophy Patterns of MAPT-Related Frontotemporal Dementia With Disease Progression Modeling. *Neurology*. 2021;97(9):e941-e952. doi:10.1212/WNL.0000000000012410

144. Iturria-Medina Y, Khan AF, Adewale Q, Shirazi AH. Blood and brain gene expression trajectories mirror neuropathology and clinical deterioration in neurodegeneration. *Brain*. 2020;143(2):661-673. doi:10.1093/BRAIN/AWZ400

145. McCarthy J, Borroni B, Sanchez-Valle R, et al. Data-driven staging of genetic frontotemporal dementia using multi-modal MRI. *Hum Brain Mapp*. 2022;43(6):1821-1835. doi:10.1002/HBM.25727

EXPERIMENTAL SECTION

The studies presented in this section provide clear examples on how different approaches of advanced neuroimaging can be applied in two different inherited neurodegenerative conditions, namely genetic Frontotemporal dementia (FTD) and Huntington's disease (HD).

In the **first study** (*Chapter 3*) we aimed to compare genetic and sporadic FTD, taking into account clinical features, neuroimaging and biofluid biomarkers. We included a cohort of FTD patients followed at the Neurological Clinic of the University of Brescia, with the aim to describe differences and similarities between familial and sporadic forms, and to explain how understanding genetic FTD might help in deciphering sporadic FTD.

In the second and third studies (*Chapter 4 and 5*) we included a large sample of presymptomatic and symptomatic subjects from the international Genetic FTD Initiative (GENFI).

In the **second study** (**Chapter 4**) we aimed to indirectly explore in vivo neurotransmitter pathways changes, especially in the earliest disease phases, namely in prodromal FTD. To achieve this, we used JuSpace toolbox, which is able to explore if the spatial pattern of observed brain changes in the disease of interest are related to the distribution of specific neurotrasmitters pathways.

In the **third study** (*Chapter 5*) we aimed to investigate the activity of the glymphatic system, an emerging target of neurodegenerative disorders, in genetic FTD. In particular, we applied a diffusion-based technique called diffusion tensor image analysis along the perivascular space (DTI-ALPS).

In the **fourth study** (*Chapter 6*) we included a cohort of young carriers of HD mutation very far from disease onset, followed at the HD Centre of the University College London (London, UK). We studied dynamic functional connectivity of the visual networks with the aim to demonstrate very early alterations in premanifest HD and their correlation with biofluid biomarkers.

CHAPTER 3 – STUDY 1

Differences and similarities between familial and sporadic Frontotemporal dementia: an Italian single-center cohort study

Alberto Benussi, Ilenia Libri, Enrico Premi, Antonella Alberici, Valentina Cantoni, Yasmine Gadola, Jasmine Rivolta, Marta Pengo, Stefano Gazzina, Vince D. Calhoun, Roberto Gasparotti, Henrik Zetterberg, Nicholas Ashtong, Kaj Blennow, Alessandro Padovani, Barbara Borroni

Published in *Alzheimer's and Dementia 2022*, doi: 10.1002/trc2.12326.

Abstract

Introduction. The possibility to generalize our understandings on treatments and assessments to both familial (f-FTD) and sporadic frontotemporal dementia (s-FTD) is a fundamental perspective for the near future, considering the constant advancement in potential disease-modifying therapies that target particular genetic forms of FTD. The aim of the present study is to investigate differences in clinical features and cerebrospinal fluid and blood-based biomarkers between f-FTD and s-FTD.

Materials and methods. In this longitudinal cohort study, we evaluated a consecutive sample of symptomatic FTD patients, classified as f-FTD and s-FTD according to Goldman scores (GS). All patients underwent clinical, behavioral, and neuropsychiatric symptom assessment, CSF biomarkers and serum neurofilament light (NfL) analysis, and brain atrophy evaluation with magnetic resonance imaging.

Results. Of 570 patients with FTD, 123 were classified as f-FTD and 447 as s-FTD. In the f-FTD group, 95 had a pathogenic FTD mutation while 28 were classified as GC=1 or 2; of the s-FTD group, 133 were classified as GS=3 and 314 with GS=4. f-FTD and s-FTD cases showed comparable demographic features, except for younger age at disease onset, age at diagnosis and higher years of education in the f-FTD group (all $p<0.05$). f-FTD showed worse behavioural disturbances as measured with Frontal Behavioral Inventory (FBI) negative behaviors (14.0±7.6 *vs.* 11.6±7.4, $p=0.002$), and positive behaviors (20.0±11.0 *vs.* 17.4±11.8, $p=0.031$). Serum

NfL concentrations were higher in patients with a f-FTD (70.9±37.9 pg/mL) compared with s-FTD patients (37.3±24.2 pg/mL, $p<0.001$), and f-FTD showed greater brain atrophy in the frontal and temporal regions and basal ganglia. Patients with f-FTD had significantly shorter survival than those with s-FTD ($p=0.004$).

Conclusions. f-FTD and s-FTD are very similar clinical entities, but with different biological mechanisms, and different rates of progression. The parallel characterization of both f-FTD and s-FTD will improve our understanding of the disease, and aid in designing future clinical trials through both genetic and sporadic forms of FTD.

Introduction

Frontotemporal dementia (FTD) encompasses a heterogeneous group of neurodegenerative disorders with a wide range of clinical, genetic and neuropathological features.[1] The disease is characterized by insidious and progressive personality changes, impairment of executive functions and language deficits.[2,3] Different phenotypes have been classically defined on the basis of presenting clinical symptoms, including the behavioral variant of FTD (bvFTD), which is associated with early behavioral and personality changes,[3] the agrammatic variant of primary progressive aphasia (avPPA), with progressive deficits in speech, grammar and word output, and the semantic variant of PPA (svPPA), a progressive disorder of semantic knowledge and naming.[2] The occurrence of associated motor symptoms, as in progressive supranuclear palsy (PSP), corticobasal syndrome (CBS) and motor neuron disease (FTD-MND), enriches the spectrum of FTD related disorders.[4]

The majority of cases typically present sporadically as sporadic FTD (s-FTD) but about a third of patients have an autosomal dominant family history (familial FTD [f-FTD]),[5] with mutations of three main genes, *microtubule-associated protein tau* (*MAPT*), *granulin* (*GRN*), and *chromosome 9 open reading frame 72* (*C9orf72*), together accounting for 10 to 20% of all FTD and 70% of all genetic FTD cases.[6,7] Some individuals with f-FTD have a family history consistent with an autosomal dominant syndrome or with significant familial aggregation but do not have a known underlying mutation. To estimate this, the modified Goldman score has been developed, which enables the stratification of a family history based on the number of a patient's relatives who are or were affected, with scores strongly correlating with the likelihood of identifying a causal mutation.[5] With the onset of potential disease-modifying therapies targeting the pathophysiology of specific genetic mutations, it has become fundamental to carefully characterise and compare sporadic and familial forms to advance our understanding of whether treatments and assessments developed based on studies of f-FTD are generalizable to s-FTD, and *vice versa*.

Only few studies to date have tried to assess this issue, with initial results suggesting that sporadic and familial FTD cases are clinically similar.[8,9] However, a comprehensive comparison including cerebrospinal fluid (CSF) and blood-based biomarkers, imaging and survival, is currently lacking.

These premises prompted the objective of the present study, aimed at comprehensively compare characteristics of a large cohort of f-FTD and s-FTD patients, including clinical features, imaging and biological markers of neurodegeneration, and progression rates.

Materials and methods

Participants

This retrospective study included a sample of patients diagnosed with FTD according to current clinical criteria,[2,3] consecutively recruited at the Centre for Neurodegenerative Disorders, Department of Clinical and Experimental Sciences, University of Brescia, Italy, between July 2007 and July 2021.

Each participant underwent a neurological evaluation, routine laboratory examination and a standardized neuropsychological and behavioural assessment, as previously reported.[10]

In all FTD cases, the diagnosis was supported by a routine brain structural imaging, while CSF concentrations of tau, phosphorylated tau $(p\text{-}tau)_{181}$ and $A\beta_{1\text{-}42}$ or PET amyloid were measured in a subset of cases, to rule out Alzheimer's disease, as previously reported.[11] Furthermore, in accordance with recent consensus recommendations, genetic screening for *GRN*, *C9orf72* and *MAPT* P301L mutations was performed in selected cases (i.e., for all bvFTD patients and PPA patients with a strong family history [GS < 3]). Given the low frequency of *MAPT* mutations in Italy[12] we considered only the P301L mutation and we sequenced the entire *MAPT* gene only in selected cases.

Patients with clinical signs or symptoms of motor involvement were all screened with electromyography for MND and were excluded from analysis if they had an overlap FTD-amyotrophic lateral sclerosis or FTD-MND syndrome.

A subgroup of FTD patients underwent blood sampling and a standardised magnetic resonance imaging (MRI) imaging for further group analyses. FTD patients were followed over time and data on survival recorded.

FTD cases were subgrouped according to the modified Goldman's score (GS)[13] and the presence of pathogenetic mutations. Cases with familial aggregation (f-FTD) were defined as GS 1 or 2 or carrying a pathogenic mutation, while sporadic FTD (s-FTD) were defined as GCS 3 or 4. A GS of 1 corresponds to a family history consistent with the proband's clinical syndrome with an autosomal dominant inheritance pattern, with at least three people who are affected in two generations and who are linked by a first-degree relative; a GS of 2 indicates familial aggregation of three or more affected relatives but without meeting the criteria for a score of 1; a GS of 3 denotes one other affected relative; a GS of 4 signifies no known family history of neurodegenerative disease.

Full written informed consent was obtained from all subjects according to the Declaration of Helsinki. The Brescia Ethics Committee approved the study protocol.

Neuropsychological and behavioural assessment

At baseline, patients underwent a standardized neuropsychological battery which included the mini-mental state examination (MMSE), the Rey Auditory Verbal Learning test (immediate and delayed recall), the Rey complex figure (copy and recall), the digit span, phonemic and semantic fluencies, the Token Test, the clock-drawing test, and the trail-making test (part A and part B).[14]

The level of functional independence was assessed with the basic activities of daily living (BADL) and the instrumental activities of daily living (IADL) questionnaires, whereas neuropsychiatric and behavioural disturbances were evaluated with the frontal behaviour inventory (FBI).[15] Disease severity was assessed using the global Clinical Dementia Rating (CDR) plus National Alzheimer's Coordinating Center (NACC) frontotemporal lobar degeneration (FTLD).[16,17]

Serum neurofilament light and serum p-tau$_{181}$ measurements

A subgroup of patients (n=199) underwent blood collection for serum NfL and serum p-tau$_{181}$ dosages by Single molecule array (Simoa) technology, as previously described.[18] Briefly, NfL were measured on an HD-X Analyzer using the commercial NF-Light assay according to the manufacturer's instructions (Quanterix=) with lower limit of quantitation of 0.174 pg/mL. Serum p-tau$_{181}$ was measured using the in-house Simoa assay developed at the University of Gothenburg with the lower limit of quantification of 1 pg/ml. The measurements were performed out in one round of experiments using the same batch of reagents, and the operators were blinded to all clinical information. Quality control samples had intra-assay and inter-assay coefficients of variation of less than 8% and 20%, respectively.

CSF measurements

A subgroup of patients (n=215) underwent lumbar puncture according to a standardized protocol, in the outpatient clinic, at fasting, after informed written consent had been obtained and according to standard procedures.[19] CSF total-tau and p-tau concentrations were measured by sandwich ELISA test (Innotest hTau

Antigen kit, Innotest PHOSHO-TAU 181P, Fujirebio). CSF Aβ1-42 levels were determined using a sandwich ELISA (Inottest β-amyloid [1-42], Fujirebio). Interassay variability was less than 7%.

Imaging

A subgroup of patients (n=239) was studied with three-dimensional T1-weighted Magnetization Prepared - RApid Gradient Echo (MPRAGE) MRI. Three different scanners were considered, namely 1.5-Tesla Siemens Simphony, 1.5-tesla Siemens Avanto and 3-Tesla Siemens Skyra. As the first step, the raw DICOM scans were converted into the Neuroimaging Informatics Technology Initiative format, using MRIcroGL software (https://www.nitrc.org/projects/mricrogl/). T1-weighted images were then processed and analyzed with the voxel-based morphometry (VBM) pipeline implemented in the Computational Anatomy Toolbox (CAT12 v.1742) (http://www.neuro.uni-jena.de/cat/) for SPM12 (SPM12 v.7219) (http://www.fil.ion.ucl.ac.uk/spm/software/spm12/) running on MATLAB R2019b (the MathWorks, Inc., Natick, Massachusetts, United States). The VBM pipeline consists of several stages (tissue segmentation, spatial normalization to a standard Montreal National Institute [MNI] template, modulation and smoothing), as previously described.[20] CAT12 potentially provided more robust and accurate performances compared to other VBM pipelines.[21] The normalized and modulated grey matter images were then smoothed with 10-mm full width at half-maximum Gaussian kernel.

Source based morphometry (SBM) was consequently applied to study co-varying patterns of alterations. SBM leverages independent component analysis (ICA) to extract spatially independent patterns that occur in structural images. In contrast to mass-univariate testing (*i.e.,* VBM analysis), SBM captures interrelationships between voxels to identify patterns of structural variation between different groups. Furthermore, as multivariate approach, SBM can result in less-noisy sources of interest as well as a reduced number of multiple comparisons.[22]

In line with the original paper,[22,23] to obtain a common set of sources, a group ICA (considering all subjects) was calculated by GIFT toolbox (GroupICAT v4.0c; https://trendscenter.org/software/gift/),[24] with neural network algorithm (Infomax) that attempts to minimize the mutual information of the network outputs;[25] the component number was estimated to be 18, based on the minimum description length principle.[24,26] The statistical reliability of the source decomposition was tested by using the ICASSO toolbox[26] by running

Infomax 10 times with different initial conditions and bootstrapped data sets. Individual source maps were converted to Z scores before entering group statistics, to obtain voxel values comparable across subjects. Group analysis was run testing the differences between f-FTD and s-FTD, considering age, gender, scanner type, clinical phenotype (bvFTD and PPA), disease severity (CDR plus NACC FTLD score), and total grey matter volume (GMV) as nuisance variables. The statistical threshold was set at $p<0.05$ corrected for multiple comparisons. Source matrix was used for visualization, scaling each map to unit standard deviation (SBM Z-map) and threshold at $|Z|> 2.0$. The maps of significant sources were then superimposed onto the MNI normalized template brain.

Statistical analysis

Continuous and categorical variables are reported as mean (± standard deviation) and n (%) respectively. Baseline demographic and clinical variables were compared across groups using Student's t-test or Fisher's tests, as appropriate. Differences in cognitive or behavioural scores were compared by using the rank-based nonparametric analysis of covariance (ANCOVA) method, with phenotype (*i.e.*, bvFTD and PPA) and disease severity (CDR plus NAAC FTLD) as covariates. Differences in serum NfL levels or CSF parameters between groups were compared using the ANCOVA, with age as covariate.

Survival was calculated as time from symptom onset to time of death from any cause (outcome=0) or censoring date (outcome=1). Survival analysis was carried out by the Kaplan-Meier method with log rank *post hoc* testing and by means of univariate and multivariate stepwise Cox proportional-hazard regression analysis; hazard ratios (HR) are provided with their respective 95% confidence intervals (CIs).

A two-sided *p*-value <0.05 was considered significant. Statistical analyses were performed using SPSS (v.24; SPSS, IBM).

Data availability

All study data, including raw and analysed data, and materials will be available from the corresponding author, B.B., upon reasonable request.

Results

Participant characteristics

In total, 570 participants (mean age=65.8 ± 8.3 years; 277 females [48.6%]) were included in the present study. Of these, 123 were classified as f-FTD (95 with pathogenetic mutations, namely 66 *GRN*, 26 *C9orf72* and 3 *MAPT* mutations, and 28 with either GS=1 or 2) and 447 as s-FTD (133 with GS=3 and 314 with GS=4). Demographic and neuropsychological characteristics of included patients are reported in **Table 1**. f-FTD and s-FTD cases showed comparable demographic features, except for younger age at disease onset, age at diagnosis and higher years of education in the f-FTD group (all $p<0.05$, see **Table 1**). Disease duration was similar between groups: 2.7 ± 2.1 years in the f-FTD and mean 2.6 ± 2.3 in s-FTD, p=.913.

Table 1. Demographic and clinical characteristics of familial and sporadic FTD patients.

Variable	All FTD	f-FTD	s-FTD	*p*-value
Number	570	123	447	-
Age, years	65.9 ± 8.3	63.2 ± 8.6	66.7 ± 8.0	**<0.001**†
Sex, female % (n)	48.6 (277)	48.8 (60)	48.5 (217)	0.928^
Age at onset, years	63.3 ± 8.3	60.7 ± 8.5	63.9 ± 8.1	**<0.001**†
Disease duration, years	2.6 (2.2)	2.7 (2.1)	2.6 (2.3)	0.913
Education, years	9.0 ± 4.3	9.7 ± 4.2	8.8 ± 4.3	**0.031**†
Phenotype, % (n)				**0.004**
bvFTD	66.8 (381)	64.2 (302)	67.6 (302)	
nfPPA	21.2 (121)	30.1 (37)	18.8 (84)	
svPPA	11.9 (68)	5.7 (7)	13.6 (61)	
Global cognitive functions				
CDR plus NACC FTLD	1.6 ± 0.9	1.7 ± 0.9	1.6 ± 0.9	0.065
MMSE	19.9 ± 7.6	18.4 ± 8.6	20.4 ± 7.2	0.194
Behavioural disturbances				
FBI-A	12.2 ± 7.5	14.0 ± 7.6	11.6 ± 7.4	**0.001**
FBI-B	5.9 ± 5.7	6.0 ± 5.2	5.8 ± 5.9	0.628
FBI-AB	18.0 ± 11.7	20.0 ± 11.0	17.4 ± 11.8	**0.009**
Cognitive domains				
RAVL, immediate recall	29.3 ± 12.4	28.8 ± 15.2	29.5 ± 11.0	0.609
RAVL, delayed recall	4.9 ± 3.8	5.1 ± 4.0	4.8 ± 3.7	0.228
Rey complex figure, copy	23.8 ± 13.2	22.8 ± 10.0	24.1 ± 13.9	0.590
Rey complex figure, recall	9.6 ± 7.8	9.9 ± 6.0	9.5 ± 8.2	0.487

Digit span forward	4.8 ± 1.3	4.6± 1.2	4.8 ± 1.4	0.291
Fluency, letter	18.6± 10.9	15.8 ± 11.4	19.4 ± 10.7	0.064
Fluency, semantic	23.6 ± 12.2	22.4 ± 11.9	23.9 ± 12.2	0.784
Token test	25.4 ± 8.2	24.2 ± 8.6	25.8 ± 8.1	0.212
Clock drawing test	5.5± 3.1	5.2 ± 3.1	5.7 ± 3.1	0.925
Trail making test, part A (sec)	122.8 ± 143.8	124.2± 136.7	122.5 ± 146.0	0.785
Trail making test, part B (sec)	275.5 ± 156.0	280.7 ± 164.4	274.1 ± 154.1	0.852

Note: Categorical variables were compared with chi-square test while continuous were compared with one-way ANOVA; for clinical and behavioral measures, results were corrected for phenotype, disease severity and disease duration: cognitive tests were corrected for age and education, according to Italian normative data. Significant comparisons are reported in boldface.

Abbreviations: ANOVA, analysis of variance; bvFTD , behavioral variant frontotemporal dementia; CDR plus NACC FTLD, CDR Dementia Staging Instrument plus behavior and language domains from the National Alzheimer's Coordinating Center and Frontotemporal Lobar Degeneration modules; FBI, Frontal Behavior Inventory; f-FTD, familial FTD; FTD, Frontotemporal Dementia patients; MMSE, Mini-Mental State Examination; nfPPA, non-fluent variant of primary progressive aphasia; NPI, Neuropsychiatric Inventory; RAVL, Rey Auditory Verbal Learning Test; s-FTD, sporadic FTD; svPPA, semantic variant of primary progressive aphasia.

Clinical and behavioural differences between f-FTD and s-FTD

Clinical and behavioral scores according to f-FTD and s-FTD groups are reported in **Table 1**. No significant differences in global cognitive performances between f-FTD and s-FTD were found. f-FTD showed worse behavioral disturbances as measured with FBI-A (14.0 ± 7.6 *vs.* 11.6 ± 7.4, p=0.001), and FBI-B (20.0 ± 11.0 *vs.* 17.4 ± 11.8, p=0.009).

In particular, when FBI-A subitems were analysed, f-FTD showed worse scores in personal neglect (53.5% *vs.* 37.4%, p<0.05), disorganization (75.6% *vs.* 60.7%, p<0.05) and alien hand phenomenon and/or apraxia (24.4% *vs.* 10.5%, p=0.03), after adjusting for phenotype.

f-FTD and s-FTD were similar across standard neuropsychological tests, and only a tendency in letter fluency differences were observed, with f-FTD showing greater impairment compared to s-FTD (15.8 ± 11.4 *vs.* 19.4 ± 10.7, p=0.064). No other significant differences in cognitive domains were detected.

Biological differences between f-FTD and s-FTD

Serum NfL concentrations were higher in patients with f-FTD (70.9 ± 37.9 pg/mL) compared to s-FTD patients (37.3 ± 24.2 pg/mL, p<0.001). CSF total tau, p-tau$_{181}$ and Aβ_{1-42} and serum p-tau$_{181}$ levels did not show significant differences between groups (all p-values >0.05) (see **Table 2**).

Table 2. Biological markers of familial and sporadic FTD patients.

Variable	All FTD	f-FTD	s-FTD	*p*-value
Number	215	43	172	
Biological markers				
CSF total tau, pg/mL	441.7 ± 292.0	433.2 ± 292.0	443.9 ± 296.5	0.808
CSF p-tau$_{181}$, pg/mL	62.7 ± 63.01	55.2 ± 65.0	64.6 ± 62.5	0.377
CSF Aβ_{1-42}, pg/mL	765.7 ± 383.7	804.1 ± 344.3	756.1 ± 393.3	0.390
Serum NfL, pg/mL	44.0 ± 30.6	70.9 ± 37.9	37.3± 24.2	**<0.001**
Serum p-tau$_{181}$, pg/mL	3.0 ± 6.3	2.4 ± 9.8	3.2 ± 5.0	0.454

Note: Continuous variables were compared with one-way ANCOVA, corrected for age and phenotype.

Significant comparisons are reported in boldface.

Abbreviations: Aβ, amyloid beta; ANCOVA, analyses of covariance; CSF, cerebrospinal fluid; FTD, frontotemporal dementia patients; f-FTD, familial FTD; NfL, neurofilament light; p-tau, phosphorylated tau; s-FTD, sporadic FTD.

Imaging

Twelve out the 18 estimated sources were considered, after excluding seven sources for artifacts (*i.e.*, signal near the external boundary of the brain or appearing primarily in ventricles or white matter areas). The 12 sources included frontoparietal (right and left), basal ganglia, visual, default mode network (posterior and anterior), auditory, and frontal pathway. Among them, four sources presented loading scores (as index of grey matter density) significant differences between f-FTD and s-FTD, considering comparable disease stage (p<0.01 corrected for multiple comparisons using the false discovery rate - FDR). As shown in **Figure 1**, f-FTD showed greater brain atrophy in the basal ganglia (putamen, caudate, thalamus; source 3), in the medial

and inferior frontal gyri (source 11), in the middle frontal gyri, thalamus and inferior parietal lobule (source 16), and in the temporal regions (source 17).

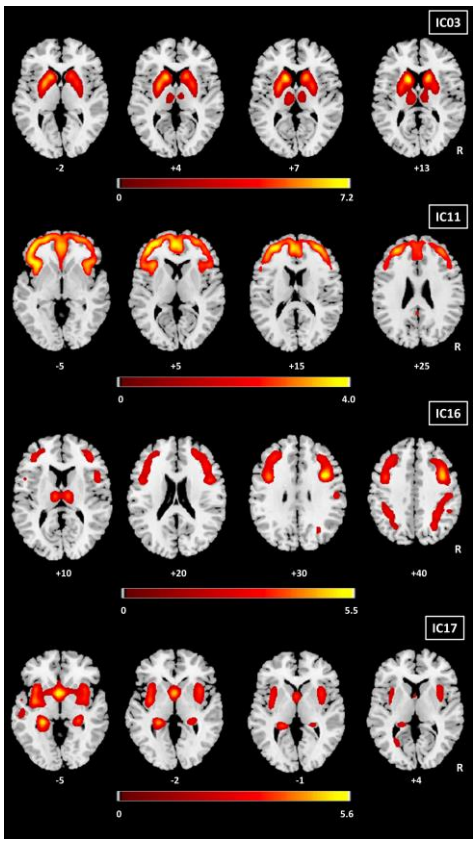

Figure 1. Source Based Morphometry (SBM) analyses showing greater brain damage in f-FTD as compared to nf-FTD. See text for details. F-FTD, familial frontotemporal dementia; IC = independent component.

Survival in f-FTD versus s-FTD

Survival analysis was available for 567 participants (447 sporadic and 123 familial FTD). Overall, 149 deaths occurred in the whole sample, with 115 (26.0%) in s-FTD and 34 (27.6%) in f-FTD. The univariate Cox regression analysis showed a significant association between survival and f-FTD (HR 1.76, 95%CI 1.20-2.60, p=0.004). Patients with f-FTD had significantly shorter survival than those with s-FTD at the Kaplan-Meier survival curves (p=0.004) (see **Figure 2**). The mean estimated survival in the whole sample was of 175.0 (95% CI 162.6-187.4) months, with 181.2 (95% CI 167.7-194.6) months in s-FTD and 122.8 (95% CI 108.8-136.8) months in f-FTD.

When predictors of survivals were considered, namely familial aggregation (f-FTD and s-FTD), serum NfL levels and behavioral disturbances (FBI-A), the multivariate Cox regression analysis showed that only serum NfL was significantly associated to survival (HR 1.02, 95%CI 1.01-1.02, p<0.001).

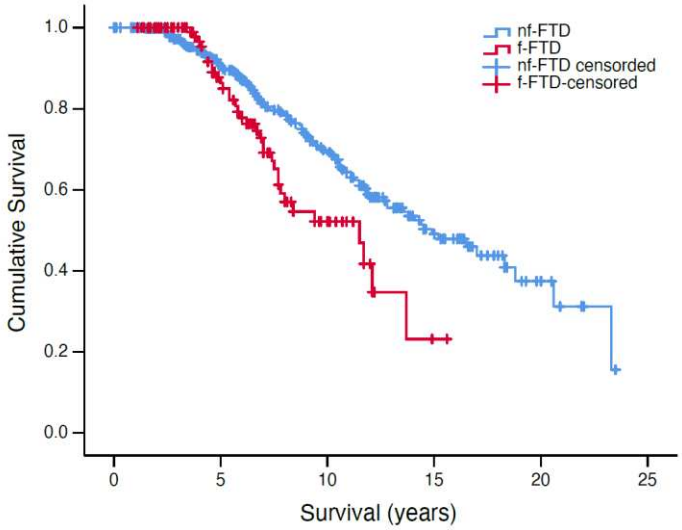

Figure 2. Survival curves in f-FTD and nf-FTD.

Kaplan-Meier survival curves in f-FTD (red line) and s-FTD (blue line). F-FTD, familial frontotemporal dementia; s-FTD, sporadic frontotemporal dementia.

f-FTD and s-FTD subgroups comparisons

When f-FTD subgroups were considered, that is, pathogenetic mutations carriers versus GS=1 or 2 patients without pathogenetic mutations, the former group presented earlier age at disease onset and earlier age at diagnosis (see **Supplementary Table 1).** No significant differences in clinical presentation or biological markers, except for increased CSF total tau (491.1 ± 290.7 *vs.* 294.9 ± 183.4, p=0.015) and serum NfL, even though not significant (78.2 ± 36.9 *vs.* 49.2 ± 31.9, p=0.067) in patients carrying pathogenetic mutations, were reported (**Supplementary Table 1**). When s-FTD subgroups were considered, that is, GS=3 versus GS=4, comparable findings between groups were found.

When only bvFTD patients were considered (n = 351), comparable results were shown, with f-FTD showing earlier age at disease onset and earlier age at diagnosis and significant higher serum NfL compared to s-FTD (see **Supplementary Table 2**). The univariate Cox regression analysis showed a significant association between survival and f-bvFTD (HR 1.72, 95%CI 1.06-2.81, p=0.03). Patients with f-bvFTD had significantly shorter survival than those with s-FTD at the Kaplan-Meier survival curves (p=0.028).

Supplementary Table 1. Demographic and clinical characteristics of familial and sporadic FTD patients according to their subgroups

Variable	f-FTD		*p*-value[†°]	s-FTD		*p*-value[†#]
	pathogenetic mutations	GS=1 or 2		GS=3	GS=4	
Number	95	28	-	133	314	
Age, years	61.9±8.4	67.2±8.1	**0.005**	67.5±7.5	66.4±8.2	0.191
Sex, female %	53.7	32.1	**0.036**[^]	48.1	48.4	0.519[^]
Age at onset, years	59.8±8.3	64.0±8.5	**0.020**	64.6±7.44	63.7±8.3	0.291
Education, years	9.7±4.1	9.9±4.4	0.799	8.9±4.6	8.7±4.2	0.578
Phenotype, bvFTD % (vs. PPA)	63.2	71.4	0.284[^]	70.7	66.2	0.598[^]
Clinical and behavioural assessment[§]						
CDR plus NACC FTLD	1.7±0.9	1.8±0.9	0.607	1.6±1.0	1.6±0.9	0.654
FBI-A	13.9±7.7	14.5±7.3	0.736	11.5±7.4	11.7±7.4	0.834
FBI-B	5.5±4.9	8.0±6.0	0.073	5.9±6.2	5.8±5.8	0.868
FBI-AB	19.5±10.9	22.1±11.4	0.525	17.7±12.6	17.3±11.5	0.916
Biological markers[*]						
CSF total tau, pg/mL	491.1±290.7	294.9±183.4	**0.015**	388.5±250.7	468.3±312.5	0.067
CSF phospho-tau$_{181}$, pg/mL	59.1±75.0	45.2±24.7	0.660	64.6±62.6	58.8±58.5	0.375
CSF Aβ_{1-42}, pg/mL	814.5±372.4	777.2±271.1	0.760	771.8±404.2	749.31±390.1	0.750
Serum NfL, pg/mL	78.2±36.9	49.2±31.9	0.067	36.5±22.0	37.6±25.4	0.905

FTD = Frontotemporal Dementia patients; f-FTD = familial FTD; s-FTD = sporadic FTD; GS = Goldman's score; bvFTD = behavioral variant frontotemporal dementia; PPA = primary progressive aphasia; CDR plus NACC FTLD = CDR Dementia Staging Instrument plus behavior and language domains from the National Alzheimer's Coordinating Center and Frontotemporal lobar degeneration modules; NPI= Neuropsychiatric inventory; FBI = Frontal Behaviour Inventory; CSF = cerebrospinal fluid; NfL = neurofilament light chain.
° pathogenetic mutations vs. GS=1 or 2; # GS=3 vs. GG=4; † Student t-test comparison, unless otherwise specified; ^ *p*-values for Chi-Square test comparison; § p-values for one-way ANCOVA adjusted for phenotype; * *p*-values for one-way ANCOVA adjusted for age.

Supplementary table 2. Demographic characteristics and biomarkers of familial and sporadic bvFTD patients.

Variable	f-FTD	s-FTD	*p*-value
Number	78	273	-
Age, years	63.1±8.1	66.5±7.8	**<0.001**†
Sex, female % (n)	43.6 (34)	41.4 (113)	0.413^
Age at onset, years	60.5±8.8	63.7±7.6	**0.003**†
Education, years	9.4±4.2	8.3±4.0	0.058†
Biological markers			
CSF total tau, pg/mL	487.2±304.7	405.1±280.2	0.160*
CSF phospho-tau$_{181}$, pg/mL	62.0±66.0	60.3±63.7	0.904*
CSF Aβ_{1-42}, pg/mL	785.2±377.5	738.3±368.3	0.541*
Serum NfL, pg/mL	70.1±35.9	37.5±24.9	**<0.001***

FTD = Frontotemporal Dementia patients; f-FTD = familial FTD; s-FTD = sporadic FTD; bvFTD = behavioural variant frontotemporal dementia; CSF = cerebrospinal fluid; NfL = neurofilament light chain. †Student t-test comparison, unless otherwise specified; ^Chi-Square test comparison; *p-values for one-way ANCOVA, adjusting for age.

Discussion

The possibility to generalize our understandings on treatments and assessments to both f-FTD and s-FTD is a fundamental perspective for the near future, considering the constant advancement in potential disease-modifying therapies that target particular genetic forms of FTD. However, this is currently a difficult task, considering the absence of a clear understanding of the differences and similarities that characterise f-FTD and s-FTD.

In the present study, we observed that f-FTD and s-FTD share similar demographic features, including sex and phenotype distribution, but with younger age at disease onset and diagnosis in the f-FTD group, and marginally lower years of education in the s-FTD group. This is in line with a previous study in bvFTD,[8] with f-FTD being on average 4.8 years younger than s-FTD, and as previously reported this was mainly driven by pathogenetic mutations (see Supplementary table 1 and Supplementary table 2). Moreover, this could be also partially explained by an ascertainment bias, considering that patients with a known family history for the disease may seek diagnosis sooner and may be more vigilant regarding the onset of subtle cognitive or behavioral symptoms.

According to previous studies,[8] patients subgroups were highly similar across behavioral and cognitive measures, with only slight differences in the FBI-A and in the letter fluency scores, despite arising from different underlying pathologies and genetic factors. The FBI-A evaluates negative or deficient behaviors, such as apathy, aspontaneity and indifference, which may depend on a deficit of glutamatergic transmission, while positive symptoms, evaluated with the FBI-B, may be the consequence of a lack of GABAergic inhibition, potentially reflecting the unique impairment of different neurotransmitter systems in FTD.

Despite a comparable clinical picture, f-FTD showed higher serum NfL concentrations by an average of 37.3 pg/mL and greater brain damage, compared to s-FTD. Moreover, f-FTD showed a shorter survival rate than s-FTD, and this finding is supported by several studies showing that disease survival is generally shorter in the genetic forms of FTD.[14,27–29]

Serum NfL levels have already been shown to be a consistent and reliable marker of disease severity in both genetic and sporadic FTD,[18,30–36] with levels increasing already in the prodromal phases of disease,[37] and correlating with disease survival.[33] Also in this study, serum NfL levels were the most significant predictors of survival.

These findings raise important issues, suggesting that there were no demographical or clinical features that may reliably distinguish f-FTD from s-FTD, providing empirical support for the applicability of clinical scores developed for s-FTD to f-FTD. Conversely, different rates of progression between groups have fundamental implications when considering potential generalizability in future pharmacological and non-pharmacological clinical trials. In view of recent advances in disease modifying therapies which target specific pathogenic routes,[47] f-FTD and s-FTD should be considered separately to measure the effects of treatment interventions, given the different disease trajectories.

We acknowledge that the present study entails several limitations. First, we did not evaluate motor features of parkinsonisms which characterise PSP or CBS-like phenotypes; previous studies have indeed shown that f-FTD may present with more severe motor symptoms, mainly driven by *MAPT* variations which present greater involvement of basal ganglia with tau disease pathology.[8] Second, not all patients underwent genetic screening, so we may not entirely exclude the presence of pathogenic variants in this group. Third, only a subset of patients underwent biological measurements or imaging analyses, but still significant differences could be observed between groups. Fourth, the lack of pathological confirmation in the s-FTD cases prevented evaluation of significant differences and distributions between proteinopathies. Finally, we considered both bvFTD and PPA together, even though clinical phenotype was included as covariate in the statistical analyses. Major strengths of our study are the large series of FTD patients and the comprehensive approach in extensively evaluating demographical, clinical, fluid biomarker, and imaging data, carried out at the same study site to minimize variability.

In conclusion, our results suggest that f-FTD and s-FTD are very similar clinical entities, but with different rates of progression. The parallel characterization of both f-FTD and s-FTD will improve our understanding of the disease, and aid in designing future clinical trials through both genetic and sporadic forms of FTD.

References

1. Bang J, Spina S, Miller BL. Frontotemporal dementia. *Lancet*. 2015;386(10004):1672-1682. http://linkinghub.elsevier.com/retrieve/pii/S0140673615004614

2. Gorno-Tempini ML, Hillis AE, Weintraub S, et al. Classification of primary progressive aphasia and its variants. *Neurology*. 2011;76(11):1006-1014. http://eutils.ncbi.nlm.nih.gov/entrez/eutils/elink.fcgi?dbfrom=pubmed&id=21325651&retmode=ref&cmd=prlinks

3. Rascovsky K, Hodges JR, Knopman D, et al. Sensitivity of revised diagnostic criteria for the behavioural variant of frontotemporal dementia. *Brain*. 2011;134(Pt 9):2456-2477. doi:Doi 10.1093/Brain/Awr179

4. Borroni B, Benussi A. Recent advances in understanding frontotemporal degeneration. *F1000Research*. 2019;8:2098. doi:10.12688/f1000research.20330.1

5. Rohrer JD, Guerreiro R, Vandrovcova J, et al. The heritability and genetics of frontotemporal lobar degeneration. *Neurology*. 2009;73(18):1451-1456. http://eutils.ncbi.nlm.nih.gov/entrez/eutils/elink.fcgi?dbfrom=pubmed&id=19884572&retmode=ref&cmd=prlinks

6. Borroni B, Padovani A. Dementia: A new algorithm for molecular diagnostics in FTLD. *Nat Rev Neurol*. 2013;9(5):241-242. http://dx.doi.org/10.1038/nrneurol.2013.72

7. Benussi A, Padovani A, Borroni B. Phenotypic heterogeneity of monogenic frontotemporal dementia. *Front Aging Neurosci*. 2015;7(SEP). doi:10.3389/fnagi.2015.00171

8. Heuer HW, Wang P, Rascovsky K, et al. Comparison of sporadic and familial behavioral variant frontotemporal dementia (FTD) in a North American cohort. *Alzheimer's Dement*. 2020;16(1):60-70. doi:10.1002/alz.12046

9. Capozzo R, Sassi C, Hammer MB, et al. Clinical and genetic analyses of familial and sporadic frontotemporal dementia patients in Southern Italy. *Alzheimer's Dement*. 2017;13(8):858-869. doi:10.1016/j.jalz.2017.01.011

10. Benussi A, Gazzina S, Premi E, et al. Clinical and biomarker changes in presymptomatic genetic frontotemporal dementia. *Neurobiol Aging*. 2019;76:133-140. doi:10.1016/j.neurobiolaging.2018.12.018

11. Borroni B, Benussi A, Archetti S, et al. Csf p-tau181/tau ratio as biomarker for TDP pathology in frontotemporal dementia. *Amyotroph Lateral Scler Frontotemporal Degener*. 2015;16(1-2):86-91. doi:10.3109/21678421.2014.971812

12. Fostinelli S, Ciani M, Zanardini R, et al. The Heritability of Frontotemporal Lobar Degeneration:

Validation of Pedigree Classification Criteria in a Northern Italy Cohort. *J Alzheimers Dis*. 2018;61(2):753-760. doi:10.3233/JAD-170661

13. Goldman JS, Farmer JM, Wood EM, et al. Comparison of family histories in FTLD subtypes and related tauopathies. *Neurology*. 2005;65(11):1817-1819. http://eutils.ncbi.nlm.nih.gov/entrez/eutils/elink.fcgi?dbfrom=pubmed&id=16344531&retmode=ref&cmd=prlinks

14. Cosseddu M, Benussi A, Gazzina S, et al. Mendelian forms of disease and age at onset affect survival in frontotemporal dementia. *Amyotroph Lateral Scler Frontotemporal Degener*. 2018;19(1-2):87-92. doi:10.1080/21678421.2017.1384020

15. Cosseddu M, Benussi A, Gazzina S, et al. Progression of behavioural disturbances in frontotemporal dementia: a longitudinal observational study. *Eur J Neurol*. 2020;27(2):265-272. doi:10.1111/ene.14071

16. Knopman DS, Kramer JH, Boeve BF, et al. Development of methodology for conducting clinical trials in frontotemporal lobar degeneration. *Brain*. 2008;131(11):2957-2968. doi:10.1093/brain/awn234

17. Miyagawa T, Brushaber D, Syrjanen J, et al. Utility of the global CDR ® plus NACC FTLD rating and development of scoring rules: Data from the ARTFL/LEFFTDS Consortium. *Alzheimer's Dement*. 2020;16(1):106-117. doi:10.1002/alz.12033

18. Rohrer JD, Woollacott IOC, Dick KM, et al. Serum neurofilament light chain protein is a measure of disease intensity in frontotemporal dementia. *Neurology*. 2016;87(13):1329-1336. doi:10.1212/WNL.0000000000003154

19. Borroni B, Malinverno M, Gardoni F, et al. Tau forms in CSF as a reliable biomarker for progressive supranuclear palsy. *Neurology*. 2008;71(22):1796-1803. doi:10.1212/01.wnl.0000335941.68602.39

20. Kurth F, Gaser C, Luders E. A 12-step user guide for analyzing voxel-wise gray matter asymmetries in statistical parametric mapping (SPM). *Nat Protoc*. 2015;10(2):293-304. doi:10.1038/nprot.2015.014

21. Farokhian F, Beheshti I, Sone D, Matsuda H. Comparing CAT12 and VBM8 for detecting brain morphological abnormalities in temporal lobe epilepsy. *Front Neurol*. 2017;8(AUG):428. doi:10.3389/fneur.2017.00428

22. Xu L, Groth KM, Pearlson G, Schretlen DJ, Calhoun VD. Source-based morphometry: The use of independent component analysis to identify gray matter differences with application to schizophrenia. *Hum Brain Mapp*. 2009;30(3):711-724. doi:10.1002/hbm.20540

23. Gupta CN, Calhoun VD, Rachakonda S, et al. Patterns of gray matter abnormalities in schizophrenia based on an international mega-analysis. *Schizophr Bull*. 2015;41(5):1133-1142.

doi:10.1093/schbul/sbu177

24. Calhoun VD, Adali T, Pearlson GD, Pekar JJ. A method for making group inferences from functional MRI data using independent component analysis. *Hum Brain Mapp*. 2002;16(2):131-131. doi:10.1002/hbm.10044

25. Mckeown MJ, Makeig S, Brown GG, et al. Analysis of fMRI data by blind separation into independent spatial components. *Hum Brain Mapp*. 1998;6(3):160-188. doi:10.1002/(sici)1097-0193(1998)6:3<160::aid-hbm5>3.3.co;2-r

26. Li YO, Adali T, Calhoun VD. Estimating the number of independent components for functional magnetic resonance imaging data. *Hum Brain Mapp*. 2007;28(11):1251-1266. doi:10.1002/hbm.20359

27. Hodges JR, Davies R, Xuereb J, Kril J, Halliday G. Survival in frontotemporal dementia. *Neurology*. 2003;61(3):349-354. http://eutils.ncbi.nlm.nih.gov/entrez/eutils/elink.fcgi?dbfrom=pubmed&id=12913196&retmode=ref&cmd=prlinks

28. Chiu WZ, Kaat LD, Seelaar H, et al. Survival in progressive supranuclear palsy and frontotemporal dementia. *J Neurol Neurosurg Psychiatry*. 2010;81(4):441-445. http://jnnp.bmj.com/cgi/doi/10.1136/jnnp.2009.195719

29. Borroni B, Grassi M, Archetti S, et al. Genetic background predicts poor prognosis in frontotemporal lobar degeneration. *Neurodegener Dis*. 2011;8(5):289-295. doi:10.1159/000322790

30. Panman JL, Venkatraghavan V, Van Der Ende EL, et al. Modelling the cascade of biomarker changes in GRN -related frontotemporal dementia. *J Neurol Neurosurg Psychiatry*. Published online 2021:494-501. doi:10.1136/jnnp-2020-323541

31. Gaetani L, Blennow K, Calabresi P, Di Filippo M, Parnetti L, Zetterberg H. Neurofilament light chain as a biomarker in neurological disorders. *J Neurol Neurosurg Psychiatry*. Published online 2019:870-881. doi:10.1136/jnnp-2018-320106

32. Steinacker P, Anderl-Straub S, Diehl-Schmid J, et al. Serum neurofilament light chain in behavioral variant frontotemporal dementia. *Neurology*. 2018;91(15):e1390-e1401. http://www.neurology.org/lookup/doi/10.1212/WNL.0000000000006318

33. Benussi A, Karikari TK, Ashton N, et al. Diagnostic and prognostic value of serum NfL and p-Tau 181 in frontotemporal lobar degeneration. *J Neurol Neurosurg Psychiatry*. 2020;91(9):960-967. doi:10.1136/jnnp-2020-323487

34. van der Ende EL, Xiao M, Xu D, et al. Neuronal pentraxin 2: a synapse-derived CSF biomarker in genetic frontotemporal dementia. *J Neurol Neurosurg Psychiatry*. 2020;91(6):612-621. doi:10.1136/jnnp-2019-322493

35. Heller C, Foiani MS, Moore K, et al. Plasma glial fibrillary acidic protein is raised in progranulin-associated frontotemporal dementia. *J Neurol Neurosurg Psychiatry*. 2020;91(3):263-270. doi:10.1136/jnnp-2019-321954

36. Solje E, Benussi A, Buratti E, Remes AM, Haapasalo A, Borroni B. State-of-the-Art Methods and Emerging Fluid Biomarkers in the Diagnostics of Dementia—A Short Review and Diagnostic Algorithm. *Diagnostics*. 2021;11(5):788. doi:10.3390/diagnostics11050788

37. Benussi A, Ashton NJ, Karikari TK, et al. Prodromal frontotemporal dementia: clinical features and predictors of progression. *Alzheimers Res Ther*. 2021;13(1):188. doi:10.1186/s13195-021-00932-2

38. Stern Y, Gazes Y, Razlighi Q, Steffener J, Habeck C. A task-invariant cognitive reserve network. *Neuroimage*. 2018;178(December 2017):36-45. doi:10.1016/j.neuroimage.2018.05.033

39. Garibotto V, Borroni B, Kalbe E, et al. Education and occupation as proxies for reserve in aMCI converters and AD: FDG-PET evidence. *Neurology*. 2008;71(17):1342-1349. http://www.neurology.org/cgi/doi/10.1212/01.wnl.0000327670.62378.c0

40. Borroni B, Padovani A, Premi E, et al. The FTLD-modified Clinical Dementia Rating scale is a reliable tool for defining disease severity in frontotemporal lobar degeneration: evidence from a brain SPECT study. *Eur J Neurol*. 2010;17(5):703-707. http://eutils.ncbi.nlm.nih.gov/entrez/eutils/elink.fcgi?dbfrom=pubmed&id=20050899&retmode=ref&cmd=prlinks

41. Premi E, Pilotto A, Alberici A, et al. FOXP2, APOE, and PRNP: new modulators in primary progressive aphasia. *J Alzheimers Dis*. 2012;28(4):941-950. http://eutils.ncbi.nlm.nih.gov/entrez/eutils/elink.fcgi?dbfrom=pubmed&id=22129783&retmode=ref&cmd=prlinks

42. Premi E, Gazzina S, Bozzali M, et al. Cognitive Reserve in Granulin-Related Frontotemporal Dementia: from Preclinical to Clinical Stages. *PLoS One*. 2013;8(9):e74762. http://dx.plos.org/10.1371/journal.pone.0074762.t001

43. Premi E, Grassi M, Van Swieten J, et al. Cognitive reserve and TMEM106B genotype modulate brain damage in presymptomatic frontotemporal dementia: A GENFI study. *Brain*. 2017;140(6):1784-1791. doi:10.1093/brain/awx103

44. Gazzina S, Grassi M, Premi E, et al. Education modulates brain maintenance in presymptomatic frontotemporal dementia. *J Neurol Neurosurg Psychiatry*. Published online 2019:1-7. doi:10.1136/jnnp-2019-320439

45. Massimo L, Zee J, Xie SX, et al. Occupational attainment influences survival in autopsy-confirmed frontotemporal degeneration. *Neurology*. 2015;84(20):2070-2075. http://www.neurology.org/cgi/doi/10.1212/WNL.0000000000001595

46. Van Loenhoud AC, Van Der Flier WM, Wink AM, et al. Cognitive reserve and clinical progression in Alzheimer disease: A paradoxical relationship. *Neurology*. 2019;93(4):E334-E346. doi:10.1212/WNL.0000000000007821

47. Giunta M, Solje E, Gardoni F, Borroni B, Benussi A. Experimental Disease-Modifying Agents for Frontotemporal Lobar Degeneration. *J Exp Pharmacol*. 2021;Volume 13:359-376. doi:10.2147/JEP.S262352

CHAPTER 4 – STUDY 2

Early neurotransmitters changes in prodromal Frontotemporal Dementia: a GENFI study

Enrico Premi*, Marta Pengo*, Irene Mattioli, Valentina Cantoni, Juergen Dukart, Roberto Gasparotti, Emanuele Buratti, Alessandro Padovani, Martina Bocchetta, Emily G. Todd, Arabella Bouzigues, David M. Cash, Rhian S. Convery, Lucy L. Russell, Phoebe Foster, David L. Thomas, John C. van Swieten, Lize C. Jiskoot, Harro Seelaar, Daniela Galimberti, Raquel Sanchez-Valle, Robert Laforce Jr, Fermin Moreno MD, Matthis Synofzik, Caroline Graff, Mario Masellis, Maria Carmela Tartaglia, James B. Rowe, Kamen A. Tsvetanov, Rik Vandenberghe, Elizabeth Finger, Pietro Tiraboschi, Alexandre de Mendonça, Isabel Santana, Chris R. Butler, Simon Ducharme, Alexander Gerhard, Johannes Levin MD, Markus Otto, Sandro Sorbi, Isabelle Le Ber, Florence Pasquier, Jonathan D. Rohrer, Barbara Borroni on behalf of the Genetic Frontotemporal dementia Initiative (GENFI)

* These authors contributed equally to this work.

Published in *Neurobiology of Disease 2023*, doi: 10.1016/j.nbd.2023.106068.

Abstract

Introduction. Neurotransmitters deficits in Frontotemporal Dementia (FTD) are still poorly understood. Better knowledge of neurotransmitters impairment, especially in prodromal disease stages, might tailor symptomatic treatment approaches.

Materials and methods. In the present study, we applied JuSpace toolbox, which allowed for cross-modal correlation of Magnetic Resonance Imaging (MRI)-based measures with nuclear imaging derived estimates covering various neurotransmitter systems including dopaminergic, serotonergic, noradrenergic, GABAergic and glutamatergic neurotransmission.

We included 392 mutation carriers (157 *GRN*, 164 *C9orf72*, 71 *MAPT*), together with 276 non-carrier cognitively healthy controls (HC). We tested if the spatial patterns of grey matter volume (GMV) alterations in mutation carriers (relative to HC) are correlated with specific neurotransmitter systems in prodromal (CDR® plus NACC FTLD=0.5) and in symptomatic (CDR® plus NACC FTLD≥1) FTD.

Results. In prodromal stages of *C9orf72* disease, voxel-based brain changes were significantly associated with spatial distribution of dopamine and acetylcholine pathways; in prodromal *MAPT* disease with dopamine and serotonin pathways, while in prodromal *GRN* disease no significant findings were reported (p<0.05, Family Wise Error corrected). In symptomatic FTD, a widespread involvement of dopamine, serotonin, glutamate and acetylcholine pathways across all genetic subtypes was found. Social cognition scores, loss of empathy and poor response to emotional cues

were found to correlate with the strength of GMV colocalization of dopamine and serotonin pathways (all p<0.01).

Conclusions. This study, indirectly assessing neurotransmitter deficits in monogenic FTD, provides novel insight into disease mechanisms and might suggest potential therapeutic targets to counteract disease-related symptoms.

Introduction

Frontotemporal dementia (FTD) is a neurodegenerative disorder characterised by progressive behavioural, linguistic, dysexecutive and motor disturbances[1,2]. Its causes are genetic in about a third of cases, with mutations in *microtubule-associated protein tau* (*MAPT*), *progranulin* (*GRN*) and *chromosome 9 open reading frame 72* (*C9orf72*) being the commonest causes[3,4]. Even if the behavioral variant of FTD is the most common presentation, each mutation group is characterized by distinctive neuropathological, clinical and imaging features (Greaves, J Neurol 2019). *C9orf72* mutation carriers frequently present psychiatric disturbances and an early episodic memory impairment (Boeve, Brain 2012; Poos, Alzh Dem 2021); they display diffuse and symmetric cortical atrophy, involving also posterior regions, thalamus and cerebellum (Whitwell, Brain 2012; Boeve, Brain 2012). On the other hand, *GRN* and *MAPT* mutation carriers exhibit more prominent language impairment (Beck, Brain 2008; Le Ber, Brain 2008). Moreover, *GRN* mutation is associated with early parietal lobe dysfunction (Beck, Brain 2008). *GRN* mutation carriers show a striking asymmetrical pattern of cortical atrophy, whereas *MAPT* mutation carriers a symmetrical brain atrophy involving mainly the anteromedial temporal lobes. Early neuroimaging alterations are described around 5-10 years before phenoconversion with a specific distribution in each group (Rohrer, Lancet Neurology 2015).

Despite the continuous advancement of knowledge on disease-related mechanisms, little is known about neurotransmitter processes that occur in FTD. Exploring neurotransmitter pathways involved might shed more light on disease pathogenesis; moreover, since each mutation group is characterized by different clinical and imaging features, we might hypothesize that diverse neurotransmitter pathways are involved. As a consequence, research in this field might aid in identify tailored therapeutic targets for symptomatic interventions.

Although impairment of dopaminergic, serotoninergic, GABAergic and glutamatergic pathways in autopsy studies has been demonstrated [5], clinical trials have failed to report substantial benefits from neurotransmitter modulation on clinical symptoms in FTD [6]. This discrepancy may be due to weaknesses in research methodology and small studies in unstratified populations.

Recent advancements in positron emission tomography (PET) and single photon computed emission tomography (SPECT) tracer development resulted in novel tracers that can reliably measure the availability of specific receptors. However, the need of large samples and of comparing multiple tracers in the same subjects

have prevented reliable results on *in vivo* neurotransmitter pathways in neurodegenerative disorders, and especially in FTD. Indeed, only a few small series studies or case reports are available in FTD and in FTD-related mutations [7–13].

To fill this gap, JuSpace toolbox has been recently developed with the aim to gather neurotransmitter pathways abnormalities combining MRI-based measures and a list of included PET and SPECT maps covering various neurotransmitter pathways [14]. JuSpace considers spatial pattern of brain alterations based on MRI measures derived by comparison between different groups (e.g. patients versus healthy controls), and it performs a correlation between these alterations and each receptor/transporter map included in the toolbox [15]. JuSpace therefore is able to explore if the spatial pattern of observed brain changes in the disease of interest are related to the distribution of specific neurotransmitters pathways, as derived from independent healthy volunteer populations.

In the present study, we aimed to indirectly unravel neurotransmitter pathways changes, in particular in the earliest disease phases, namely in prodromal FTD, and to assess correlation with clinical symptoms. To achieve this, we applied JuSpace tool on a large sample of subjects from the international Genetic FTD Initiative (GENFI), considering individuals at different disease stages and with different pathogenetic mutations, and we evaluated impairment of dopamine, serotonin, glutamate, GABA, noradrenaline and acetylcholine systems.

Materials and methods

Subjects

Data for this study were drawn from the GENFI multicenter cohort study, which consists of 26 research centers in Europe and Canada. Inclusion and exclusion criteria have been previously described [16]. Local ethics committees approved the study at each site and all participants provided written informed consent according to the Declaration of Helsinki.

We considered both symptomatic patients fulfilling current clinical criteria for FTD [1,2], and asymptomatic participants *at risk* to carry *GRN, C9orf72* or *MAPT* mutations. Between January 2012 and March 2020, we considered 668 participants, of which 392 were mutation carriers (157 with *C9orf72,* 164 with *GRN*, and 71 with *MAPT* mutations) and 276 were mutation non-carriers. Mutation carriers were grouped according to disease severity, as measured by Clinical Dementia Rating Dementia Staging Instrument plus behaviour and language domains from the National Alzheimer's Coordinating Center and Frontotemporal lobar degeneration modules (CDR® plus NACC FTLD, from here on referred as CDR)[17] into asymptomatic subjects (CDR=0), prodromal FTD (CDR=0.5) or symptomatic FTD patients (CDR$\geq$1). Mutation non-carriers were considered as healthy control group (HC).

Included subjects underwent a careful recording of demographic data and a standardized clinical and neuropsychological assessment, as previously published [18].

MRI acquisition

MRI protocol was common to all the GENFI sites, and adapted for different scanners. Each subject underwent a 3T MRI at each local site from three different manufacturers (Philips Healthcare, GE Healthcare Life Sciences, Siemens Healthcare Diagnostic). The protocol included a volumetric T1-weighted MRI scan (magnetization-prepared rapid gradient echo, MPRAGE), as previously reported [16]. During scanning, subjects were asked to keep their eyes closed, not to think of anything in particular, and not to fall asleep.

MRI preprocessing and analyses

T1-weighted images were processed and analysed with the voxel-based morphometry (VBM) pipeline implemented in the Computational Anatomy Toolbox (CAT12 v.1742) (www.neuro.uni-jena.de/cat) for SPM12 (SPM12 v.7219) (www.fil.ion.ucl.ac.uk/spm/software/spm12) running on MATLAB R2019b (the MathWorks, Inc., Natick, Massachusetts, United States). The VBM pipeline consists of several stages (tissue segmentation, spatial normalization to a standard Montreal National Institute [MNI] template, modulation and smoothing), as previously described [19]. CAT12 potentially provides more robust and accurate performances compared to other VBM pipelines [20]. The normalized and modulated grey matter images were then smoothed with 8 mm full width at half-maximum Gaussian kernel to reduce the probability of misalignment errors, increasing the chance to detect differences over small regions of the brain.

To test for group differences in grey matter volume (GMV) a General Linear Model using SPM12 was implemented, considering age, gender and site as nuisance variables. The statistical threshold was set to $p<0.05$ corrected for multiple comparisons (whole-brain family-wise error, FWE).

Spatial correlation with neurotransmitter density maps

We used the JuSpace toolbox to test if the spatial patterns of GMV alterations in asymptomatic, prodromal and symptomatic FTD subjects (relative to HC) are correlated with specific neurotransmitter systems [15]. We considered a list of included PET and SPECT maps in JuSpace toolbox, covering various neurotransmitter systems [15].

JuSpace creates a spatial pattern of GMV, comparing two different groups (e.g. patients versus healthy controls), and therefore aims to assess if the spatial patterns of brain changes observed in patients (as compared to healthy controls) are related to the distribution of specific neurotransmitters systems, these latter derived from independent healthy volunteer populations [15]. Thus, it performs a correlation between these alterations and each receptor/transporter map included in the toolbox.

Confounding effects of age, gender and site were regressed out from all images prior to these analyses [15].

We considered serotonin transmission, i.e. the 5-hydroxytryptamine 1a (5-HT1a) receptor, the 5-HT1b receptor, the 5-HT2a receptor, and the serotonin transporter SERT; dopamine transmission, i.e. the D1

receptor, the D2 receptor, the dopamine transporter (DAT), and the FluoroDOPA, the GABAa receptors, the vesicular acetylcholine transporter (VAChT), the metabotropic glutamate receptor type 5 (mGLUR5), and the noradrenaline transporter (NAT). Each map included in Juspace toolbox was derived by PET data with the exception of DAT, which was derived from SPECT data, and each map was built up with specific numbers of healthy volunteers (Supplementary Table 1 for details). Using JuSpace toolbox, native normalized, modulated and smoothed grey matter images were parceled in regions of interest using the Neuromorphometrics Atlas (MICCAI 2012 Grand Challenge and Workshop on Multi-Atlas Labeling, www.masi.vuse.vanderbilt.edu/workshop2012/index.php/Challenge_Details). Mean regional values of GMV were extracted for all patients and HC. Spearman correlation coefficients (Fisher's Z transformed) were calculated between these z-transformed GMV maps of the patients and the spatial distribution of the respective neurotransmitter maps included in JuSpace toolbox. Exact permutation-based p-values as included in JuSpace (10,000 permutations randomly assigning group labels using orthogonal permutations) were computed to check if the distribution of the observed Fisher's z-transformed individual correlation coefficients were significantly different from zero. All analyses were Family Wise Error (FWE) corrected for the number of tests. Spearman correlation coefficients (Fisher's Z transformed) were calculated between these z-transformed GMV maps and the spatial distribution of the respective neurotransmitter maps. Exact permutation-based p-values as implemented in JuSpace (10,000 permutations randomly assigning group labels using orthogonal permutations) were computed to test if the observed correlation coefficients across patients deviate from a null distribution.

Statistical analysis

Comparisons of demographic and clinical characteristics were performed by the Student's t-test for continuous variables and the χ^2 test for categorical variables.

Spearman correlation was used to assess the relationship between each neurotransmitter output obtained with Juspace (i.e., the GMV-neurotransmitters correlation, Fisher's Z transformed) and clinical or behavioural data. Statistical significance was set at $p<0.05$, corrected for multiple comparisons (Family Wise Error-FWE) (SPSS Statistics 22.0, Chicago, USA).

Data availability

All study data, including raw and analysed data, and materials will be available from the GENFI Coordinator upon reasonable request. The software applied is publicly available at https://github.com/juryxy/JuSpace.

Results

Participants

Demographic characteristics of mutation carriers and non-carriers are reported in **Table 1**. In the present study, we considered 157 *C9orf72* expansion carriers, namely 85 asymptomatic, 33 prodromal and 39 symptomatic subjects; 164 with *GRN* mutation carriers, namely 107 asymptomatic, 33 prodromal and 24 symptomatic subjects, and 71 *MAPT* mutation carriers, namely 39 asymptomatic, 18 prodromal and 14 symptomatic subjects.

Standard voxel-wise analyses of GMV demonstrated the typical pattern of brain atrophy in mutations subgroups, according to disease stage, as previously published[16,21–27] (see **Supplementary Figure 1**).

Table 1. Demographic and clinical characteristics of the studied group.

Variable	HC	*C9orf72*	*GRN*	*MAPT*	p-value*
Number	276	157	164	71	
Age, years	46.5±13.2	49.6±13.2	48.5±12.9	44.6±12.8	0.02
Sex, female %	57.6	54.1	59.8	52.1	0.14^
Education, years	14.3±3.3	14.0±3.2	14.2±3.8	14.6±3.0	0.56

Demographic characteristics are expressed as mean ± standard deviation, unless otherwise specified. HC = Healthy controls, *C9orf72 = chromosome 9 open reading frame 72* mutation carriers; *GRN = progranulin* mutation carriers; *MAPT = microtubule-associated protein tau* mutation carriers; *Student-t test, unless otherwise specified; ^ Chi-Square test.

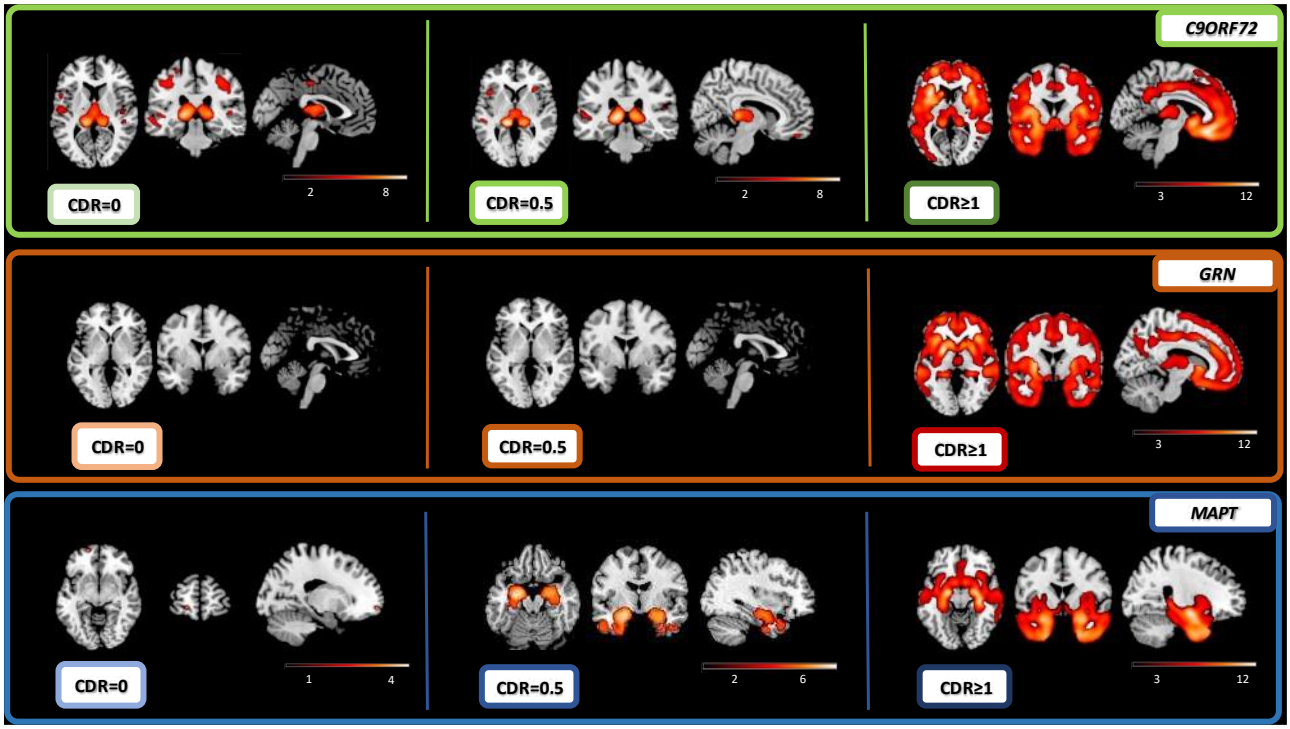

Supplementary Figure 1. Voxel-wise analyses in C9orf72, GRN and MAPT mutation carriers as compared to HC.

C9orf72 = *chromosome 9 oper reading frame 72* mutation carriers; *GRN* = *progranulin* mutation carriers; *MAPT* = *microtubule-associated protein tau* mutation carriers; CDR = Clinical Dementia Rating Staging Instrument plus behavior and language domains from the National Alzheimer's Coordinating Center and Frontotemporal lobar degeneration modules. Only clusters surviving correction for multiple comparisons ($p < 0.05$ family wise error [FWE] whole-brain) were shown. Significant clusters were superimposed on a standardized MRI T1 3D template.

Neurotransmitters deficits in C9orf72 expansion carriers

In prodromal stage of *C9orf72* disease (CDR=0.5), as compared to HC, voxel-based brain changes were significantly associated with spatial distribution of dopamine transporter DAT (r=-0.13, *p*=0.02) and acetylcholine transporter (r=-0.12, *p*=0.02). In fully symptomatic stage (CDR≥1), additional voxel-based brain changes were significantly associated with spatial distribution of

5-HT1a receptors (r=-0.30, *p*=0.01), D1 receptors (r=-0.28, *p*=0.01), FDOPA (r=-0.13, *p*=0.02), and mGluR5 (r=-0.20, *p*=0.01) (see **Figure 1** and **Table 2**). The negative correlation coefficients indicate GMV reduction in patients as compared to HC in areas with high neurotransmitters density.

There was no significant difference in spatial distribution in asymptomatic expansion carriers (CDR=0) as compared to HC.

Neurotransmitters deficits in GRN mutation carriers

No voxel-based brain changes were significantly associated with neurotransmitter spatial distribution in prodromal *GRN* disease (CDR=0.5). In fully symptomatic stage (CDR≥1), as compared to HC, voxel-based brain changes were significantly associated with spatial distribution of 5-HT1a receptors (r=-0.25, *p*=0.01), D1 receptors (r=-024, *p*=0.01), dopamine transporter DAT (r=-0.14, *p*=0.01), FDOPA (r=-0.11, *p*=0.02), acetylcholine transporter (r=-0.16, *p*=0.02), and mGluR5 (r=-0.23, *p*=0.01) (see **Figure 1** and **Table 2**).

There was no significant difference in spatial distribution in asymptomatic mutation carriers (CDR=0) as compared to HC.

Neurotransmitters deficits in MAPT mutation carriers

In prodromal stage of *MAPT* disease (CDR=0.5), as compared to HC, voxel-based brain changes were significantly associated with spatial distribution of 5-HT1a receptors (r=-0.34, *p*=0.01), D1 receptors (r=-0.20, *p*=0.01), dopamine transporter DAT (r=-0.30, *p*=0.01), FDOPA (r=-0.16, *p*=0.01), and SERT (r=-0.16, *p*=0.01). In fully symptomatic stage (CDR≥1), additional voxel-based brain changes were significantly associated with spatial distribution of 5-HT1b receptors (r=0.14, *p*=0.02) and acetylcholine transporter (r=-0.18, *p*=0.02) (see **Figure 1** and **Table 2**).

There was no significant difference in spatial distribution in asymptomatic mutation carriers (CDR=0) as compared to HC.

Table 2. Results of spatial correlation analyses for included participants according to mutation subtype and disease stage.

	CDR=0.5		CDR≥1	
Mutation	***r***	***p*-value**	***r***	***p*-value**
C9orf72				
5HT1a	-0.08	0.38	**-0.30**	**0.01**
5HT1b	0.01	0.98	-0.01	0.91
5HT2a	-0.01	0.98	-0.09	0.26
SERT	-0.09	0.08	-0.08	0.91
D1	-0.01	0.09	**-0.28**	**0.01**
D2	-0.08	0.26	0.02	0.91
DAT	**-0.13**	**0.02**	**-0.22**	**0.01**
FDOPA	-0.05	0.64	**-0.13**	**0.02**
GABAa	0.07	0.98	-0.07	0.91
NAT	-0.08	0.16	0.04	0.55
VAchT	**-0.12**	**0.02**	**-0.20**	**0.01**
mGluR5	-0.07	0.45	**-0.20**	**0.01**
GRN				
5HT1a	-0.05	0.94	**-0.25**	**0.01**
5HT1b	-0.03	0.94	-0.02	0.73
5HT2a	-0.04	0.94	-0.08	0.14
SERT	0.02	0.94	-0.02	0.73
D1	-0.06	0.94	**-0.24**	**0.01**
D2	0.02	0.94	0.01	0.73
DAT	-0.03	0.94	**-0.14**	**0.01**
FDOPA	-0.02	0.94	**-0.11**	**0.02**
GABAa	-0.01	0.94	-0.01	0.73
NAT	0.01	0.94	0.06	0.22
VAchT	-0.08	0.44	**-0.16**	**0.01**
mGluR5	-0.09	0.36	**-0.23**	**0.01**
MAPT				
5HT1a	**-0.34**	**0.01**	**-0.50**	**0.01**
5HT1b	0.09	0.30	**0.14**	**0.02**
5HT2a	-0.01	0.97	0.02	0.73
SERT	**-0.16**	**0.01**	**-0.26**	**0.01**
D1	**-0.20**	**0.01**	**-0.37**	**0.01**
D2	0.04	0.97	0.13	0.07
DAT	**-0.30**	**0.01**	**-0.45**	**0.01**
FDOPA	**-0.16**	**0.01**	**-0.36**	**0.01**
GABAa	-0.01	0.97	0.06	0.73
NAT	0.01	0.97	0.11	0.08
VAchT	-0.12	0.14	**-0.18**	**0.02**
mGluR5	-0.05	0.97	-0.05	0.73

Fisher's z-transformed correlation coefficients (*r*) for each neurotransmitter map are reported, with corresponding *p*-values. The negative correlation coefficients indicate GMV reduction in patients as compared to HC in areas with high neurotransmitters density.

Significant results in boldface; *p*-values corrected for multiple comparison (FWE correction).

CDR = Clinical Dementia Rating Dementia Staging Instrument plus behaviour and language domains from the National Alzheimer's Coordinating Center and Frontotemporal lobar degeneration; 5HT = 5-hydroxytryptamine; SERT = serotonin transporter; D = dopamine; DAT= dopamine transporter; FDOPA= Fluorodopa; GABAa = γ-Aminobutyric acid type A; NAT = noradrenaline; VAChT = Vesicular acetylcholine transporter; mGLUR5 = metabotropic glutamate receptor type 5.

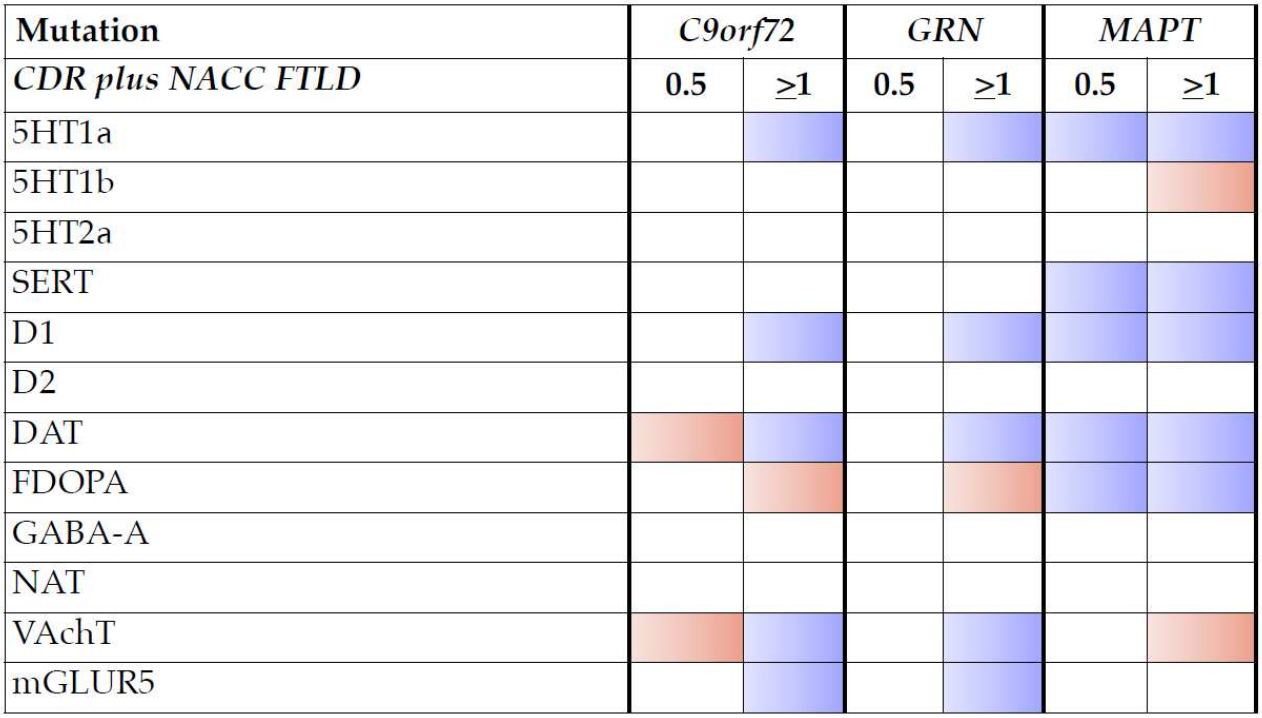

Figure 1. Results of spatial correlation analyses according to mutation and disease stage.

Significant correlations for each neurotransmitter map in the different genetic groups are represented, considering each mutation group (*C9orf72*, *GRN*, *MAPT*) and disease stage according to Clinical Dementia Rating Dementia Staging Instrument plus behaviour and language domains from the National Alzheimer's Coordinating Center and Frontotemporal lobar degeneration modules (CDR plus NACC FTLD, here referred as CDR).

5HT = 5-hydroxytryptamine; SERT = serotonin transporter; D = dopamine; DAT= dopamine transporter; FDOPA= Fluorodopa; GABAa = γ-Aminobutyric acid type A; NAT = noradrenaline; VAChT = Vesicular acetylcholine transporter; mGLUR5 = metabotropic glutamate receptor type 5.

p-values<0,01 in blue and *p*-values<0.05 in red, corrected for multiple comparisons (Bonferroni's correction).

Neurotransmitter impairment and social cognition in monogenic FTD

In order to explore a possible association between neurotransmitter impairments and clinical outcomes, we assessed the relationship between GMV-neurotransmitters correlation coefficients and social cognition/loss of empathy data in monogenic FTD patients (CDR>0). We considered only GMV-neurotransmitters correlation coefficients significantly impaired in FTD and we excluded those highly correlated to each other (Spearman correlations coefficients>0.80), namely FDOPA. Thus, we included in the present analyses 5-HT1a receptors, D1 receptors, DAT, VAchT, and mGLUR5.

We considered *a)* Ekman facial emotion recognition task and *Faux-pas* recognition test (mini-SEA) scores (the lower the scores the worse the performances)[28], and *b)* loss of empathy and *c)* poor response to social/emotional cues, as reported by caregiver (which were rated on a 5-point scale: 0 = absent, 0.5 = questionable/very mild, 1 = mild, 2 = moderate, and 3 = severe). Significant threshold was set at $p \leq 0.002$, after correction for multiple comparisons.

In *C9orf72* expansion carriers, mini-SEA scores (n=58) were positively correlated with the strength of GMV colocalization of 5HT1a receptors (r=0.449, p<0.001) and D1 receptors (r=0.402, *p*=0.002); loss of empathy (n=71) was negatively correlated with D1 receptors (r=-0.423, *p*<0.001) and poor response to emotional cues (n=71) with 5HT1a receptors (r=-0.406, p<0.001) and D1 receptors (r=-0.454, *p*<0.001). No other significant correlations between cognitive data and GMV neurotransmitters co-localization at pre-established statistical threshold were reported.

In *GRN* mutation carriers, loss of empathy (n=57) was negatively correlated with D1 receptors (r=-0.439, *p*=0.001) and poor response to emotional cues (n=57) with D1 receptors (r=-0.542, *p*<0.001) and DAT (r=-0.497, *p*<0.001).

The relatively low number of prodromal or symptomatic *MAPT* mutation carriers prevented us to run correlation analyses in this group.

Supplementary Table 1. Receptor/transporters considered in the present study.

Receptor/ transporter	Neurotransmitter	Tracer	Modality	N healthy volunteers	Reference
D1	dopamine	[11C]SCH23390	PET	13	Kaller et al, 2017[29]
D2	dopamine	[11C]Raclopide	PET	7	Alakurtti et al, 2015[30]
DAT	dopamine	[123I]FP-CIT	SPECT	174	Dukart et al, 2018[14]
Fluoro-DOPA	dopamine	[18F]Fluorodopa	PET	12	Gomez et al, 2018[31]
5-HT1a	serotonin	[11C]WAY-100635	PET	36	Hansen et al, 2021[32]
5-HT2a	serotonin	[11C]Cimbi-36	PET	29	Beliveau et al, 2017[33]
SERT	serotonin	[11C]DASB	PET	100	Beliveau et al, 2017[33]
GABAa	GABA	[11C]Flumazenil	PET	6	Dukart et al, 2018[14]
VAChT	acethylcoline	[18F]FEOBV	PET	18	Aghourina et al, 2017[34]
mGLUR5	glutamate	[11C]ABP688	PET	73	Smart et al, 2019[35]
NAT	noradrenaline	[^{11}C]O-MRB	PET	11	Hesse et al, 2017[36]

5HT = 5-hydroxytryptamine; SERT = serotonin transporter; VAChT = Vesicular acetylcholine transporter; mGLUR5 = metabotropic glutamate receptor type 5; NAT = noradrenaline transporter.

Discussion

In the last years, a giant step forward has been made in the knowledge of genetic basis of FTD and gene-related pathogenetic mechanisms, and more recently experimental therapeutic trials targeting *C9orf72*, *GRN*, or *MAPT* have been proposed.

Despite this, neurotransmitter impairment in monogenic FTD and differences according to causative gene have not been assessed yet. Restoring these deficits, individually or in combination, has the potential advantage to improve clinical and behavioral symptoms and may help in further understanding of the disease.

In the present work, we investigated if the spatial distribution of grey matter atrophy observed in different subtypes of monogenic prodromal and symptomatic FTD are related to the localization of specific neurotransmitters pathways as derived from independent healthy volunteer populations[15]. These data have been obtained by JuSpace toolbox, which compares PET and SPECT derived neurotransmitter maps with other imaging modalities such as MRI data[15]. In our study, we considered grey matter atrophy as an imaging biomarker of neurodegeneration; however, other biomarkers might be even more sensitive, in particular in the prodromal phase (e.g. measures derived from functional imaging data).

We reported that grey matter alterations in the prodromal disease stages specifically co-localised with different neurotransmitters pathways, involving dopamine and cholinergic systems in *C9orf72* expansion carriers, dopamine and serotonin in *MAPT* mutation carriers, and with no significant detectable changes in *GRN* mutation carriers. Indeed, it has been reported that TDP-43 proteinopathy, the pathological hallmark of *C9orf72* expansions, may cause dopamine alterations[28] and that *C9orf72* expansion carriers exhibit more pronounced memory deficits as compared to *MAPT* and *GRN* mutation carriers[28], tasks for which cholinergic system is key. On the other hand, in regard to *MAPT* mutations, it has been proposed a link between dopamine and serotonin neurotransmission and phosphorylation state of tau protein[37,38], with tau being able to disrupt the survival of dopaminergic and serotoninergic neurons in *Drosophila* and in animal models[39,40]. Finally, the lack of significant findings in *GRN* mutation carriers is in line with previous imaging studies reporting less functional and structural brain abnormalities in the prodromal stages than other genetic subtypes[23,41–43].

Conversely, symptomatic disease was associated with a broad involvement of different circuits and significant changes of dopaminergic, serotoninergic and cholinergic pathways in all monogenic FTD subtypes. We also found additional glutamatergic pathway involvement in *C9orf72* and *GRN* symptomatic mutations carriers. Of

note, GABAergic and noradrenergic pathways resulted spared in monogenic FTD. These findings confirm and extend previous literature data on autopsy studies as well as a recent study on a large group of PPA patients[44], but also suggest an additional involvement of cholinergic system in monogenic FTD which is absent in sporadic disease[5,45]. As compared to previous studies[5], we indeed failed to confirm a co-localization of grey matter alteration and the GABAergic system.

Interestingly, we also suggest that dopamine and serotonin pathways may be associated with social cognition deficits and loss of empathy, which represents an early clinical feature in FTD[46]. Dopamine, in addition to be linked to movement disorders, has long been known for its role in reward processing and emotional recognition[47,48], and most recently a central role of serotonin circuits has been recognized in emotion regulation and social behaviour[49–51].

Most studies evaluating pharmacological approaches in FTD have not reported clear-cut results[6]. Findings herein reported argue for further considering pharmacological manipulation of specific neurotransmitters, specifically considering FTD subtypes and disease stage to counteract related symptoms. In this view, investigating neurotransmitter pathways involved might aid in identifying biochemical alterations, which together with clinical, biological and neuroimaging biomarkers might be helpful to characterize more in detail the different FTD subtypes. In comparison to other biomarkers, exploring neurotransmitter impairment might hold the advantage to identify tailored therapeutic targets to improve symptomatic treatment.

Nonetheless, we acknowledge that this study entails some limitations. First, future implemented neurotransmitters maps in JuSpace may further refine the present findings. Moreover, the maps available have been recently obtained, and present some limitations that might to be addressed, e.g. the variability in the number of controls cases in each map and receptor density assessment is not necessarily related to neurotransmitter density. Moreover, JuSpace toolbox has not yet been validated in aging populations with substantial atrophy (anche se di questo non sono sicura…). Second, we considered prodromal monogenic FTD, and these results cannot be extended to prodromal sporadic disease. Third, other toolbox mapping neurotransmitter systems and their implementation, such as NeuroMaps, may be also considered[52]. Finally, JuSpace toolbox indirectly assess neurotransmitter impairment, and confirmation with *post mortem* studies is warranted to confirm the results observed.

In conclusions, this study suggests that JuSpace is a helpful tool to indirectly assess neurotransmitter deficits in neurodegenerative dementias and may provide novel insight into disease mechanisms and intervention pharmacological targets.

References

1. Rascovsky K, Hodges JR, Knopman D, et al. Sensitivity of revised diagnostic criteria for the behavioural variant of frontotemporal dementia. *Brain*. 2011;134(Pt 9):2456-2477. doi:10.1093/BRAIN/AWR179
2. Gorno-Tempini ML, Hillis AE, Weintraub S, et al. Classification of primary progressive aphasia and its variants. *Neurology*. 2011;76(11):1006-1014. doi:10.1212/WNL.0B013E31821103E6
3. Borroni B, Padovani A. Dementia: a new algorithm for molecular diagnostics in FTLD. *Nat Rev Neurol*. 2013;9(5):241-242. doi:10.1038/NRNEUROL.2013.72
4. Greaves C V., Rohrer JD. An update on genetic frontotemporal dementia. *J Neurol*. 2019;266(8):2075-2086. doi:10.1007/s00415-019-09363-4
5. Murley AG, Rowe JB. Neurotransmitter deficits from frontotemporal lobar degeneration. *Brain*. 2018;141(5):1263-1285. doi:10.1093/BRAIN/AWX327
6. Panza F, Lozupone M, Seripa D, et al. Development of disease-modifying drugs for frontotemporal dementia spectrum disorders. *Nat Rev Neurol*. 2020;16(4):213-228. doi:10.1038/S41582-020-0330-X
7. Sperfeld AD, Collatz MB, Baier H, et al. FTDP-17: an early-onset phenotype with parkinsonism and epileptic seizures caused by a novel mutation. *Ann Neurol*. 1999;46(5):708-715. doi:10.1002/1531-8249(199911)46:5<708::aid-ana5>3.0.co;2-k
8. Miyoshi M, Shinotoh H, Wszolek ZK, et al. In vivo detection of neuropathologic changes in presymptomatic MAPT mutation carriers: a PET and MRI study. *Parkinsonism Relat Disord*. 2010;16(6):404-408. doi:10.1016/J.PARKRELDIS.2010.04.004
9. Meloni M, Farris R, Solla P, Mascia MM, Marrosu F, Cannas A. C9ORF72 Intermediate Repeat Expansion in a Patient With Psychiatric Disorders and Progressive Cerebellar Ataxia. *Neurologist*. 2017;22(6):245-246. doi:10.1097/NRL.0000000000000147
10. Carecchio M, Galimberti D, Fenoglio C, et al. Evidence of pre-synaptic dopaminergic deficit in a patient with a novel progranulin mutation presenting with atypical parkinsonism. *J Alzheimers Dis*. 2014;38(4):747-752. doi:10.3233/JAD-131151
11. Leuzy A, Zimmer ER, Dubois J, et al. In vivo characterization of metabotropic glutamate receptor type 5 abnormalities in behavioral variant FTD. *Brain Struct Funct*. 2016;221(3):1387-1402.

doi:10.1007/S00429-014-0978-3

12. Takeshige H, Nakayama S, Nishioka K, Li Y, Motoi Y, Hattori N. Marked Reduction in the Striatal Dopamine Transporter Uptake During the Early Stage of Motor Symptoms in Patients with the MAPT N279K Mutation. *Intern Med*. 2018;57(20):3015-3019. doi:10.2169/INTERNALMEDICINE.0454-17

13. Murley AG, Rouse MA, Simon Jones P, et al. GABA and glutamate deficits from frontotemporal lobar degeneration are associated with disinhibition. 2020;143(11). doi:10.1093/BRAIN/AWAA305

14. Dukart J, Holiga Š, Chatham C, et al. Cerebral blood flow predicts differential neurotransmitter activity. *Sci Rep*. 2018;8(1). doi:10.1038/S41598-018-22444-0

15. Dukart J, Holiga S, Rullmann M, et al. JuSpace: A tool for spatial correlation analyses of magnetic resonance imaging data with nuclear imaging derived neurotransmitter maps. *Hum Brain Mapp*. 2021;42(3):555-566. doi:10.1002/HBM.25244

16. Rohrer JD, Nicholas JM, Cash DM, et al. Presymptomatic cognitive and neuroanatomical changes in genetic frontotemporal dementia in the Genetic Frontotemporal dementia Initiative (GENFI) study: a cross-sectional analysis. *Lancet Neurol*. 2015;14(3):253-262. doi:10.1016/S1474-4422(14)70324-2

17. Miyagawa T, Brushaber D, Syrjanen J, et al. Utility of the global CDR ® plus NACC FTLD rating and development of scoring rules: Data from the ARTFL/LEFFTDS Consortium. *Alzheimers Dement*. 2020;16(1):106-117. doi:10.1002/ALZ.12033

18. Premi E, Calhoun VD, Diano M, et al. The inner fluctuations of the brain in presymptomatic Frontotemporal Dementia: The chronnectome fingerprint. *Neuroimage*. 2019;189:645-654. doi:10.1016/J.NEUROIMAGE.2019.01.080

19. Kurth F, Gaser C, Luders E. A 12-step user guide for analyzing voxel-wise gray matter asymmetries in statistical parametric mapping (SPM). *Nat Protoc*. 2015;10(2):293-304. doi:10.1038/NPROT.2015.014

20. Farokhian F, Beheshti I, Sone D, Matsuda H. Comparing CAT12 and VBM8 for Detecting Brain Morphological Abnormalities in Temporal Lobe Epilepsy. *Front Neurol*. 2017;8(AUG). doi:10.3389/FNEUR.2017.00428

21. Beck J, Rohrer JD, Campbell T, et al. A distinct clinical, neuropsychological and radiological

phenotype is associated with progranulin gene mutations in a large UK series. *Brain*. 2008;131(Pt 3):706-720. doi:10.1093/BRAIN/AWM320

22. Boeve BF, Boylan KB, Graff-Radford NR, et al. Characterization of frontotemporal dementia and/or amyotrophic lateral sclerosis associated with the GGGGCC repeat expansion in C9ORF72. *Brain*. 2012;135(Pt 3):765-783. doi:10.1093/BRAIN/AWS004
23. Cash DM, Bocchetta M, Thomas DL, et al. Patterns of gray matter atrophy in genetic frontotemporal dementia: results from the GENFI study. *Neurobiol Aging*. 2018;62:191-196. doi:10.1016/J.NEUROBIOLAGING.2017.10.008
24. Josephs KA, Whitwell JL, Jack CR, et al. Voxel-based morphometry patterns of atrophy in FTLD with mutations in MAPT or PGRN. *Neurology*. 2009;72(9):813-820. doi:10.1212/01.WNL.0000343851.46573.67
25. Mahoney CJ, Beck J, Rohrer JD, et al. Frontotemporal dementia with the C9ORF72 hexanucleotide repeat expansion: clinical, neuroanatomical and neuropathological features. *Brain*. 2012;135(Pt 3):736-750. doi:10.1093/BRAIN/AWR361
26. Sha SJ, Takada LT, Rankin KP, et al. Frontotemporal dementia due to C9ORF72 mutations: clinical and imaging features. *Neurology*. 2012;79(10):1002-1011. doi:10.1212/WNL.0B013E318268452E
27. Whitwell JL, Weigand SD, Boeve BF, et al. Neuroimaging signatures of frontotemporal dementia genetics: C9ORF72, tau, progranulin and sporadics. *Brain*. 2012;135(Pt 3):794-806. doi:10.1093/BRAIN/AWS001
28. Funkiewiez A, Bertoux M, de Souza LC, Lévy R, Dubois B. The SEA (Social cognition and Emotional Assessment): a clinical neuropsychological tool for early diagnosis of frontal variant of frontotemporal lobar degeneration. *Neuropsychology*. 2012;26(1):81-90. doi:10.1037/A0025318
29. Kaller S, Rullmann M, Patt M, et al. Test-retest measurements of dopamine D 1-type receptors using simultaneous PET/MRI imaging. *Eur J Nucl Med Mol Imaging*. 2017;44(6):1025-1032. doi:10.1007/S00259-017-3645-0
30. Alakurtti K, Johansson JJ, Joutsa J, et al. Long-term test-retest reliability of striatal and extrastriatal dopamine D2/3 receptor binding: Study with [11C]raclopride and high-resolution PET. *J Cereb Blood Flow Metab*. 2015;35(7):1199-1205. doi:10.1038/JCBFM.2015.53

31. Gómez FJG, Huertas I, Ramírez JAL, Solís DG. Elaboración de una plantilla de SPM para la normalización de imágenes de PET con 18F-DOPA. *Imagen Diagnóstica*. 2018;9(01):23-25. doi:10.33588/IMAGENDIAGNOSTICA.901.2

32. Hansen JY, Shafiei G, Markello RD, et al. Mapping neurotransmitter systems to the structural and functional organization of the human neocortex. *bioRxiv*. Published online October 30, 2021:2021.10.28.466336. doi:10.1101/2021.10.28.466336

33. Beliveau V, Ganz M, Feng L, et al. A High-Resolution In Vivo Atlas of the Human Brain's Serotonin System. *J Neurosci*. 2017;37(1):120-128. doi:10.1523/JNEUROSCI.2830-16.2016

34. Aghourian M, Legault-Denis C, Soucy JP, et al. Quantification of brain cholinergic denervation in Alzheimer's disease using PET imaging with [18 F]-FEOBV. *Mol Psychiatry*. 2017;22(11):1531-1538. doi:10.1038/MP.2017.183

35. Smart K, Cox SML, Kostikov A, et al. Effect of (Z)-isomer content on [11 C]ABP688 binding potential in humans. *Eur J Nucl Med Mol Imaging*. 2019;46(5):1175-1178. doi:10.1007/S00259-018-4237-3

36. Hesse S, Müller U, Rullmann M, et al. The association between in vivo central noradrenaline transporter availability and trait impulsivity. *Psychiatry Res Neuroimaging*. 2017;267:9-14. doi:10.1016/J.PSCYCHRESNS.2017.06.013

37. Koppel J, Jimenez H, Adrien L, H. Chang E, Malhotra AK, Davies P. Increased tau phosphorylation follows impeded dopamine clearance in a P301L and novel P301L/COMT-deleted (DM) tau mouse model. *J Neurochem*. 2019;148(1):127-135. doi:10.1111/JNC.14593

38. Ramos-Rodriguez JJ, Molina-Gil S, Rey-Brea R, Berrocoso E, Garcia-Alloza M. Specific serotonergic denervation affects tau pathology and cognition without altering senile plaques deposition in APP/PS1 mice. *PLoS One*. 2013;8(11). doi:10.1371/JOURNAL.PONE.0079947

39. Wu TH, Lu YN, Chuang CL, et al. Loss of vesicular dopamine release precedes tauopathy in degenerative dopaminergic neurons in a Drosophila model expressing human tau. *Acta Neuropathol*. 2013;125(5):711-725. doi:10.1007/S00401-013-1105-X

40. Khan K, Betters R, Lee G, Hefti MM, Marcinkiewcz CA. 1,5 1. Published online 2022.

41. Borroni B, Alberici A, Cercignani M, et al. Granulin mutation drives brain damage and

reorganization from preclinical to symptomatic FTLD. *NBA*. 2012;33(10):2506-2520. doi:10.1016/j.neurobiolaging.2011.10.031

42. Premi E, Cauda F, Costa T, et al. Looking for Neuroimaging Markers in Frontotemporal Lobar Degeneration Clinical Trials: A Multi-Voxel Pattern Analysis Study in Granulin Disease. *J Alzheimers Dis*. 2016;51(1):249-262. doi:10.3233/JAD-150340

43. Premi E, Giunta M, Iraji A, et al. Dissemination in time and space in presymptomatic granulin mutation carriers: a GENFI spatial chronnectome study. *Neurobiol Aging*. 2021;108:155-167. doi:10.1016/J.NEUROBIOLAGING.2021.09.001

44. Premi E, Dukart J, Mattioli I, et al. Unravelling Neurotransmitters Impairment in Primary Progressive Aphasias. *SSRN Electron J*. 2022;(October 2022):1-9. doi:10.2139/ssrn.4099029

45. Benussi A, Alberici A, Buratti E, et al. Toward a Glutamate Hypothesis of Frontotemporal Dementia. *Front Neurosci*. 2019;13. doi:10.3389/FNINS.2019.00304

46. Toller G, Cobigo Y, Callahan P, et al. Multisite ALLFTD study modeling progressive empathy loss from the earliest stages of behavioral variant frontotemporal dementia. *Alzheimers Dement*. Published online January 2, 2023. doi:10.1002/ALZ.12898

47. Fernandez RW et al. Modulation of social space by dopamine in *Drosophila melanogaster*, but no effect on the avoidance of the *Drosophila* stress odorant Supplementary material. *Biol Lett*. Published online 2017.

48. Schuster BA, Sowden S, Rybicki AJ, et al. Dopaminergic Modulation of Dynamic Emotion Perception. *J Neurosci*. 2022;42(21):4394-4400. doi:10.1523/JNEUROSCI.2364-21.2022

49. Canli T, Lesch KP. Long story short: the serotonin transporter in emotion regulation and social cognition. *Nat Neurosci*. 2007;10(9):1103-1109. doi:10.1038/NN1964

50. Kanen JW, Arntz FE, Yellowlees R, et al. Serotonin depletion amplifies distinct human social emotions as a function of individual differences in personality. *Transl Psychiatry*. 2021;11(1). doi:10.1038/S41398-020-00880-9

51. Duerler P, Vollenweider FX, Preller KH. A neurobiological perspective on social influence: Serotonin and social adaptation. *J Neurochem*. 2022;162(1):60-79. doi:10.1111/JNC.15607

52. Markello RD, Hansen JY, Liu ZQ, et al. neuromaps: structural and functional interpretation of brain

maps. *Nat Methods*. 2022;19(11):1472-1479. doi:10.1038/S41592-022-01625-W

CHAPTER 5 – STUDY 3

Impaired glymphatic system in genetic Frontotemporal Dementia: a GENFI study

Enrico Premi, Matteo Diano, Irene Mattioli, Daniele Altomare, Valentina Cantoni, Martina Bocchetta, Roberto Gasparotti, Emanuele Buratti, Marta Pengo, Arabella Bouzigues, Lucy L. Russell, Phoebe H. Foster, Eve Ferry-Bolder, Carolin Heller, John C. van Swieten, Lize C. Jiskoot, Harro Seelaar, Fermin Moreno, Raquel Sanchez-Valle, Daniela Galimberti, Robert Laforce, Caroline Graff, Mario Masellis, Maria Carmela Tartaglia, James B. Rowe, Elizabeth Finger, Rik Vandenberghe, Alexandre de Mendonça, Chris R. Butler, Alexander Gerhard, Simon Ducharme, Isabelle Le Ber, Pietro Tiraboschi, Isabel Santana, Florence Pasquier, Matthis Synofzik, Johannes Levin, Markus Otto, Sandro Sorbi, Jonathan D. Rohrer, Barbara Borroni, on behalf of GENFI

Under revision

Abstract

Introduction. The glymphatic system is an emerging target in neurodegenerative disorders. Here we investigated the activity of the glymphatic system in genetic Frontotemporal Dementia (FTD) with a diffusion-based technique called diffusion tensor image analysis along the perivascular space (DTI-ALPS).

Materials and methods. We investigated 291 subjects with symptomatic or presymptomatic FTD (112 with *C9orf72* expansion, 119 with *GRN* mutations, and 60 with *MAPT* mutations), and 49 non-carriers (healthy controls, HC). We computed the DTI-ALPS index by calculating diffusivities in the x, y, and z axes of the plane of the lateral ventricle body. Clinical stage and blood-based markers were considered. A subset of 180 participants underwent cognitive follow-ups for a total of 640 evaluations.

Results. The DTI-ALPS index was lower in symptomatic FTD (estimated marginal mean±standard error, 1.21±0.02) than in HC (1.29±0.02, p=0.005) and presymptomatic mutation carriers (1.30±0.01, p<0.001), with no significant differences between mutations. Lower DTI-ALPS was associated with worse disease severity (β=-1.16, p<0.001). A trend towards a significant association between lower DTI-ALPS and higher plasma

neurofilament light chain was reported (β=-0.28, *p*=0.063). Analysis of longitudinal data demonstrated that worsening of disease severity was faster in subjects with low DTI-ALPS at baseline than in those with average (*p*=0.010) or high (*p*=0.010) DTI-ALPS index.

Conclusion. Using a non-invasive imaging approach, as a proxy for glymphatic system function, we demonstrated glymphatic system abnormalities in symptomatic stages of genetic FTD. Such measures of the glymphatic system may elucidate pathophysiological processes in human FTD and facilitate early phase trials of genetic FTD.

Introduction

Frontotemporal Dementia (FTD), marked by changes in behavior, language and executive control, in association with multiple neuropathological substrates and heterogeneous genetic background.[1–3]

Clinical phenotypes mainly encompass behavioral variant FTD (bvFTD) and Primary Progressive Aphasias (PPA).[1,2] The pathogenic mechanisms of FTD are determined by intracellular accumulation of aberrant proteins, including mainly tau (frontotemporal lobar degeneration-tau, FTLD-tau) or TAR DNA-binding protein 43 (TDP-43, FTLD-TDP).[4,5] Around 30% of FTD is familial, most commonly caused by autosomal dominant genetic mutations within *microtubule-associated protein tau* (*MAPT*), *progranulin* (*GRN*), and *chromosome 9 open reading frame 72* (*C9orf72*) genes.[6]

Genetic FTD cases represent a privileged scenario in which to study the earliest phases of the disease in presymptomatic individuals, and assess the changes in defined neuropathological subtypes, such as FTLD-tau, associated with *MAPT* mutations, or FTLD-TDP, due to *GRN* or *C9orf72* genetic variations.[7]

Impairment of the glymphatic function, the brain waste clearing system,[8] has recently been suggested to play a role in several neurodegenerative disorders.[9–14] The glymphatic pathway promotes the flow of cerebrospinal fluid (CSF) into the brain along arterial perivascular spaces and subsequently into the brain interstitium through an astrocytic aquaporin-4 dependent mechanism. The pathway then directs the CSF flow towards the venous perivascular and perineuronal spaces, ultimately clearing solutes into meningeal and cervical lymphatic drainage vessels.[15,16]

Despite the expanding concepts on glymphatic physiology and pathology, the *in vivo* assessment of the glymphatic function is still hampered by the need of non-invasive imaging techniques for its quantification.[17] Recent studies have demonstrated the possibility of measuring glymphatic functions using Magnetic Resonance Imaging (MRI).[18] In particular, the diffusion tensor image analysis along the perivascular space (DTI-ALPS) technique has been utilized to estimate the efficiency of the glymphatic system by the DTI-ALPS-index, as a measure of perivascular clearance activity in the human brain.[18] This index showed its significant consistency with the classical detection clearance rate calculated on glymphatic MRI after intrathecal administration of gadolinium.[19]

DTI-ALPS is impaired in several neurological conditions.[10–13,17,20,21] More recently, significantly decreased DTI-ALPS values were reported in behavioral variant FTD[14] and, in agreement with these findings, glymphatic dysfunction was associated with accumulation of tau and TDP-43 proteins in animal models.[22–24]

However, a few questions still need to be addressed. It is not yet known whether the glymphatic dysfunction *i)* is an early event in FTD, already detectable in presymptomatic disease stages; *ii)* is associated with a specific FTLD proteinopathy or may represent a common pathway related to neurodegeneration; *iii)* is a marker of disease severity; *iv)* correlates with markers of neuronal dysfunction or axonal damage, such as plasma neurofilament light chain (NfL) or glial fibrillary acid protein (GFAP),[25,26] and/or *v)* predicts disease progression over time.

These questions prompted the current cross-sectional and longitudinal study. Our specific aim was to evaluate glymphatic system abnormalities in presymptomatic and symptomatic individuals with pathogenic mutations within the *MAPT*, *GRN* and *C9orf72* genes, to provide novel insight into the pathophysiology of genetic FTD.

Materials and methods

Participants

From the GENFI cohort study, individuals carrying a pathogenic FTD variation and their non-carrier family members were recruited from research centres across Europe and Canada (www.genfi.org.uk). Inclusion and exclusion criteria have been previously described.[27] Here we considered a consecutive sample of 340 participants recruited from January 30, 2012 to January 30, 2021. Among them, 112 were *C9orf72* expansion carriers (68 presymptomatic and 44 symptomatic), 119 *GRN* mutation carriers (88 presymptomatic and 31 symptomatic), 60 *MAPT* mutation carriers (43 presymptomatic and 17 symptomatic), and 49 were non-carriers cognitively unimpaired individuals (i.e., healthy controls, HC).

All participants underwent the GENFI standardized assessment at enrollment.[7] During the first visit, demographic information was collected. The years to expected onset were calculated as the difference between age at assessment and mean age at onset within the family, as previously described.[28] We assessed disease stage using the Clinical Dementia Rating (CDR)® Dementia Staging Instrument plus National Alzheimer's Coordinating Centre (NACC) behaviour and language domains (CDR plus NACC FTLD),[29] hereinafter referred to as CDR-FTLD.

CDR-FTLD = 0 defined the presymptomatic stage in mutation carriers, whilst CDR-FTLD >0 defined the symptomatic stage. Among 291 mutation carriers, 282 participants underwent CDR-FTLD at baseline. A subgroup of mutation carriers also underwent CDR-FTLD at different follow-ups (180 with at least two evaluations, 105 with at least three, 55 with at least four, 15 with at least five, and 3 with at least six), for a total of 640 evaluations.

Local ethics committees approved the study at each site and all participants provided written informed consent; the study was conducted according to the Declaration of Helsinki.

MRI acquisition

MRI protocol was common to all the GENFI sites, and adapted for different scanners; no pre-study phantom harmonization was performed at local level. Each subject underwent a 3 tesla (3T) MRI at their local site, which have scanners from three different manufacturers (Philips Healthcare, GE Healthcare Life Sciences, Siemens Healthcare Diagnostic). The protocol included a volumetric T1-weighted (magnetization-prepared

rapid gradient echo, MPRAGE) scan and a diffusion-weighted imaging (DWI) scan (consisting of with either four or five b0 images and 61 diffusion-weighted images or 64 diffusion-weighted images both with a bvalue of 1,000 s/mm^2, depending on the different acquisition sites), as previously reported.[7,27]

MRI preprocessing and analyses

Structural grey matter data. T1-weighted images were processed with the voxel-based morphometry (VBM) pipeline implemented in the Computational Anatomy Toolbox (CAT12 v.1742) (www.neuro.uni-jena.de/cat) for SPM12 (SPM12 v.7219) (www.fil.ion.ucl.ac.uk/spm/software/spm12) running on MATLAB R2019b (the MathWorks, Inc., Natick, Massachusetts, United States). The VBM pipeline steps consist in tissue segmentation, spatial normalization to a standard Montreal National Institute template, modulation and smoothing.[31] The pipeline was also used to calculate the total intracranial volume (TIV) values for each subject.

Diffusion-weighted data. DWI scans were preprocessed using Mrtrix3 and FSL software.[32] DWI scans were analyzed using the FDT tool of the FMRIB Software Library (FSL, v6.0). DWI data were denoised and corrected for eddy current-induced distortions and subject movements. These slices are replaced by non-parametric predictions by Gaussian Process. Diffusion tensor measures of fractional anisotropy (FA) and mean diffusivity (MD) were calculated running DTIFIT script, which fits a diffusion tensor model at each voxel, and subsequently registered to the study template.

DTI-ALPS index computation. The DTI-ALPS method is based on the assumption that the perivascular interstitial fluid movement in the white matter at the level of the lateral ventricle body is dominant along the parallelly aligned medullary veins (X axis), which run perpendicular to the ventricular wall; the Y axis is given by projection fibres running in the head-foot direction, mainly adjacent to the lateral ventricle, and the Z axis represents association fibres, running in the anterior-posterior direction outside the projection fibres.[18] In the projection area, dominant fibres run in the Z-axis direction, perpendicular to both the X- and Y-axes, whereas in the association area, dominant fibres run in the Y-axis direction, perpendicular to both the X and Z-axes. The DTI-ALPS index is calculated from the diffusivity in each direction of the projection and association fibers regions at the lateral ventricular body level and estimates the effect of the glymphatic system impairment on the diffusivity along the perivascular space of medullary veins. In calculating the DTI-ALPS index, the FA maps of each subject were registered linearly first and nonlinearly subsequently into the high-resolution

FSL_HCP1065_FA standard space image. Spherical Region of Interest (ROIs) measuring 5 mm in radius were placed *a priori* in the projection and association areas at the level of the lateral ventricle bodies in the left and right hemispheres onto the same FA template (see **Supplementary Figure 1**). The ROIs were then automatically registered to the subjects' FA map, and all subjects underwent visual inspection (by MD and IM) to check correct ROI placement. If ROIs were not correctly placed, due to artifacts or poor image quality, the subject was excluded from the study (n=57, 14.3%). Finally, in line with previous literature data, 3 DTI-ALPS indices were calculated using the following formula:[18,33]

$$DTI\ -\ ALPS = \frac{mean(Dxx\ proj, Dxx\ assoc)}{mean(Dyy\ proj, Dzz\ assoc)}$$

The left and right DTI-ALPS (L-DTI-ALPS and R-DTI-ALPS) indexes were calculated as a ratio of the mean of the X-axis diffusivity in the projection area (Dxx,proj) and X-axis diffusivity in the association area (Dxx,assoc) to the mean of the Y-axis diffusivity in the projection area (Dyy,proj) and the Z-axis diffusivity in the association area (Dzz,assoc) on each hemisphere, respectively.

The bilateral mean DTI-ALPS index (hereinafter referred to as DTI-ALPS) was calculated as the average of the R-DTI-ALPS and R-DTI-ALPS.

A DTI-ALPS index closes to 1.0 reflects lower diffusivity with greater glymphatic system impairment, whereas higher values indicate greater diffusivity and less glymphatic system impairment. In all the analyses, the bilateral mean DTI-ALPS index has been used as primary measure.[18]

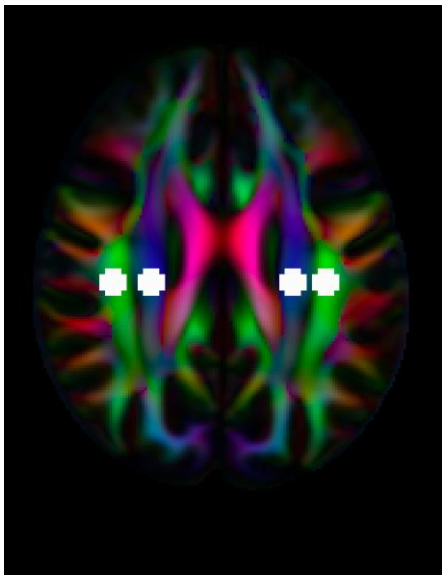

Supplementary Figure 1. Region of interest (ROI) anatomical placement for DTI-ALPS. Graphical representation of ROI placement on standard fractional anisotropy (FA) template (FSL_HCP1065_FA standard space). Two 5 mm spherical ROIs were placed *a priori* in the projection (blue fibers) area and two 5 mm spherical ROIs in the association (green fibers) area at the level of the lateral ventricle bodies, on the left and right hemispheres.

Plasma NfL and plasma GFAP quantification

In a subset of participants, plasma was collected by venipuncture and centrifuged (2,000 g, 10 minutes, at room temperature), according to GENFI protocol. [30] Serum was frozen at -80°C within 3 hours after collection, shipped and analysed without any previous thaw–freeze cycle. Samples were measured using the multiplex Neurology 4-Plex A kit (102153, Quanterix, Lexington, USA) on the SIMOA HD-1 Analyzer following manufacturer's instructions, as previously published.[30] The lower limit of detection of the assay for NfL and GFAP were 0.104 and 0.221 and pg/mL, respectively. Quality control samples had a mean intra-assay and inter-assay coefficient of variation of <10%. Technicians were blinded to the genotypic and clinical status of the samples. Plasma NfL and GFAP measures were available for 284 and 235 participants, respectively.

Statistical analyses

Differences among groups in the sociodemographic and clinical features were assessed using Kruskal-Wallis rank sum tests for continuous variables, or tests for equality of proportions for categorical variables.

Associations between DTI-ALPS and other variables were assessed using linear models adjusted for covariates, namely age, sex, and MRI site. When plasma markers were considered, site where samples were analyzed was added as covariate as well.

In order to assess the association between DTI-ALPS at baseline and longitudinal change in disease severity (CDR-FTLD), baseline DTI-ALPS scores of mutation carriers were converted into Z-scores using mean and

standard deviation (SD) of HC, and mutation carriers were classified as having "high" (Z-score > 1), "average" (Z-score between -1 and 1), or "low" (Z-score < -1) baseline DTI-ALPS. Subsequently, the association between DTI-ALPS at baseline and longitudinal change in disease severity was assessed using a linear mixed model with longitudinal CDR-FTLD as the dependent variable, DTI-ALPS groups (i.e., "high", "average", and "low"), time (years) from baseline, and their interaction as independent variables; age, sex, CDR-FTLD at baseline, and site as covariates; random intercepts and slopes at the subject level were computed.

When the number of groups in the comparison was larger than two, post-hoc pairwise comparisons were adjusted using the False Discovery Rate correction. Significance was set at $p<0.05$. All statistical analyses were performed with R, version 4.3.0 (The R Project for Statistical Computing, https://www.r-project.org/).

Results

Participants

Table 1 illustrates demographic and clinical features of the 340 study participants. As expected, HC (median age: 42 years; median CDR-FTLD score: 0) and presymptomatic mutation carriers (median age: 38-46 years; median CDR-FTLD score: 0) were younger and had better global cognition and functioning than symptomatic mutation carriers (median age: 61-62 years, $p<0.05$; median CDR-FTLD score: 2, $p<0.05$). In presymptomatic mutation carriers, the expected age at onset was similar in the three genetic groups ($p=0.447$). In symptomatic mutation carriers, bvFTD was the most prevalent clinical phenotype, and its prevalence was higher in *C9orf72* (93%, 28/30) than in *GRN* mutation carriers (61%, 17/28, $p=0.023$).

Glymphatic system according to clinical, genetic and neuropathological features

Figure 1 shows the distribution of DTI-ALPS according to disease stage and genetic group.

The DTI-ALPS index was lower in all symptomatic mutation carriers (estimated marginal mean ± standard error, 1.21±0.02) than in HC (1.29±0.02, $p=0.005$) and all presymptomatic mutation carriers (1.30±0.01, $p<0.001$), denoting glymphatic impairment in symptomatic FTD (**Figure 1A**).

Disaggregating also by genetic group, DTI-ALPS was lower in symptomatic *C9orf72* expansion carriers (1.20±0.02) than in HC (1.29±0.02, $p=0.023$) and in presymptomatic *C9orf72* mutation carriers (1.28±0.02, $p=0.023$), and in symptomatic *GRN* mutation carriers (1.24±0.03) than in presymptomatic *GRN* mutation carriers (1.32±0.02, $p=0.023$), with a similar yet not statistically significant trend also in *MAPT* mutation carriers (1.22±0.03 in symptomatic vs 1.28±0.02 in presymptomatic) (**Figure 1B** and **Table 1**).

As reported in **Table 1**, similar results were found when R-DTI-ALPS or L-DTI-ALPS were considered instead of the global DTI-ALPS.

No significant differences in the DTI-ALPS index were found when comparing bvFTD (1.19±0.03) to PPA (1.24±0.05, $p=0.295$), nor in the L-DTI-ALPS index (bvFTD vs. PPA, 1.19±0.03 vs. 1.24±0.05, $p=0.370$) or R-DTI-ALPS index (1.19±0.03 vs. 1.24±0.05, $p=0.317$) (see **Table 1**).

No significant differences in the DTI-ALPS index were found when comparing FTLD-TDP (symptomatic *C9orf72* and *GRN* mutation carriers, 1.20±0.02) to FTLD-tau (symptomatic *MAPT* mutation carriers, 1.19±0.04, $p=0.819$).

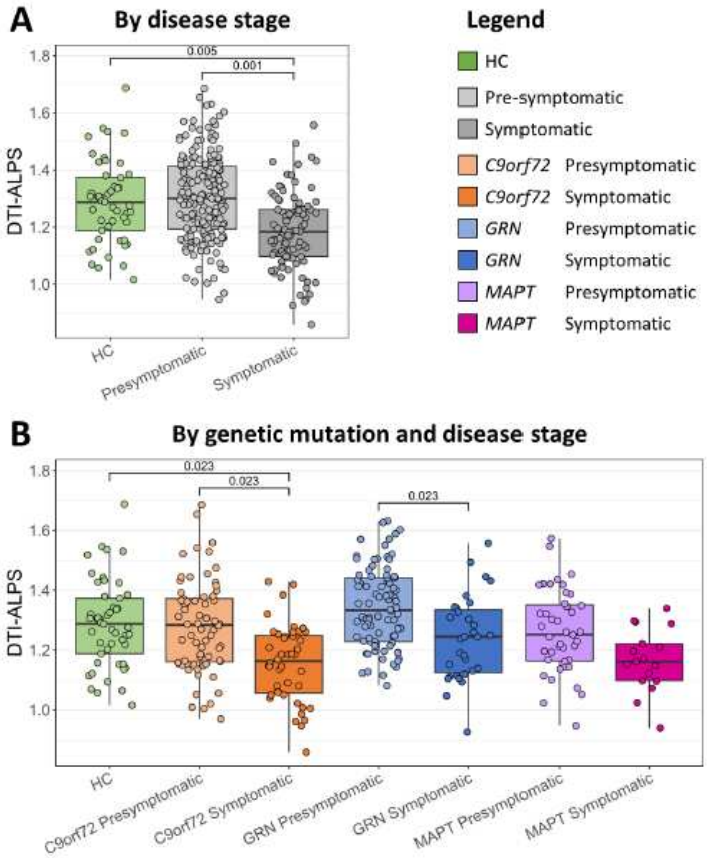

Figure 1. **Distribution of DTI-ALPS across disaggregating by disease stage (panel A) or by genetic mutation and disease stage (panel B).**

DTI-ALPS = diffusion tensor image analysis along the perivascular space; HC = healthy controls.

Comparisons of interest were "HC vs Presymptomatic", "HC vs Symptomatic", and "Presymptomatic vs Symptomatic" in A (i.e., 3 pairwise comparisons in total); and "HC vs all groups" and "Presymptomatic vs Symptomatic" within the three genetic groups in B (i.e., 9 pairwise comparisons in total).

Post-hoc pairwise comparisons of interest were adjusted using the False Discovery Rate correction.

Associations between glymphatic system and disease severity, expected years of onset, and plasma biomarkers

In all mutation carriers combined, lower DTI-ALPS was associated with worse disease severity (CDR-FTLD: β=-1.16, p<0.001) (**Figure 2A**). In presymptomatic mutation carriers, a trend of statistical significance was found between having lower DTI-ALPS and closer expected years of onset (β=-9.94, p=0.096) (**Figure 2B**).

In all mutation carriers, lower DTI-ALPS was associated with higher plasma NfL, although with a trend of statistical significance (β=-0.28, *p*=0.063) (**Figure 2C**). No significant association was observed between DTI-ALPS and plasma GFAP (β=-0.10, *p*=0.379) (**Figure 2D**).

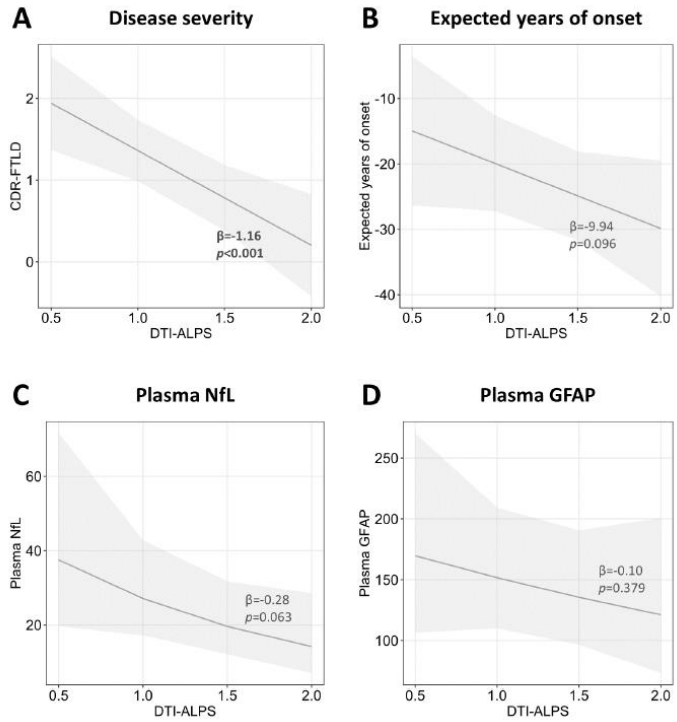

Figure 2. **Association of DTI-ALPS with disease severity (i.e., CDR-FTLD) (panel A), expected years of onset (panel B), plasma NfL (panel C), and plasma GFAP (panel D) in mutation carriers.**
DTI-ALPS = diffusion tensor image analysis along the perivascular space; CDR-FTLD = CDR® Dementia Staging Instrument plus National Alzheimer's Coordinating Centre behaviour and language domains; NfL = neurofilament light; GFAP = glial fibrillary acid protein.
Plasma NfL and GFAP values were log-transformed.

Association between the glymphatic system status at baseline and longitudinal worsening in disease severity

All mutation carriers with low (β=0.20, *p*<0.001) or average (β=0.05, *p*=0.023) DTI-ALPS at baseline showed worsening in disease severity, while those with high DTI-ALPS remained stable over time (β=0.02, *p*=0.646)

(**Figure 3**). Worsening in disease severity was faster in mutation carriers with low DTI-ALPS at baseline than in those with average (p=0.010) or high (p=0.010) DTI-ALPS at baseline (**Figure 3**).

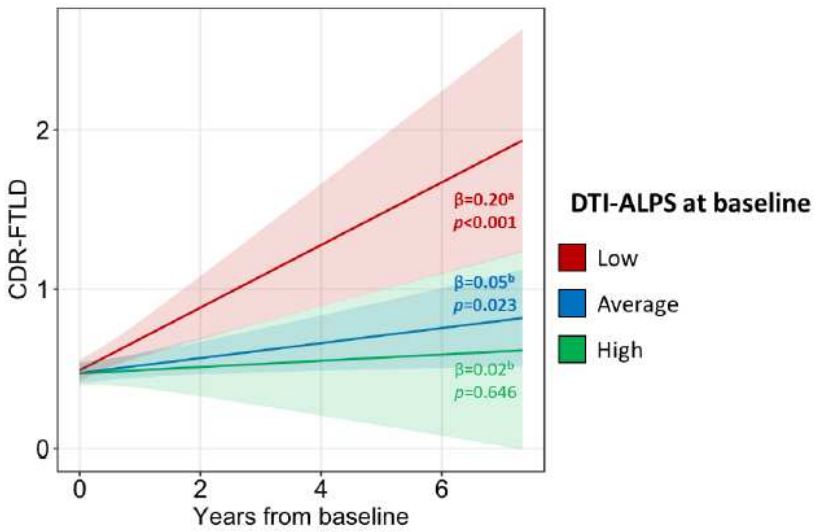

Figure 3. Association between DTI-ALPS at baseline and longitudinal worsening in disease severity.
DTI-ALPS = diffusion tensor image analysis along the perivascular space; CDR-FTLD = CDR® Dementia Staging Instrument plus National Alzheimer's Coordinating Centre behaviour and language domains.
Baseline DTI-ALPS scores of mutation carriers were converted into Z-scores using mean and standard deviation of healthy controls, and mutation carriers were classified as having "high" (Z-score > 1), "average" (Z-score between -1 and 1), or "low" (Z-score < -1) baseline DTI-ALPS.
Post hoc comparisons: [a] > [b].

Discussion

The glymphatic system represents a potential novel therapeutic target for the treatment of neurodegenerative disorders, while innovative non-invasive imaging techniques can quantify glymphatic system *in vivo* to elucidate pathophysiology. In the present study, we reported that glymphatic system, as indirectly measured by DTI-ALPS index, is impaired in genetic FTD, irrespective of specific genetic mutation, and consequently independently of FTLD-related proteinopathy. Glymphatic system dysfunction was not an early event, and was undetectable in the presymptomatic disease stages, although it is unclear if this reflects late emergence of glymphatic deficits or limited sensitivity of non-invasive methods.

We have used the non-invasive MRI index, the DTI-ALPS, as a measure of diffusivity along the perivascular space. This we interpret as a measure of glymphatic function, at least for what concerns its perivascular component.[18]

Recent work has consistently reported impairment of DTI-ALPS index as a proxy of glymphatic system function in neurodegenerative disorders, and in sporadic FTD as well. [10–14,17,20,21] This confirms and extends previous research data, claiming that glymphatic system impairment is not disease-specific but reflects brain distress and neurodegeneration.[34] In this perspective, a preserved glymphatic system might be protective against disease progression and clinical worsening, even in carriers of FTD-related mutations; while an altered glymphatic system might be associated with worse clinical outcomes over time.

These results support the hypothesis that brain clearance system continues to decline with disease progression, leading to increased tau or TDP-43 pathological burden, and further raising the protein concentration to a level that favors aggregation. Glymphatic system dysfunction may participate in the symptom worsening of genetic FTD through its role in the clearance of pathogenetic proteins, autoimmune cell infiltration, and promotion of inflammatory activation. [17]

In this view, we also reported a mild negative association between glymphatic function and expected age at onset of symptoms, and between glymphatic function and markers of neurodegeneration, such as NfL, [25,26,30] although not statistically significant.

Interestingly, longitudinal assessment of participants in the GENFI cohort allowed us to demonstrate that glymphatic function may clearly predict disease progression over time, suggesting that DTI-ALPS index may be regarded as marker of progression, possibly predicting transition toward progressive stages.

These results suggest the potential of glymphatic change as a therapeutic target in FTD, counteracting disease progression by enhancing the brain endogenous waste clearance pathways. The evidence for specific interventions remains indirect, e.g. that sleep deprivation can suppress brain clearance via the glymphatic dysfunction,[35,36,37] and consequently behavioral or pharmacological interventions that preserve night sleep could be considered. Although the study of sleep disturbances in FTD is in its infancy, there is emerging evidence that hypothalamic dysfunction, manifesting as disturbances in sleep, is an integral component of neurodegeneration in FTD.[38] In addition to sleep, another potential molecular target could be represented by aquaporin-4, a key protein involved in the glymphatic system function,[39] already demonstrated to be impaired in FTD patients in the GENFI cohort.[40] In the near future, both pharmacological strategies or non-pharmacological approaches (e.g., diet), might be considered to modulate acquaporin-4 metabolism.[41,42,43]

We acknowledge that this study entails some limitations. First, the DTI-ALPS index was calculated based on the diffusion of perivascular space and may not be directly equivalent to the glymphatic function, although it has been shown to be reliable and has been widely applied in multiple diseases. Second, we assessed DTI-ALPS index of the whole brain rather than a regional function measurement, even though we tested left and right hemispheres with no substantial differences across clinical phenotypes.

Notwithstanding these limitations, we believe that using a non-invasive diffusion-based imaging approach, as a proxy of the glymphatic system function, we have successfully demonstrated that glymphatic system is impaired in the symptomatic stages of genetic FTD, irrespective of the clinical syndrome or neuropathological features. Moreover, glymphatic system impairment was associated with disease stage and predicted its clinical progression. The glymphatic system may therefore represent a novel potential target for future treatment approaches in genetic FTD.

References

1 Rascovsky K, Hodges JR, Knopman D, *et al.* Sensitivity of revised diagnostic criteria for the behavioural variant of frontotemporal dementia. *Brain* 2011; **134**: 2456–77.

2 Gorno-Tempini ML, Hillis AE, Weintraub S, *et al.* Classification of primary progressive aphasia and its variants. *Neurology* 2011; **76**: 1006–14.

3 Pengo M, Premi E, Borroni B. Dissecting the Many Faces of Frontotemporal Dementia: An Imaging Perspective. *Int J Mol Sci* 2022; **23**. DOI:10.3390/IJMS232112867.

4 Neumann M, Mackenzie IRA. Review: Neuropathology of non-tau frontotemporal lobar degeneration. *Neuropathol Appl Neurobiol* 2019; **45**: 19–40.

5 Josephs KA, Hodges JR, Snowden JS, *et al.* Neuropathological background of phenotypical variability in frontotemporal dementia. *Acta Neuropathol* 2011; **122**: 137–53.

6 Borroni B, Padovani A. Dementia: a new algorithm for molecular diagnostics in FTLD. *Nat Rev Neurol* 2013; **9**: 241–2.

7 Premi E, Grassi M, Van Swieten J, *et al.* Cognitive reserve and TMEM106B genotype modulate brain damage in presymptomatic frontotemporal dementia: a GENFI study. *Brain* 2017; **140**: 1784–91.

8 Xu J, Su Y, Fu J, *et al.* Glymphatic dysfunction correlates with severity of small vessel disease and cognitive impairment in cerebral amyloid angiopathy. *Eur J Neurol* 2022; **29**: 2895–904.

9 Hsu JL, Wei YC, Toh CH, *et al.* Magnetic Resonance Images Implicate That Glymphatic Alterations Mediate Cognitive Dysfunction in Alzheimer Disease. *Ann Neurol* 2023; **93**: 164–74.

10 Kamagata K, Andica C, Takabayashi K, *et al.* Association of MRI Indices of Glymphatic System With Amyloid Deposition and Cognition in Mild Cognitive Impairment and Alzheimer Disease. *Neurology* 2022; **99**: E2648–60.

11 Saito Y, Hayakawa Y, Kamagata K, *et al.* Glymphatic system impairment in sleep disruption: diffusion tensor image analysis along the perivascular space (DTI-ALPS). *Jpn J Radiol* 2023; published online June 27. DOI:10.1007/S11604-023-01463-6.

12 Bae YJ, Kim J-M, Choi BS, *et al.* Glymphatic function assessment in Parkinson's disease using diffusion tensor image analysis along the perivascular space. *Parkinsonism Relat Disord* 2023; **114**: 105767.

13 Jeong SH, Jeong H, Sunwoo MK, *et al.* Association between choroid plexus volume and cognition in Parkinson's disease. *Eur J Neurol* 2023; published online July 27. DOI:10.1111/ENE.15999.

14 Jiang D, Liu L, Kong Y, *et al.* Regional Glymphatic Abnormality in Behavioral Variant Frontotemporal Dementia. *Ann Neurol* 2023; published online June 14. DOI:10.1002/ANA.26710.

15 Iliff JJ, Wang M, Liao Y, *et al.* A paravascular pathway facilitates CSF flow through the brain parenchyma and the clearance of interstitial solutes, including amyloid β. *Sci Transl Med* 2012; **4**. DOI:10.1126/SCITRANSLMED.3003748.

16 Rasmussen MK, Mestre H, Nedergaard M. The glymphatic pathway in neurological disorders. *Lancet Neurol* 2018; **17**: 1016–24.

17 Carotenuto A, Cacciaguerra L, Pagani E, Preziosa P, Filippi M, Rocca MA. Glymphatic system impairment in multiple sclerosis: relation with brain damage and disability. *Brain* 2022; **145**: 2785–95.

18 Taoka T, Masutani Y, Kawai H, *et al.* Evaluation of glymphatic system activity with the diffusion MR technique: diffusion tensor image analysis along the perivascular space (DTI-ALPS) in Alzheimer's disease cases. *Jpn J Radiol* 2017; **35**: 172–8.

19 Zhang W, Zhou Y, Wang J, *et al.* Glymphatic clearance function in patients with cerebral small vessel disease. *Neuroimage* 2021; **238**. DOI:10.1016/J.NEUROIMAGE.2021.118257.

20 Butler T, Zhou L, Ozsahin I, *et al.* Glymphatic clearance estimated using diffusion tensor imaging along perivascular spaces is reduced after traumatic brain injury and correlates with plasma neurofilament light, a biomarker of injury severity. *Brain Commun* 2023; **5**. DOI:10.1093/BRAINCOMMS/FCAD134.

21 Hicks A, Sinclair B, Shultz S, *et al.* Associations of Enlarged Perivascular Spaces With Brain Lesions, Brain Age, and Clinical Outcomes in Chronic Traumatic Brain Injury. *Neurology* 2023; **101**: 10.1212/WNL.0000000000207370.

22 Zamani A, Walker AK, Rollo B, *et al.* Impaired glymphatic function in the early stages of disease in a TDP-43 mouse model of amyotrophic lateral sclerosis. *Transl Neurodegener* 2022; **11**. DOI:10.1186/S40035-022-00291-4.

23 Ishida K, Yamada K, Nishiyama R, *et al.* Glymphatic system clears extracellular tau and protects from tau aggregation and neurodegeneration. *J Exp Med* 2022; **219**. DOI:10.1084/JEM.20211275.

24 Harrison IF, Ismail O, Machhada A, *et al.* Impaired glymphatic function and clearance of tau in an Alzheimer's disease model. *Brain* 2020; **143**: 2576–93.

25 Benussi A, Karikari TK, Ashton N, *et al.* Diagnostic and prognostic value of serum NfL and p-Tau181 in frontotemporal lobar degeneration. *J Neurol Neurosurg Psychiatry*. 2020;**91(9):**960-967.

26 Benussi A, Ashton N, Karikari T, *et al.* Serum Glial Fibrillary Acid Protein (GFAP) is a marker of disease severity in Frontotemporal Lobar Degeneration. *J Alzheimer Dis.* 2020;**77(3):**1129-.1141

27 Rohrer JD, Nicholas JM, Cash DM, *et al.* Presymptomatic cognitive and neuroanatomical changes in genetic frontotemporal dementia in the Genetic Frontotemporal dementia Initiative (GENFI) study: a cross-sectional analysis. *Lancet Neurol* 2015; **14**: 253–62.

28 Moore KM, Nicholas J, Grossman M, *et al.* Age at symptom onset and death and disease duration in genetic frontotemporal dementia: an international retrospective cohort study. *Lancet Neurol* 2020; **19**: 145–56.

29 Miyagawa T, Brushaber D, Syrjanen J, *et al.* Utility of the global CDR® plus NACC FTLD rating and development of scoring rules: Data from the ARTFL/LEFFTDS Consortium. *Alzheimers Dement* 2020; **16**: 106–17.

30 Heller C, Chan E, Foiani MS, *et al.* Plasma glial fibrillary acidic protein and neurofilament light chain are measures of disease severity in semantic variant primary progressive aphasia. *J Neurol Neurosurg Psychiatry* 2020; **92**: 455–6.

31 Kurth F, Gaser C, Luders E. A 12-step user guide for analyzing voxel-wise gray matter asymmetries in statistical parametric mapping (SPM). *Nat Protoc* 2015;1**0(2):**293–304

32 Tournier JD, Smith R, Raffelt D, et al. MRtrix3: A fast, flexible and open software framework for medical image processing and visualisation. ***NeuroImage*** 2019 Nov;**202**:116137.

33 Taoka T, Ito R, Nakamichi R, Kamagata K, et al. Reproducibility of diffusion tensor image analysis along the perivascular space (DTI-ALPS) for evaluating interstitial fluid diffusivity and glymphatic function: CHanges in Alps index on Multiple conditiON acquIsition eXperiment (CHAMONIX) study. *Jpn J Radiol* 2022;40(2):147–58

34 Nedergaard M, Goldman SA. Glymphatic failure as a final common pathway to dementia. *Science* 2020;**370(6512)**:50-56

35 Achariyar TM, Li B, Peng W, *et al.* Glymphatic distribution of CSF-derived apoE into brain is isoform specific and suppressed during sleep deprivation. *Mol Neurodegener* 2016;**11(1)**:74

36 Shokri-Kojori E, Wang GJ, Wiers CE, et al. β-Amyloid accumulation in the human brain after one night of sleep deprivation. *Proc Natl Acad Sci U S A* 2018 Apr24;115(17):4483-4488.

37 Komaroff AL. Does Sleep Flush Wastes From the Brain? *JAMA* 2021;**325(21):**2153-21

38 Hwang YT, Piguet O, Hodges JR, Grunstein R, Burrell JR. Sleep and orexin: A new paradigm for understanding behavioural-variant frontotemporal dementia? *Sleep Med Rev* 2020;**54**:101361

39 Arighi A, Arcaro M, Fumagalli GG, *et al.* Aquaporin-4 cerebrospinal fluid levels are higher in neurodegenerative dementia: looking at glymphatic system dysregulation. *Alzheimers Res Ther* 2022;**14(1)**:135

40 Bergström S, Öijerstedt L, Remnestål J, *et al.* A panel of CSF proteins separates genetic frontotemporal dementia from presymptomatic mutation carriers: a GENFI study. *Mol Neurodegener* 2021;**16(1):**79

41 Kitchen P, Salman MM, Halsey AM, *et al.* Targeting Aquaporin-4 Subcellular Localization to Treat Central Nervous System Edema. *Cell* 2020;**181(4):**784-799.e19

42 Silverglate B, Gao X, Lee HP, *et al.* The aquaporin-4 water channel and updates on its potential as a drug target for Alzheimer's disease. *Expert Opin Ther Targets* 2023; **1-8**.

43 Zhang J, Zhan Z, Li X, *et al.* Intermittent Fasting Protects against Alzheimer's Disease Possible through Restoring Aquaporin-4 Polarity. *Front Mol Neurosci* 2017;**10**:395

Table 1. **Demographic and clinical features of the study participants and DTI-ALPS values disaggregating by genetic mutation and disease stage.**

Features	HC	*C9orf72*		*GRN*		*MAPT*		*p*-value
	n=49	Presymptomatic n=68	Symptomatic n=44	Presymptomatic n=88	Symptomatic n=31	Presymptomatic n=43	Symptomatic n=17	
Age, years	42 (10)b	43 (15)^{b}	62 (11)^{a}	46 (19)^{b,a1}	61 (10)^{a}	38 (13)^{b,b1}	61 (6)^{a}	**<0.001**
Sex, female %	35% (17)	41% (28)	66% (29)^{a}	32% (28)^{b}	58% (18)	44% (19)	65% (11)	**0.002**
Expected age at onset, years	-	-18 (15)	-	-16 (19)	-	-14 (11)	NA	0.447
Education, years	16 (5)^{a}	15 (4)^{a}	12 (4)^{b}	16 (3)^{a}	13 (6)^{b}	16 (3)^{a}	16 (5)^{a}	**<0.001**
Phenotype, bvFTD %	-	-	93% (28)^{a} [14]	-	61% (17)^{b} [3]	-	93% (13) [3]	**0.003**
CDR-FTLD	0.0 (0.0)^{b}	0.0 (0.0)^{b}	2.0 (1.8)^{a}	0.0 (0.0)^{b}	2.0 (2.0)^{a}	0.0 (0.2)^{b}	2.0 (1.0)^{a}	**<0.001**
TIV	1415 (189)	1429 (235)	1497 (216)	1451 (185)	1430 (158)	1463 (168)	1387 (262)	0.278
DTI-ALPS index								
DTI-ALPS	1.29 (0.02)^{a}	1.28 (0.02)^{a}	1.20 (0.02)^{b}	1.32 (0.02)^{a1}	1.24 (0.03)^{b1}	1.28 (0.02)	1.22 (0.03)	**0.002**
Left DTI-ALPS	1.30 (0.02)^{a}	1.28 (0.02)^{a}	1.19 (0.03)^{b}	1.33 (0.02)^{a1}	1.23 (0.03)^{b1}	1.28 (0.03)	1.24 (0.04)	**0.002**
Right DTI-ALPS	1.29 (0.02)	1.28 (0.02)	1.21 (0.03)	1.32 (0.02)	1.27 (0.03)	1.27 (0.03)	1.20 (0.04)	**0.024**

DTI-ALPS = diffusion tensor image analysis along the perivascular space; HC = healthy controls; *C9orf72 = chromosome 9 open reading frame 72*; *GRN = progranulin*; *MAPT = microtubule-associated protein tau*; bvFTD = behavioural variant FTD; CDR-FTLD = CDR® Dementia Staging Instrument plus National Alzheimer's Coordinating Centre (NACC) behaviour and language domains; TIV = total intracranial volume.

Values are medians (interquartile ranges) for continuous variables, or percentages (raw numbers) for categorical variables, unless otherwise specified. DTI-ALPS values are estimated marginal means (standard errors). Post hoc comparisons (False Discovery Rate, FDR correction): $^{a} > {}^{b}$, $^{a1} > {}^{b1}$. [number in square brackets]: number of missing data. P values refer to pairwise comparisons (HC vs other groups, *C9orf72* presymptomatic vs symptomatic, *GRN* presymptomatic vs symptomatic, and *MAPT* presymptomatic vs symptomatic).

CHAPTER 6 – STUDY 4

Visual networks dynamic functional connectivity is associated with neurofilament light and expected clinical onset in premanifest Huntington's disease

This study is the result of a collaboration between the Centre for Neurodegenerative diseases of the University of Brescia, directed by Prof. Barbara Borroni, and the Huntington's disease Centre of the University College London (London, UK), directed by Prof. Sarah Tabrizi. It will be submitted soon.

Abstract

Introduction. Dynamic functional network connectivity (dFNC) has never been evaluated in premanifest Huntington's Disease (HD). New approaches focused on the spatial chronnectome can capture both spatial network configurations and their dynamic changes over time. The aim of this study is to investigate dFNC of the visual networks in 60 premanifest HD (preHD) very far from onset (~ 24 years) and 59 healthy controls (HC) followed at the HD Centre, University College London.

Materials and methods. We considered time-varying patterns of the visual primary network (VPN) and the visual secondary network (VSN), each summarized into four distinct recurring spatial states. Dwell time (DT) (the time each individual spends in each spatial state of each network), fractional occupancy (FO) (the total percentage of time spent by each individual in a state of a specific network), the total transition number (NT) (the total number of transitions between states performed by subjects for each network) and homogeneity (a measure of the spatio-temporal variations in each network) were considered.

Results. PreHD presented a lower number of transitions in VSN (5.05 ± 2.30 vs 6.34 ± 2.29, p = 0.01 FDR-corrected). VPN homogeneity predicted cerebrospinal fluid neurofilament light concentration (CSF NfL) (p = 0.05 FDR-corrected, beta = 0.29), whereas VSN number of transitions predicted the EYO (p = 0.03 FDR-corrected, beta -0.32). We found no association between dFNC measures, putamen volume and neuropsychological performances.

Conclusion. Our results demonstrated that premanifest HD very far from onset presented early alterations of the visual networks dFNC, which predicted the concentration of CSF NfL and EYO. These findings are relevant to a thorough characterization of the very early disease stage, with implications for understanding the physiopathology, the development of neuroimaging biomarkers and for finding the best timepoint for therapeutic interventions.

Introduction

Huntington's disease (HD) is a devasting monogenic, autosomal-dominant neurodegenerative disorder characterized by motor, cognitive and psychiatric features[1]. Early changes in structural and functional neuroimaging and biological biomarkers can be detected during the premanifest stage, even decades before the disease onset[2–8]. Nowadays, many clinical trials are ongoing to evaluate potential disease-modifying treatments. Exploring initial alterations during the premanifest phase gives novel insights into the pathophysiological process and is crucial to identify the best timepoint for therapeutic intervention and possible biomarkers for clinical trials.

Previous studies demonstrated changes in functional connectivity in premanifest HD (preHD) gene carriers on average 10-15 years before expected onset [9–13]. However, recent studies conducted on a cohort of young HD gene carriers very far from disease onset (approximately 24 years) did not find any difference in functional connectivity between preHD subjects and controls[14,15]. In spite of this, McColgan et al demonstrated an association between increased functional connectivity in posterior cortical regions and a measure of disease pathology burden (cerebrospinal fluid neurofilament light, CSF NfL). Interestingly, these alterations occurred among brain regions characterized by regional expression of genes specific to neuronal GABAergic and glutamatergic cells. The involvement of posterior cortical areas is well-documented in *post-mortem*[16] as well as in neuroimaging studies in HD[2,17,18]. In particular, structural neuroimaging investigations found an early engagement of the occipital cortex in preHD[2,19,20] and functional connectivity evidence supported the presence of posterior connectivity alterations even in the premanifest HD stages[21,22].

Static functional connectivity analyses were performed in previous studies in preHD, considering each network composed of fixed brain regions with a static spatial pattern over time. However, this appears an oversimplification, as the resting brain is highly dynamic, with reoccurring patterns of brain functional connectivity[23]. Initial approaches to capture the dynamic functioning of the brain

focused on the variations in the temporal coupling between spatially static brain networks[23–25]. An alternative avenue (the so-called "spatial chronnectome") allows capture of time-varying spatial patterns of brain networks[26,27]. Specifically, each functional brain network may assume different configurations in space during the scan period[26]. Therefore, each network results in different spatial states, which recruit distinct neuroanatomical areas. Dynamic functional network connectivity (dFNC) approaches might be more sensitive than traditional resting state functional MRI (rs-fMRI) analyses in the pre-symptomatic phase of inherited neurodegenerative diseases, as already demonstrated in genetic Frontotemporal dementia.[28,29]

To the best of our knowledge, only one study explored dFNC in HD, considering prodromal and early manifest HD patients[30]. However, this approach has never been applied to characterize preHD. This observation prompted the present study, which aims to explore dFNC alterations in a preHD cohort on average 24 years from disease onset, and their association with fluid biomarkers, expected clinical onset and disease burden score. In particular, we explored visual networks spatial chronnectome, in consideration of the increasing evidence of an early involvement of the occipital regions in preHD. A characterization of early dFNC changes might substantially contribute to explore the pathophysiology and to detect early brain alterations in preHD very far from onset, with implications for the development of therapy targets, to define the best timepoint for therapeutic interventions and to monitor the efficacy of new molecules in clinical trials.

Materials and Methods

Participants

We considered 64 preHD and 68 healthy control (HC) participants matched for age, sex and education of the Huntington's Disease-Young Adult Study (HD-YAS)[8], recruited at the HD Centre, University College London (London, UK) . 4 preHD were excluded: 3 for contraindications to MRI acquisition and 1 for a large artefact at MRI. We excluded 9 HC: 8 because of contraindications to MRI scan, 1 had evidence of a concomitant neurological disease at the MRI (not previously known), 1 presented an anatomical malformation and 1 was excluded for head-motion. Therefore, we included 60 preHD and 59 HC. PreHD subjects were gene-positive with a CAG repeat >39, disease burden score <240[31] and a Unified Huntington's Disease Rating Scale Total Motor Score ≤5[32]. HC were gene-negative family members or individuals with no familial history of HD. Exclusion criteria for YAS study were: recent drug or alcohol abuse and/or dependance, neurological or significant psychiatric comorbidity, brain trauma or contraindication to MRI. All participants underwent detailed clinical, neurological, cognitive and neuropsychiatric testing, neuroimaging, blood sampling and optional CSF collection, as previously reported[8]. The study was approved by the local Research Ethics Committee and all participants gave written informed consent prior to study entry.

Biofluid collections

Biofluids were collected using standardized, validated conditions, methods and equipment, as previously reported[33]. Blood samples were analysed to determine the concentration of different biological biomarkers, namely neurofilament light (NfL), total tau and glial fibrillary acidic protein (GFAP). Cerebrospinal fluid (CSF) was examined to measure the concentration of total huntingtin (HTT, mutant huntingtin and wild-type huntingtin), mutant HTT, NfL, YKL-40 (also known as Chitinase-3-like protein), total tau, neurogranin, interleukin-6 (IL-6), interleukin-8 (IL-8), GFAP, ubiquitin carboxyl-terminal hydrolase L1 (UCH-L1).

MRI acquisition

MRI data were acquired on a 3 T Prisma Scanner (Siemens Healthcare) with a 64-channel head coil. T2-weighted echo planar imaging (EPI) sequences sensitized to blood oxygenation level dependent (BOLD) contrast were considered in the present study. Resting-state functional MRI (fMRI) data were collected using a standard 2D EPI sequence: TR = 3.36 s; TE = 30 ms; 49 slices were acquired with 2.5 mm slice thickness with in-plane field of view of 192 x 192 mm2 with 3 x 3 mm2 resolution with 165 volumes. Pulsatile information was collected using the Nonin 8600FO pulse-oximeter and a Siemens breathing belt for respiratory data. Both were recorded along with a scanner pulses using Cambridge Electronics device CED Micro 1401 Mk II connected to a laptop running Spike v2. During scanning, subjects were asked to keep their eyes closed, not to think of anything in particular, and not to fall asleep.

Neuroimaging preprocessing and analyses

Functional data were preprocessed using the toolbox for Data Processing and Analysis for Brain Imaging (DPABI, http://rsfmri.org/dpabi)[34] based on the Statistical Parametric Mapping (SPM12, https://www.fil.ion.ucl.ac.uk/spm/) software. For each subject, the first 5 volumes were discharged to account for magnetization equilibration. The remaining 160 volumes underwent slice-timing correction and were realigned to the first volume. Any subject who had a maximum displacement in any direction larger than 2.5 mm, or a maximum rotation (x, y, z) larger than 2.5°, was excluded. We considered framewise displacement (FD)[35] as a nuisance variable accounting for head motion during MRI scanning. This motion parameter was subsequently included as a covariate in the statistical analysis (see below). Data were subsequently spatially normalized to the EPI unified segmentation template (considering that EPI normalization is able to reduce variability across subjects)[36] in Montreal Neurological Institute coordinates derived from SPM12 software ad resampled to 3x3x3 cubic voxels. Spatial smoothing with an isotropic Gaussian kernel with the full width at half-

maximum of 6 mm was applied, followed preprocessing pipeline previously published for spatial chronnectome analysis[26].

Functional Networks Decomposition

The functional data were processed using the GIFT toolbox (GIFT toolbox, https://trendscenter.org/software/gift), and a spatially constrained multivariate objective optimization Independent Component Analysis with reference (MOO-ICAR)[37,38] was used to obtain spatial maps for selected large-scale networks, namely the visual primary and secondary networks (VPN and VSN, respectively), from a recently published set of 12 brain networks[26]. Spatial maps are used as reference templates to calculate functional networks for each subject by maximizing independence in the context of the spatial constraint. These template maps include the brain networks with non-artefactual neuronal origin and assign the remaining data to be noise. These preprocessed data were also used for static functional network connectivity statistical analysis, considering the VPN and VSN derived from MOO-ICAR preprocessing analysis as well as for spatial chronnectome analysis.

Dynamic coupling maps calculation (dCM), k-means clustering, dwell time (DT), fractional occupancy (FO), total transitions number (TN) and homogeneity calculation

The spatial chronnectome analysis was performed using the dynamic functional network connectivity (dFNC) toolbox implemented in GIFT (GIFT toolbox, http://trendscenter.org/software/gift). Sliding window length or number of clusters were chosen according to previous literature on dynamic connectivity[26]. The single time courses were detrended (to remove baseline drifts from the scanners and/or physiological pulsations), orthogonalized with respect to 12-motion parameters, despiked (replacement of outlier time points with 3rd order spline fitting to clean neighboring points) and filtered using a 5th order Butterworth filter (0.01 to 0.14 Hz). For each considered network, the temporal coupling between a specific brain network and every voxel of the brain was calculated using the sliding-window correlation approach resulting in one dCM per window. This procedure takes all

the potential associations into account and fully captures the relationship between each voxel and the brain network (for example, if a given voxel is highly correlated with two networks, correlation analysis allows the detection of both of these associations). We used the tapered window obtained by convolving a rectangle (width = 30 TRs) with a Gaussian (σ = 3 TRs) and the sliding step size of one TR resulting in 108 windows per subject[26].

K-means clustering was applied to summarize the dCMs of each brain network into a set of spatial states, which allows to investigate the dynamic properties of the brain network via temporal variations of these distinct spatial states. The number of spatial states was set to 4, according to Iraji et al[26]. For each brain network, k-means clustering was applied on the 12852 (119 subjects x 108 windows) dCMs of the brain network. K-means clustering was repeated 100 times with different initializations using the k-means technique to increase the chances of escaping local minima[39]. The correlation distance metric was used to measure the similarity between data points (i.e., the dCMs), as it is more effective in the detection of spatial patterns irrespective of voxel intensities. Using temporal profiles of the spatial states, we calculated the following measures, as dynamic indexes summarizing the dynamic properties of each network : 1. The mean dwell time (DT): the average of the amount of time that subjects stay in a given state once entering that state; 2. The fractional occupancy (FO): the total percentage of time that subjects spent in a given state; 3. The total transition number (NT): the total number of transitions between states performed by subjects for each network; 4. Homogeneity: a measure of the spatio-temporal variations for each network. It varies between 0 and 1; higher homogeneity values represent fewer spatio-temporal variations.

Static Functional Network Connectivity (sFNC) analysis

MOO-ICAR preprocessing was used to estimate individual networks[26]. Back-reconstruction step considered the estimation of subject-specific networks and their related time courses based on the selected 2 networks (VPN and VSN)[26,40]. A univariate general linear model was then performed to

compare preHD versus HC, considering age, gender and FD Powers as covariates ($p<0.001$ uncorrected for multiple comparisons and $p<0.05$ family-wise error whole brain).

Statistical analysis

Comparisons of demographic and clinical characteristics were assessed by Student's t-test for continuous variables and chi-square test for categorical variables.

A univariate general linear model (GLM) was performed to study the main effect of group (preHD vs HC), considering age, gender and FD as nuisance variables. FD was added as covariate to mitigate against the effects of motion[35].

Regression analyses were performed to predict expected years to onset, disease burden score, biofluid biomarkers, putamen volume and neuropsychological performances from dynamic connectivity indexes (dwell time, fractional occupancy, total transition number and homogeneity), considering age, gender and FD as nuisance variables.

All the statistical analyses were performed on STATA and significant level was set at <0.05, after correction for multiple comparisons[41].

Results

Demographic, clinical and biological characteristics of participants

119 participants were included in the present study, namely 60 premanifest HD (age = 29.27 ± 5.59 years, female 53.3%) and 59 controls (age = 29.15 ± 5.41 years, female 61%). PreHD and HC were matched for age, gender and education. Demographic and clinical characteristics are reported in **Table 1**.

Table 1. Demographic and clinical characteristics of participants.

Variable	HC (n=59)	PreHD (n=60)	p-values
Age (years)	29.15 ± 5.41	29.27 ± 5.59	0.62
Female (%)	61%	53.3%	0.46^
Education (years)	16.37 ± 2.23	16.32 ± 2.16	0.89
Framewise displacement	0.13 ± 0.06	0.14 ± 0.07	0.50
NART	103.51 ± 8.22	102.28 ± 7.40	0.39
TMS	0.12 ± 0.33	0.53 ± 1.12	0.98
TFC	13 ± 0	13 ± 0	_
CAG repeat length	_	42.11 ± 1.63	_
Disease burden score	_	188.97 ± 39.9	_
Estimated years to onset	_	23.68 ± 5.90	_

Variables are expressed as mean ± standard deviation, unless otherwise specified.

HC = Healthy Controls; PreHD = Presymptomatic HD; NART = National Adult Reading Test; TMS = Total Motor Score; TFC = Total Functional Capacity

p-values are determined by means of independent sample t-test comparison student t test, unless otherwise specified. ^ *p*-values for Chi-Square test comparison.

We found no differences between preHD and HC concerning the clinical and neuropsychological assessments (data not shown). CSF NfL and plasma NfL were significantly higher in preHD compared to HC ($p < 0.001$ FDR corrected, $p = 0.01$ FDR corrected, respectively), whereas the concentration of the other fluid biomarkers was not significantly different between the two groups (**Figure 1**). Putamen volume was significantly reduced in preHD compared to HC ($p = 0.04$ FDR

corrected), whereas caudate volume was not (p = 0.33 FDR corrected). PreHD and HC showed no differences in the other structural neuroimaging biomarkers considered, namely whole brain, grey matter, white matter and ventricles volumes (data not shown).

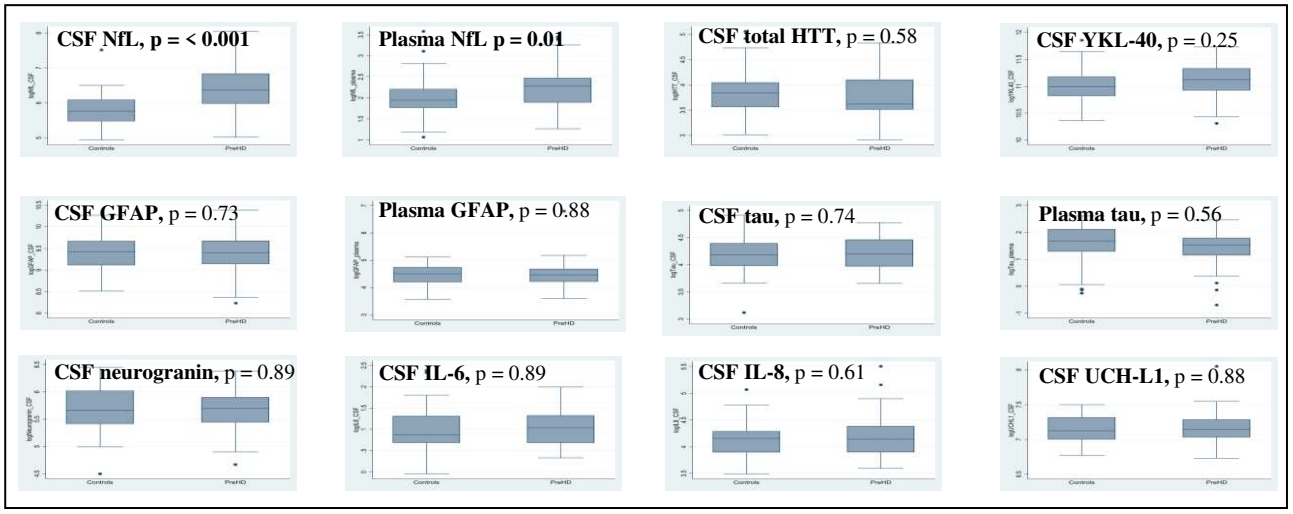

Figure 1. Biofluid measures

Boxplot of the concentrations of biofluid biomarkers in controls (left boxplot) and premanifest HD (right boxplot). All analytes were log transformed. p-values for one-way ANCOVA are expressed after adjusting for age and gender. All results are expressed after correction for multiple comparisons via False Discovery Rate (FDR). NfL = neurofilament light; IL = interleukin; HTT = huntingtin; UCH-L1 = ubiquitin carboxyl-terminal hydrolase L1.

Dwell time, fractional occupancy, number of transitions and homogeneity in premanifest HD compared to controls

Visual primary network (VPN). When considering the VPN, preHD spent more time (DT) in spatial state 1 (20.31 ±18.84 sec vs 13.19 ±14.14 sec, p = 0.03 uncorrected). Accordingly, the fraction of time (FO) spent in spatial state 1 was higher in preHD compared to HC (0.26 ±0.23 vs 0.17 ±0.20, p = 0.03 uncorrected). PreHD showed a trend towards a higher fraction of time (FO) in spatial state 3 (p = 0.06, uncorrected) (see **Table 2, Figure 2**). Homogeneity of VPN was higher in preHD compared to HC (0.956 ±0.005 vs 0.955 ±0.006, p = 0.038 uncoorected), whereas the number of transitions between states was not significantly different between the two groups (**Table 3**).

Visual secondary network (VSN). When analyzing the VSN, preHD spent more time (DT) in spatial state 3 (22.23 ±24.35 sec vs 12.79 ±12.61 sec, p = 0.014 uncorrected). Accordingly, the fraction of time (FO) spent in spatial state 3 was higher in preHD compared to HC (0.26 ±0.25 vs 0.16 ±0.17, p = 0.02 uncorrected) (see **Table 2, Figure 3**). The number of transitions of VSN was significantly lower in preHD compared to HC (5.05 ±2.30 vs 6.34 ±2.29, p = 0.002 uncorrected, p = 0.01 FDR corrected) (see **Table 3**).

Table 2. **Mean dwell time and Fractional occupancy in each spatial state according to considered dynamic functional visual networks in HC and premanifest HD.**

Large-scale networks	Dwell Time			Fractional occupancy		
	HC	preHD	p-values	HC	preHD	p-values
Visual primary network						
Spatial state 1	13.19 ±14.14	20.31 ±18.84	**0.03**	0.17 ±0.20	0.26 ±0.23	**0.03**
Spatial state 2	15.96 ±15.48	16.58 ±13.68	0.75	0.22 ±0.20	0.25 ±0.21	0.38
Spatial state 3	20.34 ±17.37	15.59 ±13.31	0.12	0.27 ±0.22	0.19 ±0.16	***0.06***
Spatial state 4	17.63 ±10.92	16.11 ±11.03	0.40	0.33 ±0.20	0.29 ±0.22	0.20
Visual secondary network						
Spatial state 1	15.90 ±13.80	21.49 ±26.06	0.11	0.27 ±0.19	0.28 ±0.25	0.81
Spatial state 2	20.98 ±17.92	18.40 ±16.72	0.43	0.29 ±0.19	0.24 ±0.24	0.23
Spatial state 3	12.79 ±12.61	22.23 ±24.35	**0.014**	0.16 ±0.17	0.26 ±0.25	**0.02**
Spatial state 4	17.94 ±17.27	13.72 ±11.42	0.16	0.28 ±0.19	0.23 ±0.19	0.13

p-values are obtained by means of univariate General Linear Model, corrected for age, gender and framewise displacement. Results reported are not corrected for multiple comparisons.

Table 3. Number of transitions and homogeneity for each network considered and regression analysis results.

Large-scale networks	Dynamicity measures			Regression analysis (preHD)		
	HC	preHD	p-values	CSF NfL	DBS	EYO
Visual primary network						
Transitions number	5.92 ±2.22	5.98 ±2.21	0.85	p = 0.74	p = 0.22	p = 0.31
Homogeneity	0.955 ±0.006	0.956 ±0.005	**0.038**	**p = 0.02*** β= 0.29	*p = 0.08*	*p = 0.09*
Visual secondary network						
Transitions number	6.34 ±2.29	5.05 ±2.30	**0.002****	p = 0.63	**p = 0.04** β= 0.25	**p = 0.01***** β= -0.32
Homogeneity	0.954 ±0.006	0.956 ±0.007	0.124	p = 0.10	p = 0.94	p= 0.92

On the left part of the table means ±standard deviation are reported for HC and preHD, with the corresponding p-value, obtained by means of a Univariate General Linear Model, corrected for age, gender and framewise displacement.

On the right, results of regression analyses are reported, considering number of transitions and homogeneity as independent predictors; CSF NfL, DBS and EYO as dependent variables; age, gender and framewise displacement as covariates. p values and beta coefficient are shown.

Results reported are not corrected for multiple comparisons; however, some of them were significant after FDR correction. *p = 0.05 FDR corrected. ** p = 0.01 FDR corrected. *** p = 0.03 FDR corrected.

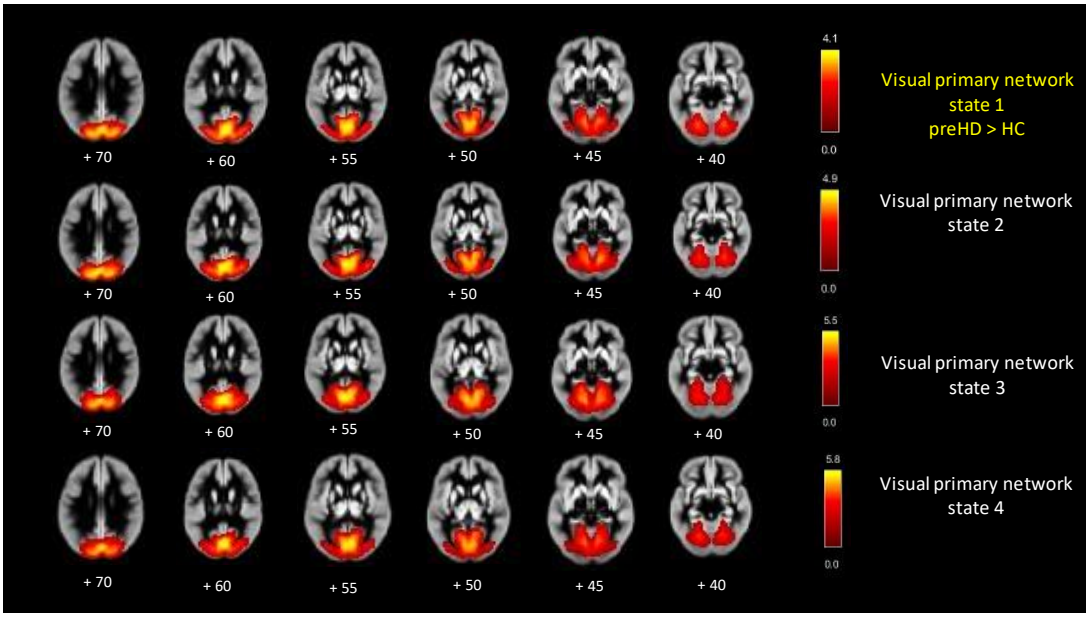

Figure 2. Spatial states of the visual primary network (VPN) and mean dwell time differences between premanifest HD and healthy controls.

The spatial states of the visual primary network. Significant dwell-time differences between groups were reported. Maps of each spatial states are displayed on a standardized axial T1 MRI template, z-axis coordinates are reported under each slice. VPN = visual primary network; preHD = premanifest HD; HC = healthy controls.

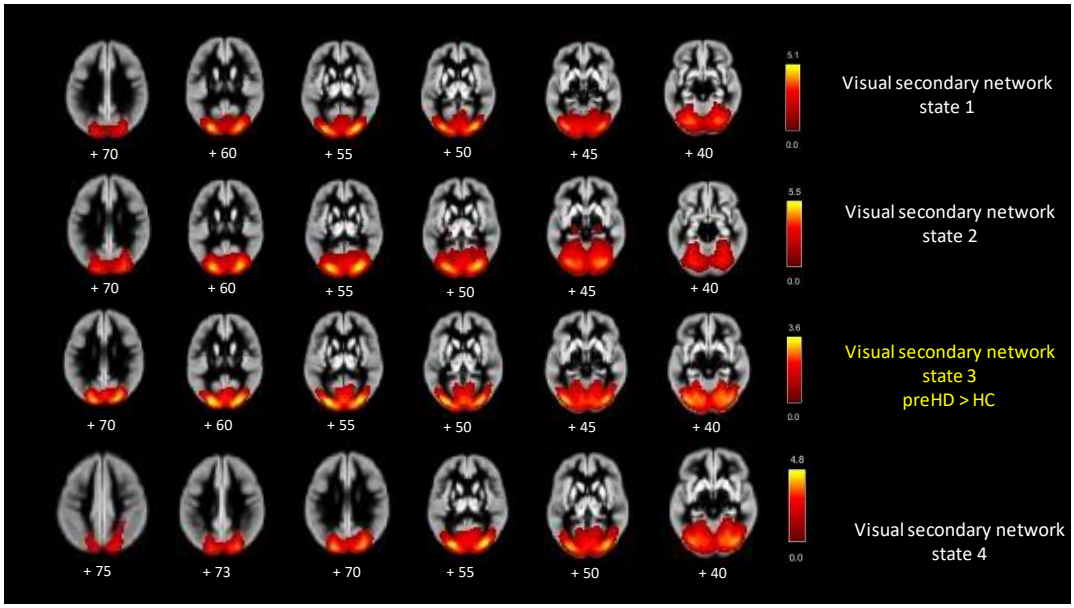

Figure 3. Spatial states of the visual secondary network (VSN) and mean dwell time differences between premanifest HD and healthy controls.

The spatial states of the visual secondary network. Significant dwell-time differences between groups were reported. Maps of each spatial states are displayed on a standardized axial T1 MRI template, z-axis coordinates are reported under each slice.VSN = visual secondary network; preHD = premanifest HD; HC = healthy controls.

Associations between biofluid biomarkers and dynamic connectivity measures in premanifest HD

When considering VPN, homogeneity significantly predicted the concentration of NfL in the CSF (p = 0.02 uncorrected, beta = 0.29, p = 0.05 FDR corrected) but not in plasma. We did not find any associations between other biofluid biomarkers and dynamic connectivity measures.

Associations between Expected Years to Onset and Disease Burden Score and dynamic connectivity measures in premanifest HD

Investigating VSN, the number of transitions significantly predicted the Expected Years to Onset (p = 0.01, beta = -0.32, p = 0.03 FDR corrected) and the Disease Burden Score (p = 0.04 uncorrected, beta = 0.25). Specifically, lower number of transitions was predictive of closer expected onset and higher DBS.

Associations between structural neuroimaging, neuropsychological assessment and dynamic connectivity measures in premanifest HD

We did not find an association between putamen volume and dynamic connectivity measures. An association between neuropsychological assessments and dynamic measures was not detected.

Static functional network connectivity (sFNC)

When sFNC was assessed, within network connectivity between preHD and HC of the two considered networks (VPN and VSN) showed no significant differences at the pre-established threshold ($p<0.001$ uncorrected).

Discussion

This is the first study exploring dynamic functional connectivity in premanifest HD. In particular, we have included a preHD cohort very far from onset to explore two networks of interest, namely the VPN and the VSN, in consideration of our previous finding of an association between posterior connectivity and CSF NfL in the same cohort[15]. Then, we applied an advanced spatial chronnectome approach[26] to evaluate not only static functional network connectivity, but also to assess the distinct conformational spatial states of each network and their dynamic patterns over time. For each network, we computed connectivity measures, both global (number of transitions between states and homogeneity) and specific for each spatial state of (dwell time and fractional occupancy).

One of the two main findings of the present study is the demonstration of an early involvement of visual networks in preHD very far from onset. Even though initial studies showed conflicting results, especially in preHD stage, increasing evidence from post-mortem, structural and functional neuroimaging supports the engagement of occipital areas, even many decades before clinical onset. A *post-mortem* study described a 32% reduction in the number of nerve cells in primary visual area in seven HD brains in advanced disease stages compared to seven controls[16]. Neuropathological *post-mortem* findings are not available in preHD; however, neuroimaging can provide in vivo evidence of occipital regions involvement in both premanifest and manifest HD. Robust neuroimaging results demonstrated occipital atrophy[2,18,42–45] and a reduction of visual network connectivity in manifest HD[10,46], associated with worse visuomotor cognition[18,19,45] and higher disease burden score[45]. Atrophy in the occipital lobe appears crucial at the time of clinical conversion; a recent study found that in the period surrounding motor diagnosis the trajectory of volumetric change is variable across the cortical mantle, with the highest rates of cortical atrophy in the occipital regions[20]. Moreover, CAG-repeat length was most predictive of the individual rate of volume decline within occipital regions.

An increasing body of literature supports an early involvement of visual areas many decades before the disease onset. This is confirmed in both structural[2] and functional[10,12] neuroimaging studies. Interestingly, McColgan and Gregory described an anterior-posterior dissociation, with increased functional connectivity in anterior regions and a decreased functional connectivity in posterior areas in preHD 10-15 years before onset[12]. Regions characterized by increased functional connectivity showed weaker structural connectivity. McColgan and colleagues went even further, exploring also structural and functional connectivity in YAS cohort (approximately 24 years before onset); an association between increased functional connectivity in posterior regions and NfL was described, whereas no correlation was found when considering structural connectivity[47]. Structural differences in cortical regions were not described in the same cohort[8]. On the basis of these study, we might infer that fMRI is more sensitive in detecting very early alterations in occipital regions[15], whereas changes in structural connectivity and cortical thickness become evident later in the disease course[2,22]. Our study further expanded this result, highlighting that dynamic functional network connectivity might be even more sensitive than a static analysis. Indeed, McColgan et al found no significant differences between preHD and HC, whereas the number of transitions in VSN in our study significantly differed between the two groups, even after correction for multiple comparison. Overall, neuroimaging findings in preHD might suggest a posterior-anterior gradient of alterations, which is in keeping with the caudo-rostral gradient of striatal pathology in HD[44].

The second main result of our work is the association between measures of dynamic functional connectivity of each network, namely number of transitions and homogeneity, and expected years to onset, disease burden score and CSF NfL. PreHD showed a number of transitions between states in VSN significantly lower than HC. This index negatively predicted the expected years to onset and positively the disease burden score. In other words, as the number of transitions decreases in preHD, the clinical onset gets closer and the disease burden score increases. This might suggest the hypothesis that the preHD brain is less dynamic compared to controls, and this feature worsens when getting closer to the onset and with the increase of the disease burden score. Moreover, the homogeneity

index of the VPN was significantly higher in preHD compared to HC. This measure quantifies the spatiotemporal variations of each brain network; higher values represent higher spatiotemporal uniformity and lower spatiotemporal variations, thus less dynamism within each network. Homogeneity positively predicted the concentration of CSF NfL, therefore suggesting the weaker the dynamic activity, the greater the axonal damage. To the best of our knowledge, changes in number of transitions and homogeneity have never been reported in neurodegenerative diseases before, whereas they were found altered in psychiatric conditions[26]. Notwithstanding this, reduced functional dynamism and flexibity, expressed by other measures (i.d. metastate changes), are well-documented in neurodegenerative conditions[48,49], also in the premanifest stage of inherited diseases[28]. For example, in our previous study on genetic Frontotemporal dementia (FTD) we found a reduction in several measures of brain dynamism in a large cohort of presymptomatic FTD patients[28]. Number of transitions and homogeneity are the only neuroimaging measures associated with expected years to onset, disease burden score and CSF NfL in preHD very far from onset. Indeed, a previous study[8] showed slightly reduced putamen volume in preHD compared to HC; however, a relation with increase in NfL was not found. Further investigations to explore a possible role of number of transitions and homogeneity as neuroimaging biomarkers in preHD are warranted.

This study presents a number of limitations. First of all, some of the results presented did not survive corrections for multiple comparisons. Notwithstanding this, the number of transitions in VSN and their association with expected years to onset remained significant after FDR correction. This limitation might be explained by the relatively small number of participants and the fact that preHD are very far from expected onset. However, this cohort is unique in literature, since it is not frequent to find young at-risk subjects who decide to undergo the genetic test many years before the expected clinical onset. In addition, the study population is well-defined, taking into account clinical, biological (both plasma and CSF) and neuroimaging data. A second limitation might be related to movement artifacts, which are always a concern in rsfMRI studies. Although HD is a movement disorder, we included subjects very far from clinical onset, without significant abnormal movements. Moreover,

we included motion parameters estimation as well as mean FD in the preprocessing and in the statistical design, respectively. Finally, the influence of vigilance (considering that rs-fMRI data were collected eye-closed) was not evaluated.

Despite these limitations, our results appear relevant, since a deep characterization of the very early preclinical stages of the disease is crucial to elucidate initial pathophysiological mechanisms and for future therapeutic trials.

To conclude, we demonstrated an involvement of visual networks in very early premanifest HD stages. Some connectivity measures of brain dynamism and flexibility, in particular the number of transitions between states and homogeneity, deserve further investigations as possible neuroimaging biomarkers. Their association with expected disease onset and CSF NfL, respectively, should be confirmed in larger cohorts. Dynamic functional connectivity analysis considering subjects closer to disease onset might be helpful to delineate the alterations occurring during the whole premanifest HD stage.

References

1. Tabrizi SJ, Wild EJ. Huntington disease: new insights into molecular pathogenesis and therapeutic opportunities. *Nat Rev Neurol*. doi:10.1038/s41582-020-0389-4
2. Tabrizi SJ, Langbehn DR, Leavitt BR, et al. Biological and clinical manifestations of Huntington's disease in the longitudinal TRACK-HD study: cross-sectional analysis of baseline data. *Lancet Neurol*. 2009;8(9):791-801. doi:10.1016/S1474-4422(09)70170-X
3. Tabrizi SJ, Scahill RI, Owen G, et al. Predictors of phenotypic progression and disease onset in premanifest and early-stage Huntington's disease in the TRACK-HD study: analysis of 36-month observational data. *Lancet Neurol*. 2013;12(7):637-649. doi:10.1016/S1474-4422(13)70088-7
4. Paulsen JS, Langbehn DR, Stout JC, et al. Detection of Huntington's disease decades before diagnosis: the Predict-HD study. *J Neurol Neurosurg Psychiatry*. 2008;79(8):874-880. doi:10.1136/JNNP.2007.128728
5. Paulsen JS, Long JD, Ross CA, et al. Prediction of manifest Huntington's disease with clinical and imaging measures: a prospective observational study. *Lancet Neurol*. 2014;13(12):1193-1201. doi:10.1016/S1474-4422(14)70238-8
6. Byrne LM, Rodrigues FB, Blennow K, et al. Neurofilament light protein in blood as a potential biomarker of neurodegeneration in Huntington's disease: a retrospective cohort analysis. *Lancet Neurol*. 2017;16(8):601-609. doi:10.1016/S1474-4422(17)30124-2
7. Byrne LM, Rodrigues FB, Johnson EB, et al. Evaluation of mutant huntingtin and neurofilament proteins as potential markers in Huntington's disease. *Sci Transl Med*. 2018;10(458). doi:10.1126/scitranslmed.aat7108
8. Scahill RI, Zeun P, Osborne-Crowley K, et al. Biological and clinical characteristics of gene carriers far from predicted onset in the Huntington's disease Young Adult Study (HD-YAS): a cross-sectional analysis. *Lancet Neurol*. 2020;19(6):502-512. doi:10.1016/S1474-

4422(20)30143-5

9. Poudel GR, Egan GF, Churchyard A, Chua P, Stout JC, Georgiou-Karistianis N. Abnormal synchrony of resting state networks in premanifest and symptomatic Huntington disease: The IMAGE-HD study. *J Psychiatry Neurosci*. 2014;39(2):87-96. doi:10.1503/jpn.120226

10. Dumas EM, Van Den Bogaard SJA, Hart EP, et al. Reduced functional brain connectivity prior to and after disease onset in Huntington's disease. *NeuroImage Clin*. 2013;2(1):377-384. doi:10.1016/j.nicl.2013.03.001

11. Koenig KA, Lowe MJ, Harrington DL, et al. Functional connectivity of primary motor cortex is dependent on genetic burden in prodromal Huntington disease. *Brain Connect*. 2014;4(7):535-546. doi:10.1089/brain.2014.0271

12. McColgan P, Gregory S, Razi A, et al. White matter predicts functional connectivity in premanifest Huntington's disease. *Ann Clin Transl Neurol*. 2017;4(2):106-118. doi:10.1002/acn3.384

13. McColgan P, Razi A, Gregory S, et al. Structural and functional brain network correlates of depressive symptoms in premanifest Huntington's disease. *Hum Brain Mapp*. 2017;38(6):2819-2829. doi:10.1002/hbm.23527

14. Langley C, Gregory S, Osborne-Crowley K, et al. Fronto-striatal circuits for cognitive flexibility in far from onset Huntington's disease: evidence from the Young Adult Study. *J Neurol Neurosurg Psychiatry*. 2021;92(2):143-149. doi:10.1136/JNNP-2020-324104

15. McColgan P, Gregory S, Zeun P, et al. Neurofilament light-associated connectivity in young-adult Huntington's disease is related to neuronal genes. *Brain*. 2022;145(11):3953-3967. doi:10.1093/BRAIN/AWAC227

16. Rüb U, Seidel K, Heinsen H, Vonsattel JP, den Dunnen WF, Korf HW. Huntington's disease (HD): the neuropathology of a multisystem neurodegenerative disorder of the human brain. *Brain Pathol*. 2016;26(6):726-740. doi:10.1111/BPA.12426

17. Tabrizi SJ, Reilmann R, Roos RAC, et al. Potential endpoints for clinical trials in

premanifest and early Huntington's disease in the TRACK-HD study: analysis of 24 month observational data. *Lancet Neurol*. 2012;11(1):42-53. doi:10.1016/S1474-4422(11)70263-0

18. Rosas HD, Salat DH, Lee SY, et al. Cerebral cortex and the clinical expression of Huntington's disease: complexity and heterogeneity. *Brain*. 2008;131(Pt 4):1057-1068. doi:10.1093/BRAIN/AWN025

19. Johnson EB, Rees EM, Labuschagne I, et al. The impact of occipital lobe cortical thickness on cognitive task performance: An investigation in Huntington's Disease. *Neuropsychologia*. 2015;79(Pt A):138-146. doi:10.1016/J.NEUROPSYCHOLOGIA.2015.10.033

20. Johnson EB, Ziegler G, Penny W, et al. Dynamics of Cortical Degeneration Over a Decade in Huntington's Disease. *Biol Psychiatry*. 2021;89(8):807-816. doi:10.1016/J.BIOPSYCH.2020.11.009

21. Dumas EM, Van Den Bogaard SJA, Hart EP, et al. Reduced functional brain connectivity prior to and after disease onset in Huntington's disease. *NeuroImage Clin*. 2013;2(1):377-384. doi:10.1016/J.NICL.2013.03.001

22. McColgan P, Gregory S, Razi A, et al. White matter predicts functional connectivity in premanifest Huntington's disease. *Ann Clin Transl Neurol*. 2017;4(2):106-118. doi:10.1002/ACN3.384

23. Calhoun VD, Miller R, Pearlson G, Adali T. The chronnectome: time-varying connectivity networks as the next frontier in fMRI data discovery. *Neuron*. 2014;84(2):262-274. doi:10.1016/J.NEURON.2014.10.015

24. Abrol A, Damaraju E, Miller RL, et al. Replicability of time-varying connectivity patterns in large resting state fMRI samples. *Neuroimage*. 2017;163:160-176. doi:10.1016/J.NEUROIMAGE.2017.09.020

25. Allen EA, Damaraju E, Plis SM, Erhardt EB, Eichele T, Calhoun VD. Tracking whole-brain connectivity dynamics in the resting state. *Cereb Cortex*. 2014;24(3):663-676. doi:10.1093/CERCOR/BHS352

26. Iraji A, Deramus TP, Lewis N, et al. The spatial chronnectome reveals a dynamic interplay between functional segregation and integration. *Hum Brain Mapp*. 2019;40(10):3058-3077. doi:10.1002/HBM.24580

27. Iraji A, Fu Z, Damaraju E, et al. Spatial dynamics within and between brain functional domains: A hierarchical approach to study time-varying brain function. *Hum Brain Mapp*. 2019;40(6):1969-1986. doi:10.1002/HBM.24505

28. Premi E, Calhoun VD, Diano M, et al. The inner fluctuations of the brain in presymptomatic Frontotemporal Dementia: The chronnectome fingerprint. *Neuroimage*. 2019;189:645-654. doi:10.1016/J.NEUROIMAGE.2019.01.080

29. Premi E, Giunta M, Iraji A, et al. Dissemination in time and space in presymptomatic granulin mutation carriers: a GENFI spatial chronnectome study. *Neurobiol Aging*. 2021;108:155-167. doi:10.1016/j.neurobiolaging.2021.09.001

30. Espinoza FA, Liu J, Ciarochi J, et al. Dynamic functional network connectivity in Huntington's disease and its associations with motor and cognitive measures. *Hum Brain Mapp*. 2019;40(6):1955-1968. doi:10.1002/hbm.24504

31. Langbehn DR, Brinkman RR, Falush D, Paulsen JS, Hayden MR. A new model for prediction of the age of onset and penetrance for Huntington's disease based on CAG length. *Clin Genet*. 2004;65(4):267-277. doi:10.1111/J.1399-0004.2004.00241.X

32. Kieburtz K. Unified Huntington's Disease Rating Scale: reliability and consistency. Huntington Study Group. *Mov Disord*. 1996;11(2):136-142. doi:10.1002/MDS.870110204

33. Wild EJ, Boggio R, Langbehn D, et al. Quantification of mutant huntingtin protein in cerebrospinal fluid from Huntington's disease patients. *J Clin Invest*. 2015;125(5):1979-1986. doi:10.1172/JCI80743

34. Yan CG, Wang X Di, Zuo XN, Zang YF. DPABI: Data Processing & Analysis for (Resting-State) Brain Imaging. *Neuroinformatics*. 2016;14(3):339-351. doi:10.1007/S12021-016-9299-4

35. Power JD, Barnes KA, Snyder AZ, Schlaggar BL, Petersen SE. Spurious but systematic correlations in functional connectivity MRI networks arise from subject motion. *Neuroimage*. 2012;59(3):2142-2154. doi:10.1016/J.NEUROIMAGE.2011.10.018

36. Calhoun VD, Wager TD, Krishnan A, et al. The impact of T1 versus EPI spatial normalization templates for fMRI data analyses. *Hum Brain Mapp*. 2017;38(11):5331-5342. doi:10.1002/hbm.23737

37. Du Y, Fan Y. Group information guided ICA for fMRI data analysis. *Neuroimage*. 2013;69:157-197. doi:10.1016/J.NEUROIMAGE.2012.11.008

38. Du Y, Pearlson GD, Liu J, et al. A group ICA based framework for evaluating resting fMRI markers when disease categories are unclear: application to schizophrenia, bipolar, and schizoaffective disorders. *Neuroimage*. 2015;122:272. doi:10.1016/J.NEUROIMAGE.2015.07.054

39. Arthur D, Vassilvitskii S. k-means++: The Advantages of Careful Seeding.

40. Salman MS, Du Y, Lin D, et al. Group ICA for identifying biomarkers in schizophrenia: "Adaptive" networks via spatially constrained ICA show more sensitivity to group differences than spatio-temporal regression. *NeuroImage Clin*. 2019;22. doi:10.1016/J.NICL.2019.101747

41. Benjamini Y, Hochberg Y. Controlling the False Discovery Rate: A Practical and Powerful Approach to Multiple Testing. *J R Stat Soc Ser B*. 1995;57(1):289-300. doi:10.1111/J.2517-6161.1995.TB02031.X

42. Tabrizi SJ, Scahill RI, Durr A, et al. Biological and clinical changes in premanifest and early stage Huntington's disease in the TRACK-HD study: The 12-month longitudinal analysis. *Lancet Neurol*. 2011;10(1):31-42. doi:10.1016/S1474-4422(10)70276-3

43. Rosas HD, Liu AK, Hersch S, et al. Regional and progressive thinning of the cortical ribbon in Huntington's disease. *Neurology*. 2002;58(5):695-701. doi:10.1212/WNL.58.5.695

44. Vonsattel JPG, Keller C, Cortes Ramirez EP. Huntington's disease - neuropathology. *Handb*

Clin Neurol. 2011;100:83-100. doi:10.1016/B978-0-444-52014-2.00004-5

45. Wolf RC, Sambataro F, Vasic N, et al. Visual system integrity and cognition in early Huntington's disease. *Eur J Neurosci*. 2014;40(2):2417-2426. doi:10.1111/EJN.12575

46. Coppen EM, van der Grond J, Hart EP, Lakke EAJF, Roos RAC. The visual cortex and visual cognition in Huntington's disease: An overview of current literature. *Behav Brain Res*. 2018;351:63-74. doi:10.1016/J.BBR.2018.05.019

47. McColgan P, Gregory S, Zeun P, et al. Neurofilament light-associated connectivity in young-adult Huntington's disease is related to neuronal genes. *Brain*. 2022;145(11):3953-3967. doi:10.1093/brain/awac227

48. Cordes D, Zhuang X, Kaleem M, et al. Advances in functional magnetic resonance imaging data analysis methods using Empirical Mode Decomposition to investigate temporal changes in early Parkinson's disease. *Alzheimer's Dement (New York, N Y)*. 2018;4:372-386. doi:10.1016/J.TRCI.2018.04.009

49. Zhuang X, Walsh RR, Sreenivasan K, Yang Z, Mishra V, Cordes D. Incorporating spatial constraint in co-activation pattern analysis to explore the dynamics of resting-state networks: An application to Parkinson's disease. *Neuroimage*. 2018;172:64-84. doi:10.1016/J.NEUROIMAGE.2018.01.019

MODULO DI EMBARGO DELLA TESI
(da compilare solo se si richiede un periodo di segretazione della tesi)

La sottoscritta Marta Pengo Nata il 04/08/1989
a Aosta (Italia)
provincia di Aosta
Dottorato di Ricerca in Genetica molecolare, Biotecnologie e Medicina Sperimentale

DICHIARA

- che il contenuto della tesi **non può essere immediatamente consultabile per il seguente motivo**

Presentazione di alcuni risultati preliminari non ancora sottomessi a riviste scientifiche né pubblicati

La motivazione deve essere dettagliata e controfirmata obbligatoriamente dal Primo Supervisore di tesi
(Brevetto, segreto industriale, motivi di priorità nella ricerca, motivi editoriali, altro)

- che il testo completo della tesi potrà essere reso consultabile dopo:

□ 6 mesi dalla data di conseguimento titolo
X 12 mesi dalla data di conseguimento titolo

- che sarà comunque consultabile immediatamente l'abstract della tesi, che viene caricato in Esse3, profilo studente.

Luogo e Data
Milano, 15/03/2024

Firma del Dichiarante

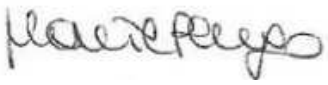
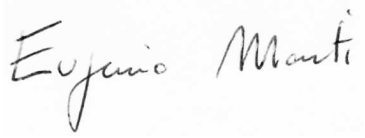
Controfirma del Primo Supervisore di tesi
per la motivazione di embargo e il periodo.